

Dissertation

zur Erlangung des Doktorgrades
der Fakultät für Chemie und Pharmazie der
Ludwig-Maximilians-Universität München

Bioresponsive HES-PEI conjugates for controlled shielding and deshielding of pDNA polyplexes



Matthäus Noga

aus Ratibor

2013

Erklärung

Diese Dissertation wurde im Sinne von § 7 der Promotionsordnung vom 28. November 2011 von Herrn Prof. Dr. Gerhard Winter betreut.

Eidesstattliche Versicherung

Diese Dissertation wurde eigenständig und ohne unerlaubte Hilfe erarbeitet.

München, 21.07.2013

(Matthäus Noga)

Dissertation eingereicht am:	25.07.2013
1. Gutachter:	Prof. Dr. Gerhard Winter
2. Gutachter:	Prof. Dr. Ernst Wagner
Mündliche Prüfung am:	25.09.2013

Für meine Familie

In Liebe und Dankbarkeit

*Es ist nicht genug zu wissen,
man muss es auch anwenden.*

*Es ist nicht genug zu wollen,
man muss es auch tun.*

Johann Wolfgang von Goethe (1749-1832)

ACKNOWLEDGEMENTS

The present thesis was prepared between November 2009 and March 2013 at the Department of Pharmacy, Pharmaceutical Technology and Biopharmaceutics at the Ludwig-Maximilians-University (LMU) in Munich.

First and foremost, I have to express my deepest gratitude to my doctoral father Prof. Dr. Gerhard Winter for making me a member of his research group and for supervising the present thesis. In particular I thank for the continuous support, inspirational scientific contributions, and the trustful professional as well as personal interaction during the last years. Thank you for the pleasant working atmosphere within your research group, making my PhD student time unforgettable.

I am deeply grateful to Dr. Ahmed Besheer for his valuable scientific and personal support, the clever guidance in the scientific daily routine and for all helpful and fruitful discussions. Ahmed is gratefully thanked for always being available for direct contact of all research issues and for being my confidential mentor. Furthermore thank you for establishing essential collaborations that formed the interdisciplinary character of my work. The success of this thesis is closely connected with his person.

I have to thank Prof. Dr. Wolfgang Frieß for all helpful and interesting discussions in the past years. Thank you for creating the pleasant working conditions together with Prof. Dr. Gerhard Winter in your labs.

This interdisciplinary thesis would not have been possible without the engaged cooperation partners. In particular, I thank Prof. Dr. Ernst Wagner and Daniel Edinger from the chair of Pharmaceutical Biotechnology for the reliable collaboration and for their essential practical and theoretical scientific advice and support during the present thesis. Prof. Dr. Ernst Wagner is gratefully thanked for farsighted and honest discussions, brilliant scientific support from the point of an outstanding gene delivery expert and for the access to cell culture and animal studies and to all other required analytical tools in the research field of polymeric delivery of nucleic acids. Thank you Daniel for being my constant companion from the first steps to the end of my PhD student time, for the fantastic team play and the pleasant time we have spent

for planning, performing and evaluating all *in vitro* and *in vivo* gene expression experiments. Animal studies would not have been possible without the great veterinary expertise of Raphaela Kläger. Wolfgang Rödl is kindly acknowledged for helping in the early stage of the project in synthesis and purification issues and for continuously providing of the LPEI material.

Prof. Dr. Joachim P. Spatz and Dr. Seraphine V. Wegner from the Max-Planck-Institute for Intelligent Systems, Stuttgart and from the Department of Biophysical Chemistry, University of Heidelberg are acknowledged for the fruitful research stay using the QCM technology for studying the enzymatic biocleavage of HES-PEI copolymers.

It is all about people. I have to thank all my colleagues from the Winter and Frieß labs for creating a comfort zone that enabled the productive working atmosphere. The social events like the hiking and skiing trips, the excursion to Freiburg/Basel and all other comings together were great fun. Particularly, I warmly thank my HESchen Stall mates Elisabeth Härtl and Christian Neuhofer for the great and trustful time we had together in our lab. Furthermore the haxball society is kindly acknowledged – I will not forget all hard-fought matches with MrKlose, Juggernaut, Nimbus, McLovin and Nullinger. Thanks to our IT experts Raimund Geidobler, Christian Neuhofer and Markus Hofer for solving any sort of technical computer problems.

Fresenius Kabi Deutschland GmbH and Serumwerk Bernburg AG are kindly acknowledged for their HES material support of the experimental work of this thesis.

Many thanks are expressed to the students Kathrin Abstiens, Michael Möhwald and Cornelia Ziegler, who did an excellent job during their internships in my lab.

I deeply thank my parents and my sister Anita for the support they gave me over all the years and for simply being my family. Finally I would like to thank my wife Sabine for her continuous encouragement, for her appreciative patience and for her love.

LIST OF ABBREVIATIONS

AA	Alpha amylase
AF4	Asymmetric flow filed flow fractionation
AFM	Atomic force microscopy
BSA	Bovine serum albumin
DLS	Dynamic light scattering
DMEM	Dulbecco's Modified Eagle's Medium
DMSO	Dimethyl sulfoxide
DNA	Deoxyribonucleic acid
DSC	Differential scanning calorimetry
DTT	Dithiothreitol
EDTA	Ethylenediaminetetraacetic acid
FACS	Fluorescence-activated cell sorting
FCS	Fetal calf serum
FD	Freeze-drying
FT	Freeze-thawing
HBG	HEPES-buffered glucose
HBS	HEPES-buffered saline
HBSuc	HEPES-buffered sucrose
HBTre	HEPES-buffered trehalose
HEPES	N-(2-hydroxyethyl) piperazine-N'-(2-ethansulfonic acid)
HES	Hydroxyethyl starch
¹ H NMR	Nuclear magnetic resonance
HUH7 cells	Human hepatoma HUH7 cells
LPEI22	Linear polyethylenimine (Mw of 22 kDa)
MALS	Multi-angle light scattering
MTT	Methylthiazoletetrazolium
Mw	Weight average molecular weight
NP	Nanoparticle
N/P ratio	Molar ratio of PEI nitrogen to DNA phosphate
N2A cells	Murine neuroblastoma N2A cells
PBS	Phosphate buffered saline
PDI	Polydispersity index

pDNA	Plasmid DNA
PEG	Poly(ethylene glycol)
Px	Polyplex
QCM-D	Quartz crystal microbalance with dissipation
RI	Refractive index
RLU	Relative light units
SE-HPLC	Size exclusion high performance liquid chromatography
TEM	Transmission electron microscopy
T _g	Glass transition temperature
T _g '	Glass transition temperature of the maximal freeze-concentrate
ZP	Zeta potential

TABLE OF CONTENTS

CHAPTER I - GENERAL INTRODUCTION

1	Medical nanotechnology	2
2	Polymeric gene delivery	2
3	Functionalization of polymeric non-viral delivery systems - A step closer to artificial viruses	4
3.1	Targeting ligands	4
3.2	Domains for endosomolysis and the nuclear entry	5
3.3	Shielding agents	6
4	Importance of shielding and deshielding in gene delivery	7
5	Enzyme-triggered shedding approaches for nanomedicines	8
5.1	Extracellular and intracellular shedding	8
5.2	Enzymatic deshielding strategies	10
5.2.1	Strategy I: Enzymatic cleavage of a bioresponsive linker between stealth polymer and the anchor	10
5.2.2	Strategy II: Fully biodegradable stealth coats for long-circulating nanosystem	13
6	Alternative shielding agent: Hydroxyethyl starch (HES)	14
7	Objectives of the thesis	17
8	References	18

CHAPTER II - CONTROLLED SHIELDING AND DESHIELDING OF GENE DELIVERY POLYPLEXES USING HYDROXYETHYL STARCH AND ALPHA-AMYLASE

1	Introduction	29
----------	---------------------------	-----------

2	<i>Experimental Section</i>	31
2.1	Materials	31
2.2	Methods	31
2.2.1	Acid hydrolysis of HES70	31
2.2.2	Determination of the molar mass of acid-hydrolyzed HES using asymmetric flow field flow fractionation (AF4)	31
2.2.3	Biodegradation of HES70 and HES20 with pancreatic α -amylase (AA)	32
2.2.4	Synthesis and purification of HES-PEI conjugates	32
2.2.5	Nuclear magnetic resonance spectroscopy	33
2.2.6	Copper assay	33
2.2.7	Size exclusion chromatography	33
2.2.8	Preparation and characterization of polyplexes	34
2.2.9	Particle size and zeta potential determination	34
2.2.10	Treatment of polyplexes with pancreatic α -amylase (AA)	35
2.2.11	Erythrocyte aggregation assay	35
2.2.12	Cell culture experiments	35
2.2.13	Luciferase reporter gene expression studies	36
2.2.14	Metabolic activity of transfected cells	36
2.2.15	Flow cytometry experiment	36
3	Results	37
3.1	Acid-induced fragmentation of HES70	37
3.2	HES degradation experiments with pancreatic α -amylase	37
3.3	Polycation modification: HES-conjugation to PEI22	39
3.4	Characterization of polymeric HES-PEI conjugates	39
3.5	Biophysical characterization of the generated polyplexes	42
3.6	Treatment of polyplexes with pancreatic α -amylase	43
3.7	Erythrocyte aggregation assay	47
3.8	Cell culture experiments - Luciferase reporter gene transfection efficiency	47

3.9	Effect of AA activity	49
3.10	Binding and uptake experiments using flow cytometry	50
4	Discussion.....	52
5	Conclusions.....	55
6	Acknowledgements	55
7	References	56

CHAPTER III - THE EFFECT OF MOLAR MASS AND DEGREE OF HYDROXYETHYLATION ON THE CONTROLLED SHIELDING AND DESHIELDING OF HYDROXYETHYL STARCH-COATED POLYPLEXES

1	Introduction.....	63
2	Experimental Section.....	64
2.1	Materials	64
2.1.1	Synthesis and characterization of HES-PEI conjugates.	64
2.1.2	Investigation of the biodegradation of HES homopolymers with AA using AF4-MALS	65
2.1.3	Quartz crystal microbalance with dissipation (QCM-D)	65
2.1.4	Preparation of HESylated polyplexes	66
2.1.5	Treatment of polyplexes with pancreatic α -amylase (AA)	66
2.1.6	Cell culture experiments.....	67
2.1.7	<i>In vitro</i> luciferase reporter gene expression studies	67
2.1.8	Metabolic activity of transfected cells.....	67
2.1.9	<i>In vivo</i> transfection with HESylated polyplexes in tumor-bearing mice.....	68
3	Results	70
3.1	Biodegradation studies	70
3.2	Effect of molar mass and degree of hydroxyethylation on the luciferase reporter gene transfection efficiency <i>in vitro</i>	74

3.3	Gene transfer studies of HES-PEI polyplexes <i>in vivo</i>	76
4	Discussion.....	78
5	Conclusions.....	81
6	Acknowledgements	82
7	References	82

CHAPTER IV - CHARACTERIZATION AND BIOCOMPATIBILITY OF HYDROXYETHYL STARCH-POLYETHYLENIMINE COPOLYMERS FOR DNA DELIVERY

1	Introduction.....	87
2	Experimental section	88
2.1	Materials	88
2.2	Methods	88
2.2.1	Synthesis and characterization of HES-PEI co-polymers	88
2.2.2	Preparation and biophysical characterization of polymer-based transfection particles	89
2.2.3	Dynamic light scattering (DLS)	89
2.2.4	Transmission Electron Microscopy (TEM).....	89
2.2.5	Atomic Force Microscopy (AFM)	90
2.2.6	Zeta potential measurement	90
2.2.7	DNA binding evaluation using ethidium bromide (EtBr) binding assay	90
2.2.8	Colloidal stability of HESylated PEI-based DNA complexes	90
2.2.9	Polyplex stability in protein-containing medium	91
2.2.10	Evaluation of the cytotoxicity of plain HES-decorated PEIs	91
2.2.11	Erythrocyte aggregation assay	92
2.2.12	Hemolysis assay	92

3	Results	93
3.1	HES-PEI conjugates synthesis and characterization	93
3.2	Physicochemical characterization of the generated polyplexes.....	94
3.2.1	Particle size	94
3.2.2	Surface charge	95
3.3	DNA condensation by HES-PEI.....	96
3.4	Stability of HES-decorated polyplexes.....	97
3.5	Biocompatibility of HES-PEI conjugates.....	99
3.5.1	Cytotoxicity of HES-PEI to HUH7 cells.....	99
3.5.2	Hemocompatibility of modified LPEIs	100
4	Discussion.....	103
5	Conclusion	105
6	Acknowledgements	106
7	References	106

CHAPTER V - EFFECT OF HES-DECORATION ON STORAGE STABILITY OF pDNA POLYPLEXES – A BENCHMARK STUDY AGAINST PEG

1	Introduction.....	111
2	Experimental section	112
2.1	Materials	112
2.2	Methods	112
2.2.1	Synthesis and characterization of HESPEI co-polymers using ¹ H-NMR, copper assay, and SEC.....	112
2.2.2	Preparation of LPEI-based pDNA polyplexes.	113
2.2.3	Polyplex stability against shelf-freezing (SF) and liquid nitrogen (LN ₂) immersion stress.....	113

2.2.4	Excipient screening.	114
2.2.5	Lyophilization studies of HES-decorated polyplexes.	114
2.2.6	Biophysical characterization of pDNA polyplexes.	114
2.2.7	Thermoanalytical analysis.	115
2.2.8	Karl-Fischer titration.	115
2.2.9	Cell culture experiments.	115
2.2.10	Luciferase reporter gene expression studies.	116
2.2.11	Metabolic activity of transfected cells.	116
3	Results	117
4	Discussion.....	125
5	Conclusions	129
6	Acknowledgements	129
7	References	130

CHAPTER VI –FINAL SUMMARY OF THE THESIS

I General introduction

This chapter contains sections from mini-review (in revision):

Noga M, Winter G, Besheer A. Enzyme-responsive stealth coats for long-circulating nanomedicines

1 Medical nanotechnology

Progress in nanotechnology over the last decades and its application in the biomedical field emerged as nanomedicine around the beginning of the millennium. According to the European Science Foundation's (ESF) report "Forward Look on Nanomedicine" from 2005 [1], the term nanomedicine characterizes nano-sized molecular tools for diagnosing, treating or preventing disease, injury and pain aiming at comprehensive monitoring, repair and improvement of biological systems [2-4]. In particular nanoparticles (NPs), such as liposomes, micelles and polymeric NPs gained attraction as carriers for small-molecule drugs, proteins and nucleic acids. These nanocarriers are designed to fulfill a number of tasks upon parenteral application, most importantly: efficient targeted cargo delivery (e.g. promoted by homing devices for passive or active targeting), protection of the active pharmaceutical ingredient (API) from degradative environment (e.g. labile protein or oligonucleotide drugs), reduction of undesirable side effects of the API (e.g. controlled release of highly-potent drugs upon stimuli-sensitive triggering at the target site), and controlling the pharmacokinetics (e.g. provided by sustained drug delivery systems) [5-7].

2 Polymeric gene delivery

The central idea of gene therapy is introducing therapeutic genes into target regions in the human body for the purpose of curing patients suffering from inherited or acquired diseases. For this reason, the development of appropriate gene delivery systems is essential for improving the so far poor efficiency in gene transfer, as well as maintaining their safety and efficacy. Hurdles related to the use of viral vectors (e.g. immunogenicity of viral components [8-10]) and limitations of physical methods (such as gene gun, electroporation and microinjection) in reaching metastatic cancer and in the efficient delivery of genes, make non-viral vectors based on polymers an attractive alternative carrier system. However, polymeric oligonucleotide complexes - so-called polyplexes – have to overcome several biological extra- and intracellular barriers to act as efficient nucleotide delivery system, including proneness to *in vivo* aggregation, rapid clearance from the bloodstream, and selective and successful gene expression at the desired target, all together presenting a huge challenge for efficient gene transfer [11, 12]. Polymeric carriers based on polyethylenimine (PEI) are often considered the gold standard polycations for gene delivery. This can be attributed to many

reasons, including PEI's unique nucleic acid binding ability, protecting the genetic cargo against inactivation by degradation. This essential feature - paired with its high endosomolytic activity - makes the cationic polymer PEI an attractive carrier system for delivering nucleic acids [13]. Once entering the target cell by endocytosis, endosomal acidification increases PEI's cationic charge density leading to influx of chloride ions and osmotic water, a process described as proton-sponge-effect [14-16]. The continuous swelling provokes the rupture of the endo-/lysosomal membranes and the release of the genetic payload into the cytoplasm, a crucial step in intracellular trafficking as illustrated in

Figure I. 1. However, PEI's favourable endosomolytic potency is simultaneously the main disadvantage of the cationic polymer – namely its cytotoxicity promoted by the high charge density [13].

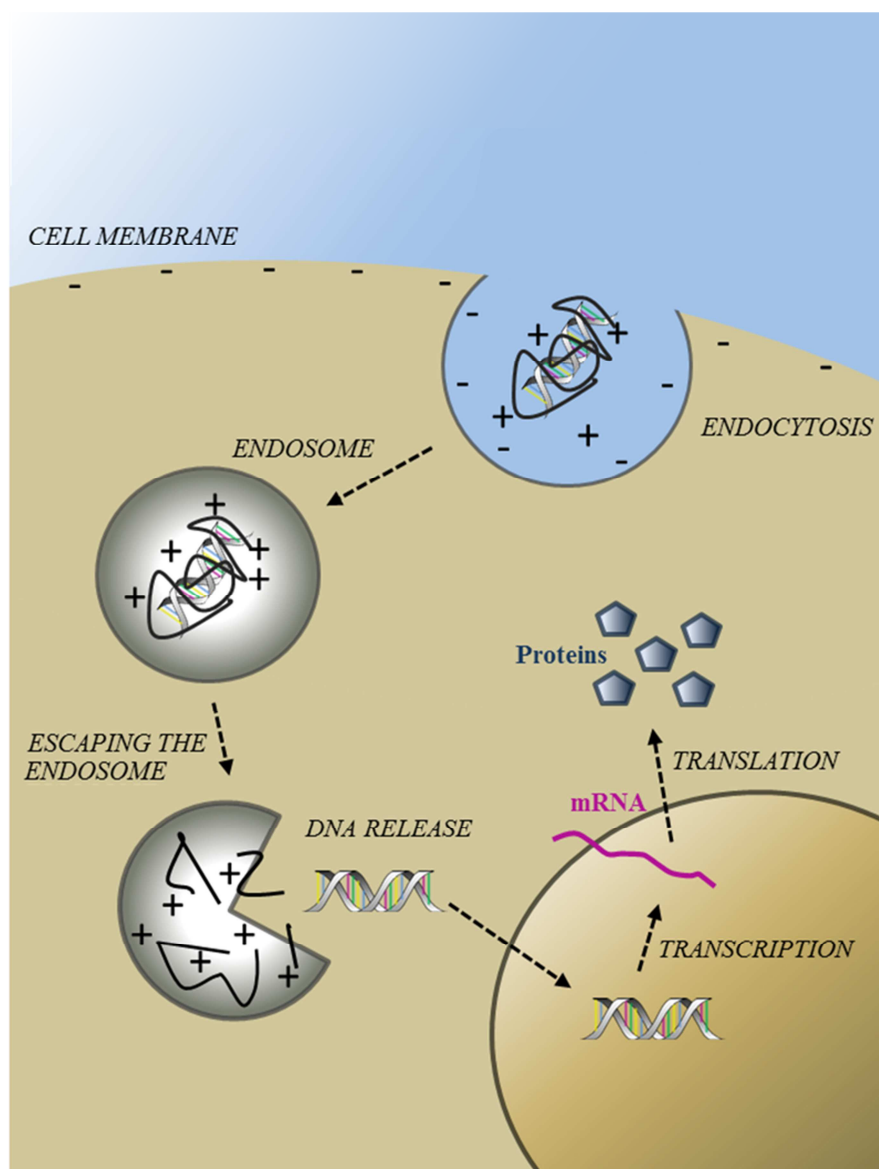


Figure 1. 1. Cellular trafficking of polymeric gene delivery systems. Cationic DNA/PEI polyplexes enter the target cell via endocytosis and escape the adversely acting endo-/lysosomal compartment due to PEIs' high charge density enabling osmotic swelling, membrane rupture and release of the payload into the cytosol. Once entered the nucleus, pDNA expression via transcription and translation results in the production of corresponding proteins.

3 Functionalization of polymeric non-viral delivery systems - A step closer to artificial viruses

In general, naked polymeric gene delivery systems are decorated with functionalized domains, mimicking artificial viruses. For successful *in vitro* and *in vivo* gene delivery, polymeric complexes are often equipped with shielding agents, targeting ligands, as well as domains facilitating endosomal lysis and the nuclear entry.

3.1 Targeting ligands

For improving the efficacy and cytotoxicity of cationic polymer carriers like PEI, naked polymer/nucleic acid polyplexes are equipped with functionalized domains. For instance, targeting ligands are exposed on the nanoparticle surface for active cell targeting via ligand-receptor interactions between the particulate system and the cell membrane structures. Several homing devices, e.g. antibodies, antibody fragments, glycoproteins, vitamins and peptides [17-21] enable enhanced cellular uptake of the carrier and its payload via receptor-mediated or related forms of endocytosis.

Mimicking the uptake behavior of natural viruses, Nie *et al.* developed dual-targeted polymeric complexes, fusing transferrin and integrin targeting [20]. Systems equipped with dual-targeting domains showed significantly increased *in vitro* gene expression, where integrin-targeting domains predominantly mediated the cellular binding and transferrin-targeting facilitated cellular uptake via receptor-mediated endocytosis [20]. Exposure of folic acid on the polyplex surface is another strategy increasing the efficiency of polymeric carrier systems. Folate receptors are abundant and over-expressed in certain tumor tissues [22], making this strategy attractive for tumor-targeted gene delivery [23]. Polyplexes based on poly(dimethylaminomethyl methacrylate) were decorated with folate-targeted PEG-coats [24]. Homing domain folate markedly increased the transfection levels of OVCAR-3 cells

related to the untargeted polyplexes [24]. Another ligand which gained great interest in gene delivery is the epidermal growth factor (EGF). Wagner and co-workers reported on EGF-conjugated PEI/DNA polyplexes for targeted gene delivery [25]. The internalization of EGF-conjugated complexes proceeded via the assumed endocytic EGF receptor-mediated pathway. EGF-conjugated PEI/DNA polyplexes resulted in up 300-fold increased gene transfection compared with the non-targeted counterpart [25]. Later the EGF-mediated internalization route was confirmed for EGF-conjugated polyplexes using live-cell imaging [26]. In another approach, the HER2-specific (human epidermal growth factor receptor-2) monoclonal antibody trastuzumab was coupled onto LPEI/DNA polyplexes [17]. The transfection efficiency in HER2-overexpressing breast cancer cell lines markedly increased compared to non-targeted LPEI polyplexes, while access of free trastuzumab in the cell culture medium diminished the level of transfection, clearly indicating HER2-mediated cellular uptake [17]. Similarly, flow cytometry analysis showed high HER2-targeting specificity for cyclodextrine-PEI-oligopeptide conjugates leading to high *in vitro* and *in vivo* gene transfection activity [27].

3.2 Domains for endosomolysis and the nuclear entry

Designing artificial viruses is often associated with the incorporation of endosomolytic domains enhancing the escape of harsh conditions present in the endo-/lysosomal compartment. PEI is a proton sponge, leading to membrane rupture and endosomal escape under the effect of endosomal acidification. In order to further enhance the endosomolytic potency of cationic polymer carriers, polyplexes with surface-attached endosomolytic domains are developed. The endosomolytically active peptide melittin gained particular interest for escaping the endosome and releasing the payload into the cytosol [28, 29]. For instance, Boeckle et al. developed smart PEI-melittin conjugates for selective membrane destabilization at the acidic pH 5 present in the endosome. Melittin-incorporation markedly increased the transfection efficiency compared to polyplexes without fusion peptide attachment [30].

Decorating polymeric gene carriers with nuclear localization signals (NLS) peptides is another promising option for efficient gene transfer. NLS peptides enable the transport of the genetic payload into the nucleus via nuclear pore complex. PEI polyplexes containing NLS signals showed markedly higher gene transfection efficiency both, *in vitro* and *in vivo* [31].

However, coupling of NLS peptides onto DNA using polymerase chain reaction (PCR) did not significantly boost the transfection performance related to PEI/DNA complexes without nuclear entry domains [32].

3.3 Shielding agents

Coating NPs with the hydrophilic polymer poly(ethylene glycol) PEG became the golden standard for imparting stealth character to nanoparticles. PEG is a neutral, hydrophilic and highly water-soluble polymer. Since the first experimental studies using PEG for the improvement of the *in vivo* biodistribution of large molecules in the 1970's [33], the PEGylation technology was established as standard in masking drugs and drug carriers from the body's immune system. Several advantages are provided by covalent attachment of PEG chains onto the target molecule: i) improvement of the drug solubility and stability, ii) extended blood circulation time, iii) reduced drug toxicity, and iv) reduced proneness of the drug to proteolytic degradation [34, 35].

Meanwhile, several PEGylated protein, peptide and particulate pharmaceuticals entered the pharmaceutical market [36-38] and generate billions of dollars in turnover (e.g. PEGylated interferon (IFN)- α 2b - PEGasys[®], Cimzia[®] - a PEGylated anti-TNF- α Fab', or Doxil[®], a doxorubicin loaded PEGylated liposome system). A large number of other candidates are on the verge of being launched onto the market or under clinical trials. PEGylation can mediate particles' escape from phagocytic uptake by making the particles "invisible" to the immune system. Surface-masking of polymeric gene delivery complexes using PEG coats is an important prerequisite for reaching distant targets after parenteral application.

Apart from PEG, several alternative polymers as hydrophilic coating were investigated, including poly[N-(2-hydroxypropyl)methacrylamide] [39-41], poly(glycerol)s [42, 43], poly(saccharide)s [44-46], poly(oxazoline)s [47], poly(amino acid)s [48, 49]. All alternative approaches are aimed at masking the drug/gene delivery system with hydrophilic polymers escaping the phagocytic system and extending their *in vivo* half-life time.

4 Importance of shielding and deshielding in gene delivery

The development and intravenous application of nano-sized particles can be used for cargo delivery to tumoral or inflammatory sites after parenteral application. Passive targeting of nanosystems to solid tumors and sites of inflammation can be achieved by extravasation into the sites of disease via the distinctive vascular architecture present in tumoral and inflammatory environment. Irregular shaped and leaky blood vessels and endothelial cells with large fenestrations allow the accumulation of long-circulating macromolecules and NPs into tumors by a phenomenon known as the enhanced permeability and retention (EPR) effect. Beside anatomical characteristics, factors like vascular endothelial growth factor (VEGF), nitric oxide (NO), prostaglandins and bradykinin promote further permeation [50, 51] (for EPR effect reviews see [52-54]).

However, a crucial prerequisite for exploiting the EPR effect is a sufficient long circulation time after parenteral application of nanomedicines, as well as sufficient colloidal particle stability in the blood stream. Cationic nanoparticles, such as naked LPEI polyplexes tend to electrostatically interact with blood components and non-target cells in the bloodstream, leading to uncontrolled *in vivo* aggregation. Aggregates of LPEI-based polyplex show a short *in vivo* half-life, due to rapid accumulation in the lung as well as elimination from the circulation by the reticuloendothelial system (RES) [55-57]. Surface-decoration of NPs with PEG became the gold standard for imparting stealth character to nanosystems as it offers several benefits: steric shielding, extended circulation times and escaping the body's phagocytic system, allowing time for passive tumor-targeting by the EPR effect. Nevertheless, stealthiness provided by PEG brings about reduced efficiency, since the non-biodegradable stealth polymer PEG can diminish cellular uptake, endosomal escape and intracellular trafficking by the effect of steric hindrance, what is known as the PEG-dilemma in gene delivery [58]. Additionally, production of anti-PEG antibodies [59] and the accelerated blood clearance of PEGylated NPs upon repeated injection [60, 61] further limit the applicability of PEGylated nanoparticles for gene delivery. For these reasons, several approaches were developed for overcoming the PEG-dilemma by shedding the interfering PEG coat after reaching the target site. Stimuli-sensitive linker molecules were designed and introduced between PEG and the nanoparticle surface, in order to get cleaved in response to triggers such as pH-value, temperature, reducing environment, ultrasound or enzyme activity [62-69].

5 Enzyme-triggered shedding approaches for nanomedicines

The majority of enzymes used for deshielding approaches belong to enzyme category 3 (for classification see Table I. 1), for instance proteases, esterases and glycosidases. Such enzymes catalyze the hydrolysis of chemically labile bonds of the corresponding coating materials, allowing site- and stimuli-specific deshielding of nanoparticles. Selective and site-specific acting makes enzymes a promising tool for controlled unmasking strategies.

Table I. 1. *Classification of enzymes according to the Nomenclature Committee of the International Union of Biochemistry and Molecular Biology.*

	Enzyme category (EC)	Catalyzed reaction
EC 1	Oxidoreductases	Catalysis of oxidative/reductive reactions
EC 2	Transferases	Catalysis of transfer reactions of functional groups
EC 3	Hydrolases	Catalysis of hydrolytic cleavage of chemical bonds
EC 4	Lyases	Catalysis of non-hydrolytic cleavage of chemical bonds
EC 5	Isomerases	Catalysis of transformation reactions of isomers
EC 6	Ligases	Catalysis of joining of chemical bonds

5.1 Extracellular and intracellular shedding

Imparting stealth character to NPs using hydrophilic coating materials is the state-of-the-art technology enabling efficient drug delivery with sufficient long residence in the bloodstream. Non-degradable stealth coats (specifically PEG coats) promote favorable features on the way to the target site (tumoral or inflammatory sites), namely increased stability and prolonged circulation time in the bloodstream by reduced undesired interactions to non-target cells and other biological components. However, after arrival at the target it would be desirable to shed down the disturbing non-degradable PEG-coat to facilitate efficient cellular uptake, endosomal escape and intracellular trafficking. Enzyme-induced surface deshielding represents a smart option for selective overcoming the PEG-dilemma due to its high selective and site-specific acting.

As illustrated in Figure I. 2, two routes of enzymatically-catalyzed shedding are in the focus of scientific interest: i) extracellular or ii) intracellular enzyme-responsive decoating.

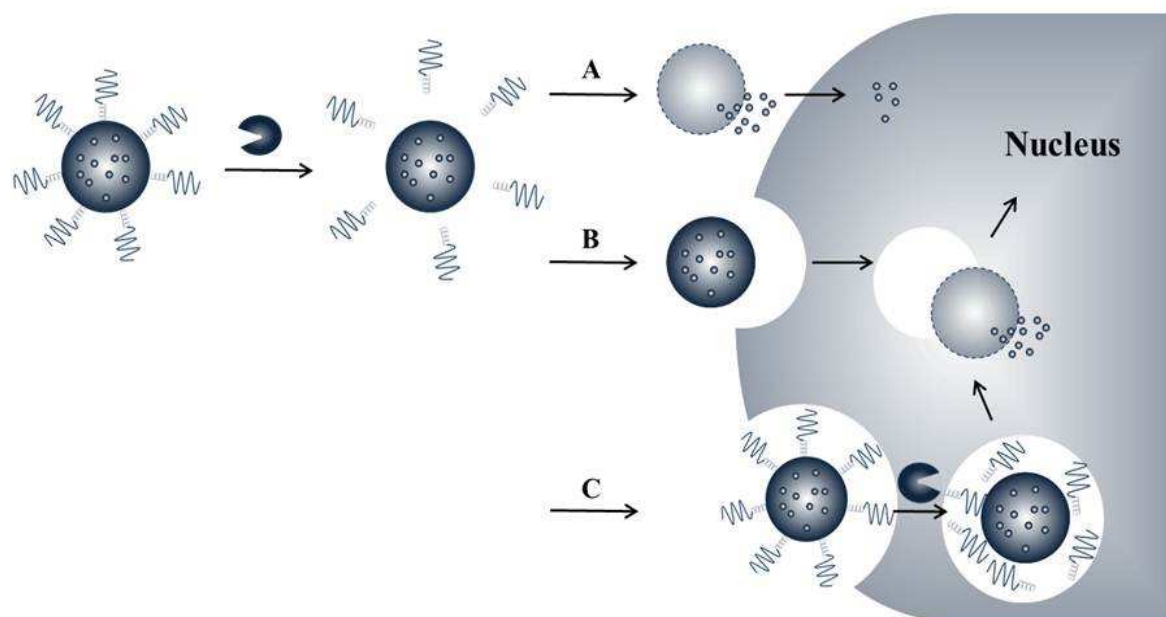


Figure I. 2. Stimuli-sensitive shedding of stealth coats – proposed mechanisms of extracellular (A/B) and intracellular (C) enzyme-induced decoating after reaching the pathological target site. A) Extracellular drug release upon controlled cleavage of the hydrophilic stealth polymer. B) Deshielding of nanoparticles in the extracellular matrix for enhanced cellular uptake by improved particle-membrane interactions due to shedding down of the sterically hindering stealth polymer coats. C) Intracellular deshielding approaches provide protection from degradative environment.

Enzyme-responsive extracellular or intracellular shedding approaches are designed to allow scenarios of interaction with target cells and release of payload. For instance, deshielding of nanoparticles under the effect of extracellular-acting enzymes is advantageous, when the release of small-molecule drugs in the extracellular matrix is desired (Figure I. 2 A). Such small molecules can then enter the target cell by passive diffusion. Furthermore, extracellular shedding approaches are beneficial - for instance - when stealth coats prevent the nanoparticles from interacting with their target cells due to shielding their targeting moieties or their positive surface charge (Figure I. 2 B) [70]. The latter is the trigger for electrostatic interaction between positively charged particle and cell membranes with negative charge. Meanwhile, if shielded particles are phagocytosed, the polymer coat can provide protection for labile drugs and genes from degradative enzymes in the endo-/lysosome, however, stealth coats can reduce the carriers' ability to escape the endo-/lysosomal compartment (Figure I. 2 C). Intracellular shedding can allow efficient escape from the endosome [71].

5.2 Enzymatic deshielding strategies

Designing enzyme-responsive stealth-coats is aimed at the combination of exploiting the advantages provided by shielding in the bloodstream, as well as functional reactivation under stimuli-sensitive shedding after arrival of the drug carrier system at the target site. Enzyme-triggered decoating provides high cleavage selectivity. Two shedding strategies exist for enzyme-responsive stealth coats for nanosystems, namely: i) cleavage of a bioresponsive linker molecule between hydrophilic shielding polymer and anchor under enzymatic effect, and ii) cleavage of the fully biodegradable stealth coating material. These strategies are explained below.

5.2.1 Strategy I: Enzymatic cleavage of a bioresponsive linker between stealth polymer and the anchor

The incorporation of enzyme-labile bonds as linker molecule between well-established PEG polymers and the anchor molecules is the most applied shedding strategy in the field of enzyme-induced deshielding. These stimuli-sensitive linker molecules are susceptible to hydrolytic cleavage by proteases and esterases. Table I. 2 provides an overview of the different published approaches of bioresponsive shedding via enzyme-labile linker molecules.

Table I. 2. *Deshielding strategy I: Enzymatically-catalyzed cleavage of bioresponsive linkers between stealth polymer and anchor.*

Enzyme class	Linker molecule	Site of shedding	Type of nanomedicine	In vivo studies	References
Proteases	MMP-sensitive peptide	Extracellularly, tumor environment	Fe ₃ O ₄ NPs	-	[72]
				+	[73]
			Quantum dots	-	[74]
			Silica NPs	+	[75]
			Liposomes	+	[58, 76]
				-	[77]
			Polycaprolactone NPs	+	[78]
	Tetrapeptide	Extracellularly, tumor environment	Liposomes	+	[79]
Esterases	Ester linker	Extracellularly, serum	Vesicles, liposomes	-	[80]
				+	[81-84]
			Solid lipid NPs	+	[85, 86]

Particularly, matrix-metalloproteinases (MMPs) have attracted great interest for enzymatically-catalyzed shedding approaches due to their high abundance in the extracellular tumor matrix. The group of MMPs is composed of a large number of versatile enzymes, classified by their substrate specificity, most notably the gelatinase (MMP-2 and MMP-9) and collagenase, and by their cellular localization in membrane-type matrix-metalloproteinases (mt-MMPs) [87]. MMPs are involved in degradation processes of the extracellular matrix (e.g. cleaving collagen) and in the tumor angiogenesis and metastasis. The predominant secretion in the tumor tissues makes MMPs a valuable trigger-system for targeted and controlled shedding approaches [87-89].

The group of Harashima developed a multifunctional envelope type nano device (MEND) for controlled tumoral delivery of genes by the EPR effect [58]. MEND was composed of pDNA-loaded liposomes equipped with an MMP-2-sensitive PEG-peptide-lipid for overcoming the PEG-dilemma. PEG coating enabled tumor accumulation, while the biodegradable PEG-peptide-lipid resulted in 65 times higher luciferase transfection levels compared to the non-degradable PEG-MENDs [58]. Similarly, PEGylated pDNA nanoparticles were generated using PEG-peptidyl lipids for controlled pDNA release in the tumor [77]. Peptide-linkers were elastase- (amino acid sequence: AAPV) or MMP-2-sensitive (amino acid sequence: GPLGV). Under enzymatic effect, the *in vitro* transfection was boosted by improved cellular uptake and intracellular trafficking [77]. Mok *et al.* reported on a PEG-shielded and MMP-2-specifically deshielded quantum dot (QD) system with different PEG chain densities [74]. Shielding diminished the cytotoxicity of heavy metal ions of the QDs. Shedding the stealth coats upon addition of MMP-2 increased the uptake of QD by uncovering of surface-immobilized cell penetrating peptides [74]. The group of Bhatia developed iron oxide NPs with MMP-2-sensitive PEG coats enabling particle self-assembly by the effect of shedding [72] and magnetofluorescent iron oxide NPs with prolonged blood circulation times (8x slower blood clearance) for passive tumor targeting and tumor imaging following enzymatic particle unmasking [73].

Other reports report on the use of masking and unmasking approaches for the controlled delivery and targeted-release of small cytotoxic molecules, such as docetaxel (DOC) or doxorubicin (DOX) [75, 78]. Liu *et al.* prepared PEGylated DOC-loaded poly(ϵ -caprolactone)-based NPs with/without gelatinase-sensitive peptide linkers [78]. The therapeutic effect of DOC-PCL NPs was benchmarked against a commercially available DOC drug (Taxotere[®]). Reversible shielded DOC-PCL nanoparticles showed higher DOC release and cellular uptake under enzymatic stimuli compared with non-reversible coated NPs. *In*

in vivo treatment revealed high tumor accumulation in the case of PEG-peptide-PCL NPs that was detectable for 72h. The developed DOC-loaded PCL NPs resulted in a higher therapeutic effect and lower cytotoxicity than the commercially available control [78]. Similarly, DOX-loaded silica nanoparticles were decorated with MMP-degradable PEG-peptide. PEGylation drastically reduced the NPs' toxicity via diminished undesired interaction with cell membranes. MMP-catalyzed dePEGylation restored the chemotoxic potency of highly-cleavable DOX-loaded silica NPs contrary to non- or low-cleavable PEGylated analogs, indicating stimuli-triggered doxorubicin release *in vitro* and *in vivo* [75].

The accelerated blood clearance (ABC) phenomenon of non-reversible PEGylated nanosystems following repeated injections is often reported in literature [60, 90]. In order to address this problem, PEGylated nanosystems can be equipped with enzymatically-cleavable PEG shields, where Zhao et al. showed that coating of solid lipid NPs using the esterase-cleavable PEG-cholesteryl hemisuccinate (PEG-CHEMS) prevented the ABC phenomenon after both s.c. and i.v. injections [85]. PEG-lipids based on cholesterol, namely PEG-CHEMS, PEG-CHMC (PEG-cholesteryl chloroformate) and PEG-CHST (tris(hydroxymethyl) amino-methane salt of cholesteryl hemisuccinate) were attached onto liposomal and vesicular systems to reduce or stop the induction of the ABC phenomenon [81]. In another approach overcoming the accelerated clearance of PEGylated NPs, the PEG-CHEMS conjugate was extended with the pH-sensitive hydrazone molecule to give a PEG-Hz-CHEMS conjugate that is susceptible to serum esterases and low pH values [83].

The effect of the degree of PEG-decoration and enzyme concentrations on the extent of enzyme-triggered cleavage of PEG-lipids was investigated by Xu and co-workers [80]. Increasing the PEG chain density on the particle surface is associated with lowered extent of biodegradation, while the rate of biocleavage was enhanced under the effect of high enzyme concentrations. The enzymatic removal of the PEG coat induced controlled release of the loaded drug [80]. Stability issues were studied using PEGylated solid lipid nanoparticles. Upon addition of carboxylesterase polysorbate or PEG- monostearate coatings were gradually degraded after 60 min resulting in a decrease in the particle size. A 24h enzyme-treatment resulted in increased nanoparticle sizes induced by particle destabilization and enzyme-triggered drug release [86]. Esterase-catalysis induced PEG detachment from the liposomes' surface and resulted in tumor-specific pDNA gene expression [84].

5.2.2 Strategy II: Fully biodegradable stealth coats for long-circulating nanosystems

Beside the use of “bio-labile” linkers between the non-cleavable shielding polymer and the anchor molecule, only few attempts were performed implementing fully biodegradable coating materials for enzymatic shedding, mostly based on poly(amino acid)s and polysaccharides. Coating nanosystems using fully enzymatically-cleavable stealth shields offers benefits in relation to the shedding approach utilizing bioresponsive linker-molecules: i) easier-achievable synthesis and purification of the synthesis products due to two-component synthesis versus three-components approaches (e.g. poly(amino acid)-anchor vs. PEG-peptide-anchor), ii) no need for incorporating unstable bonds over long-term and iii) two features provided by one component, namely shielding and deshielding ability. Shedding approaches using fully biodegradable coatings for nanosystems are listed in Table I. 3.

Table I. 3. *Deshielding strategy II: Enzymatically degradable shielding coats.*

Shielding agent	Enzyme class	Site of shedding	Type of nanomedicine	<i>In vivo</i> studies	References
Poly(amino acid)	Proteases	Extracellularly, endo-/lysosomal compartment	Liposomes, Fe ₃ O ₄ NPs	- +	[48, 91, 92] [93]
	Oxidoreductases	Mitochondrial area	Peptosoma, lactosome	+	[49, 94]
Dextrin	Glycosidases	Extracellularly, tumor environment	Polymer-protein conjugate	-	[95, 96]
				+	[97]
Hyaluronic acid	Glycosidases	Extracellularly	Polymer-protein conjugate	-	[98]
Starch	Glycosidases	Intracellularly, lysosome	Silica NPs	-	[99]

Romberg et al. generated poly(amino acid) coatings based on poly(hydroxyethyl L-glutamine) (PHEG) aiming at prolonged circulation time, liposome stabilization and drug release under enzymatic cleavage [48]. Following proteolytic shedding of the PHEG coat, dioleoyl phosphatidylethanolamine (DOPE)-based liposomes converted from the lamellar to the hexagonal state, which was monitored by dynamic light scattering as increase in the particle size and polydispersity of the liposomes and increased release of the encapsulated model-drug calcein [48]. In addition, the pharmacokinetic behavior of PHEG- and PHEA

(poly(hydroxyethyl L-asparagine))-decorated liposomes was assessed in rats. The hydrophilic coating materials significantly increased the half-life of shielded liposomes compared with the non-coated particles [93]. Poly(amino acid)s coatings are also used in the field of molecular imaging [49, 94]. Near-infrared fluorescence (NIRF)-labeled peptosomes [49] and lactosomes [94] were equipped with poly(sarcosine) shields for tumor targeting. A thin brush-layer of surface-grafted poly(sarcosine) can promote protein-repellent properties, an important prerequisite for efficient stealth polymer potency. Undesired protein interactions were diminished with increasing poly(sarcosine) surface density [100]. Incorporation of hydrophilic poly(sarcosine) onto the surface of molecular imaging nanocarriers encapsulated with a NIRF-probe allowed tumor accumulation by the EPR effect and cancer imaging [49, 94]. Similarly, different poly(saccharide) polymers showed in several studies beneficial shielding and shedding performance for protein therapeutics, both *in vitro* and *in vivo*. For instance, in the research group around Ruth Duncan, the polymer-masked-unmasked-protein therapy (PMUPT) was applied using dextrin-phospholipase A2 (PLA2)-conjugates to decrease the systemic toxicity of phospholipase A2 (PLA2) from honey bee venom and restore its antitumoral activity after enzymatic unmasking [95]. Similar PMUPT approaches were made using stealth polymers dextrin or hyaluronic acid: Conjugates of dextrin and recombinant-human epidermal growth factor (rhEGF) protected the growth factor from proteolysis by elastase, while shedding by alpha-amylase restored rhEGF's potency for increased proliferation of fibroblasts [96]. Dermal wound application with dextrin-rhEGF conjugates significantly accelerated wound healing compared to rhEGF application [97]. Coupling hyaluronic acid (HA) onto model-protein trypsin resulted in increased trypsin activity related to that of the free enzyme under the effect of the glycosidase [98]. The effect of adding pancreatin or β -D-galactosidase to starch-coated silica nanoparticles was studied on the release of the encapsulated dye. Upon enzymatic stimuli the dye was released in different manners depending on the grade of hydrolyzed starch [99].

6 Alternative shielding agent: Hydroxyethyl starch (HES)

An optimal coating material ideally comprises several beneficial characteristics: i) hydrophilic and non-charged polymer, ii) non-immunogenic and biodegradable coating material allowing efficient shielding and controlled deshielding, iii) protein-repellent properties, and iv) non-toxic cleavage-products. While PEG offers many favorable properties, its lack of

biodegradability and immunogenic potential makes alternative candidates for stealth coating very attractive. In the current dissertation, hydroxyethyl starch (HES) was proposed as a biodegradable substitute of PEG offering an opportunity for controlled shielding and enzymatically-catalyzed deshielding of nanomedicines.

HES is a water-soluble, biodegradable and semisynthetic starch derivative, mostly derived from amylopectin-rich waxy maize starch or potato starch. The polysaccharide predominantly consists of α -1,4-glycosidic D-glucose units with few sites of branching via α -1,6-glycosidic bonds (Figure I. 3). Industrial HES generation proceeds in three main stages, namely: 1st step: acid or enzymatic hydrolysis of amylopectin-rich starch (for adjustment of molecular weight), 2nd step: hydroxyethylation of cleavage products via chemical modification with ethylene oxide under alkaline conditions (for adjustment of the degree of hydroxyethylation of HES), and 3rd step: purification/fractionation of HES (for adjustment of HES' polydispersity) [101].

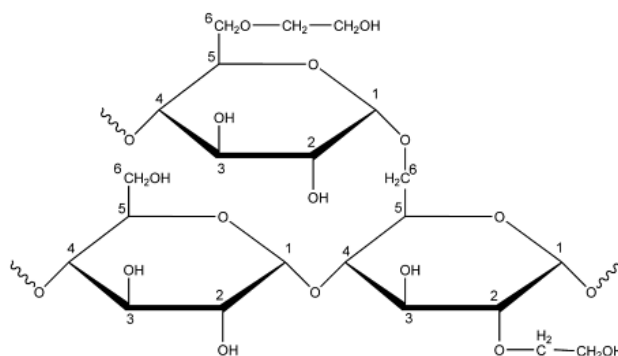


Figure I. 3. General structure of hydroxyethyl starch . Numbers represent the order of enumerated carbohydrates of the anhydroglucose unit of HES. Hydroxyethylation of amylopectin-rich starches can take place at position C2, C6 and C3 (ordered by frequency).

Hydroxyethylation of starch increases the water solubility, lowers the viscosity and - more importantly - reduces the degree of biodegradability of the polymer, increasing the systemic half-life from few minutes (starch) up to several hours (HES) [102, 103]. Additionally, HES' protein-repellent action [104, 105] has attracted great interest for the application of HES as substitute for PEG for macromolecules [101, 106, 107] and particulate systems [105, 108]. The rate and extent of enzymatic biodegradation triggered by serum α -amylases can be controlled by fine-tuning the HES' molecular characteristics. Hydroxyethylation of amylopectin-rich starches predominantly takes place at position C2 of the HES' anhydroglucose unit (AGU), less frequently at position C6 and C3. In particular, substitution of position C2 has deep impact on HES' biodegradation kinetics, where the attached hydroxyethyl residues can reduce the level of biodegradability by the effect of strong steric

hindrance. Beside the degree of hydroxyethylation, the pattern of substitution – here most notably the C2/C6 ratio – and to a lower extent the molar mass of HES, can affect the degree and kinetics of cleavage of α -1,4-glycosid bonds of HES by serum-amylases [109, 110]. In addition, a high abundance of amylases in several tumor tissues, such as breast, lung, ovarian and pancreatic cancer [111-115], makes HES-decorated nanocarriers attractive for enzyme-responsive drug and gene delivery to distant tumors. Alpha-amylases are mainly secreted by the saliva or the pancreas, act hydrolytically and are classified into enzyme-class EC 3.2.1.1 (according to the Nomenclature Committee of the International Union of Biochemistry and Molecular Biology, see chapter I.5.1). Caldwell et al. reported 1953 on stability and activity issues of amylase and found that the cleavage performance of amylase is closely linked to the presence of chloride and calcium ions [116]. The mostly common industrial use of α -amylase is the application in detergents for removal of starches [117].

The polymer HES shows great structural similarity to human glycogen, the energy reserve stored in liver and muscle cells that can be transformed to glucose in the case of energy demand. This chemical resemblance between HES and glycogen is believed to be the cause for HES' reduced immunogenicity [118]. HES solutions are in clinical application for decades as plasma volume expander in high doses showing good tolerability. Nevertheless, no effect without adverse effect. Pruritis - induced by longterm HES therapy in high dosages - is the most often adverse effect (< 10%) according to the manufacturer's expert information (Fresenius Kabi). Blood volume substitution using HES improves the hemodilution by reduction of the coagulation factors fibrinogen, Factor VIII, von Willebrand's factor, and of the platelet function, however, causing prolonged bleeding time [119-121]. Blood substitution using low molar mass HES types with low degree of substitution can minimize such effect [122]. In comparison to gelatin-, dextran- and albumin-based blood volume substitutes, HES infusions show the lowest tendency for anaphylactoid reactions with an incidence of 0.058% [123].

Beside its clinical application as plasma substitute, HES was utilized for many biomedical applications. For instance, HES-drug conjugates were generated for increased *in vivo* half-life and sustained drug release of an erythropoietin mimetic peptide and the anti-cancer drug 5-fluoruracil [124, 125]. In the field of magnetic resonance imaging, a novel macromolecular contrast agent based on HES was designed, allowing high-contrast imaging [126]. Harling *et al.* developed hydrogel microparticles based on HES for drug delivery. Lysozyme-loaded microparticles showed controlled release *in vitro* over 4 months that is expected to proceed faster under *in vivo* conditions in presence of amylase [127]. Similarly, FITC-labeled IgG was

encapsulated into hydrogel microspheres to achieve controlled release of macromolecules [128]. The use of HES as cryoprotecting agent is also described in the literature. For instance, hEHC cells for tissue engineering and human erythrocytes were cryopreserved using HES as additive [129, 130]. In another study, cross-linked HES nanocapsules with/without folic acid surface-attachment were prepared to study their unspecific or receptor-mediated cellular uptake. CLSM measurements confirmed the stealth character provided by HES, since HES nanocapsules without surface-modification resulted in markedly reduced unspecific cellular uptake related to folate-decorated HES nanocapsules [131]. In addition, the effect of particle shielding was reported on reduced phagocytic uptake of HESylated nanospheres by Besheer *et al.* [108].

7 Objectives of the thesis

Dandelion spheres are formed of thick shields surrounding a small core, which get deshielded as a response to external stimulus (namely wind). Emulating nature's design, this work describes the development and use of “nano-dandelions”: hydroxyethyl starch (HES)-coated core-shell nanoparticles with controlled shielding & deshielding for nucleic acid delivery. The concept is shielding the polyplexes in the blood stream from non-specific interactions, and enhancing the cellular uptake at the tumor site by the degradation of the coat under the action of α -amylase (Figure I. 4).

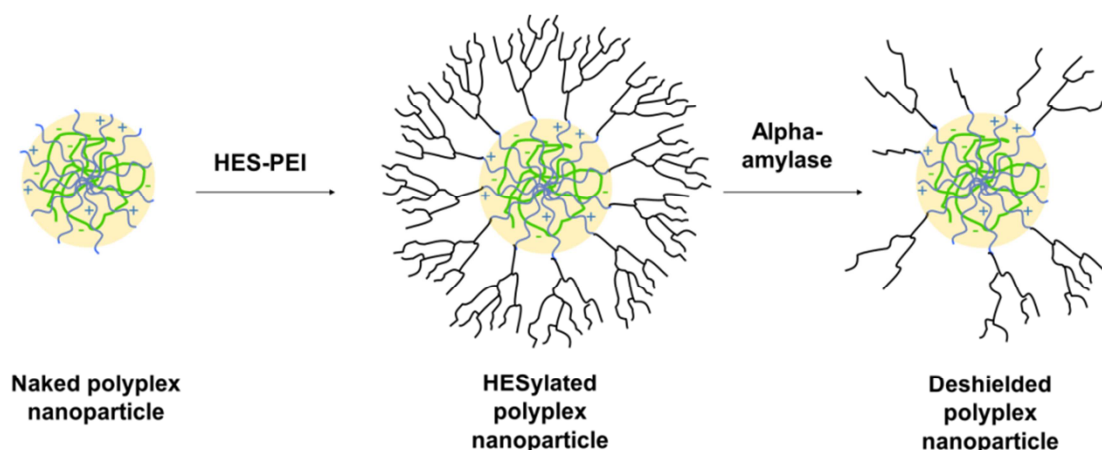


Figure I. 4. Schematic illustration of the concept of controlled shielding and enzymatically-catalyzed deshielding of HES-decorated nano-dandelions.

For this reason, the first major objective was to synthesize several HES-PEI conjugates with different molecular characteristics of HES, aiming at the generation of stable and

bioresponsive HES-decorated PEI/DNA polyplexes as a substitute for PEGylated polymeric complexes. The proof-of-concept of nanoparticle shielding and enzymatically-catalyzed polyplex surface deshielding using different HES coats and alpha-amylase was tested in several *in vitro* and *in vivo* model experiments. Additionally, the effect of lyophilization of HES-coated polyplexes on their long-term stability and gene expression activity after storage was investigated. Most of the experiments were performed with naked LPEI polyplexes and PEGylated polymeric complexes as controls.

8 References

1. European Science Foundation's Forward Look on Nanomedicine. 2005; Available from: <http://www.esf.org>.
2. **Duncan, R. and R. Gaspar**, Nanomedicine (s) under the Microscope. *Molecular pharmaceutics*, 2011. 8(6): p. 2101-2141.
3. **Duncan, R.**, Nanomedicine gets clinical. *Materials Today*, 2005. 8(8): p. 16-17.
4. **Duncan, R.**, Polymer therapeutics as nanomedicines: new perspectives. *Current Opinion in Biotechnology*, 2011. 22(4): p. 492-501.
5. **Li, S.D. and L. Huang**, Pharmacokinetics and biodistribution of nanoparticles. *Molecular Pharmaceutics*, 2008. 5(4): p. 496-504.
6. **Owens III, D.E. and N.A. Peppas**, Opsonization, biodistribution, and pharmacokinetics of polymeric nanoparticles. *International journal of pharmaceutics*, 2006. 307(1): p. 93-102.
7. **Torchilin, V.P.**, Nanocarriers. *Pharmaceutical research*, 2007. 24(12): p. 2333-2334.
8. **Hacein-Bey-Abina, S., C. von Kalle, M. Schmidt, F. Le Deist, N. Wulffraat, E. McIntyre, I. Radford, J.L. Villeval, C.C. Fraser, and M. Cavazzana-Calvo**, A serious adverse event after successful gene therapy for X-linked severe combined immunodeficiency. *New England Journal of Medicine*, 2003. 348(3): p. 255-256.
9. **McCaffrey, A.P., P. Fawcett, H. Nakai, R.L. McCaffrey, A. Ehrhardt, T.T.T. Pham, K. Pandey, H. Xu, S. Feuss, and T.A. Storm**, The host response to adenovirus, helper-dependent adenovirus, and adeno-associated virus in mouse liver. *Mol. Ther.*, 2008. 16(5): p. 931-941.
10. **Calcedo, R., L.H. Vandenberghe, G. Gao, J. Lin, and J.M. Wilson**, Worldwide epidemiology of neutralizing antibodies to adeno-associated viruses. *Journal of Infectious Diseases*, 2009. 199(3): p. 381-390.
11. **Park, T.G., J.H. Jeong, and S.W. Kim**, Current status of polymeric gene delivery systems. *Advanced Drug Delivery Reviews*, 2006. 58(4): p. 467-486.
12. **Al-Dosari, M.S. and X. Gao**, Nonviral gene delivery: principle, limitations, and recent progress. *The AAPS journal*, 2009. 11(4): p. 671-681.
13. **Boussif, O., F. Lezoualc'h, M.A. Zanta, M.D. Mergny, D. Scherman, B. Demeneix, and J.-P. Behr**, A Versatile Vector for Gene and Oligonucleotide Transfer into Cells in Culture and in vivo: Polyethylenimine. *Proceedings of the National Academy of Sciences of the United States of America*, 1995. 92(16): p. 7297-7301.
14. **Sonawane, N.D., F.C. Szoka, and A.S. Verkman**, Chloride Accumulation and Swelling in Endosomes Enhances DNA Transfer by Polyamine-DNA Polyplexes *J. Biol. Chem.* 2003 2003. 278(45): p. 44826-44831.

15. **Behr, J.-P.**, The proton sponge: a trick to enter cells the viruses did not exploit. *CHIMIA International Journal for Chemistry*, 1997. 51(1-2): p. 1-2.
16. **Akinc, A., M. Thomas, A.M. Klibanov, and R. Langer**, Exploring polyethylenimine-mediated DNA transfection and the proton sponge hypothesis. *The journal of gene medicine*, 2004. 7(5): p. 657-663.
17. **Chiu, S.-J., N.T. Ueno, and R.J. Lee**, Tumor-targeted gene delivery via anti-HER2 antibody (trastuzumab, Herceptin®) conjugated polyethylenimine. *Journal of controlled release*, 2004. 97(2): p. 357-369.
18. **Chan, P., M. Kurisawa, J.E. Chung, and Y.-Y. Yang**, Synthesis and characterization of chitosan-*g*-poly (ethylene glycol)-folate as a non-viral carrier for tumor-targeted gene delivery. *Biomaterials*, 2007. 28(3): p. 540-549.
19. **Pandey, S., P. Garg, K.T. Lim, J. Kim, Y.-H. Choung, Y.-J. Choi, P.-H. Choung, C.-S. Cho, and J.H. Chung**, The efficiency of membrane transport of vitamin B6 coupled to poly (ester amine) gene transporter and transfection in cancer cells. *Biomaterials*, 2013. 34(14): p. 3716-3728.
20. **Nie, Y., D. Schaffert, W. Rödl, M. Ogris, E. Wagner, and M. Günther**, Dual-targeted polyplexes: One step towards a synthetic virus for cancer gene therapy. *Journal of Controlled Release*, 2011. 152(1): p. 127-134.
21. **Kunath, K., T. Merdan, O. Hegener, H. Häberlein, and T. Kissel**, Integrin targeting using RGD-PEI conjugates for in vitro gene transfer. *The journal of gene medicine*, 2003. 5(7): p. 588-599.
22. **Low, P.S. and S.A. Kularatne**, Folate-targeted therapeutic and imaging agents for cancer. *Current opinion in chemical biology*, 2009. 13(3): p. 256-262.
23. **Lu, Y. and P.S. Low**, Folate-mediated delivery of macromolecular anticancer therapeutic agents. *Advanced drug delivery reviews*, 2012. 64: p. 342-352.
24. **Van Steenis, J., E. Van Maarseveen, F. Verbaan, R. Verrijck, D. Crommelin, G. Storm, and W. Hennink**, Preparation and characterization of folate-targeted pEG-coated pDMAEMA-based polyplexes. *Journal of controlled release*, 2003. 87(1): p. 167-176.
25. **Blessing, T., M. Kurs, R. Holzhauser, R. Kircheis, and E. Wagner**, Different strategies for formation of pegylated EGF-conjugated PEI/DNA complexes for targeted gene delivery. *Bioconjugate chemistry*, 2001. 12(4): p. 529-537.
26. **Mickler, F.M., L. Möckl, N. Ruthardt, M. Ogris, E. Wagner, and C. Bräuchle**, Tuning Nanoparticle Uptake: Live-Cell Imaging Reveals Two Distinct Endocytosis Mechanisms Mediated by Natural and Artificial EGFR Targeting Ligand. *Nano letters*, 2012. 12(7): p. 3417-3423.
27. **Huang, H., H. Yu, G. Tang, Q. Wang, and J. Li**, Low molecular weight polyethylenimine cross-linked by 2-hydroxypropyl- γ -cyclodextrin coupled to peptide targeting HER2 as a gene delivery vector. *Biomaterials*, 2010. 31(7): p. 1830-1838.
28. **Chen, C.-P., J.-s. Kim, E. Steenblock, D. Liu, and K.G. Rice**, Gene transfer with poly-melittin peptides. *Bioconjugate chemistry*, 2006. 17(4): p. 1057-1062.
29. **Meyer, M., A. Zintchenko, M. Ogris, and E. Wagner**, A dimethylmaleic acid-melittin-polylysine conjugate with reduced toxicity, pH-triggered endosomolytic activity and enhanced gene transfer potential. *The journal of gene medicine*, 2007. 9(9): p. 797-805.
30. **Boeckle, S., J. Fahrmeir, W. Roedl, M. Ogris, and E. Wagner**, Melittin analogs with high lytic activity at endosomal pH enhance transfection with purified targeted PEI polyplexes. *Journal of Controlled Release*, 2006. 112(2): p. 240-248.
31. **Moffatt, S., S. Wiehle, and R. Cristiano**, A multifunctional PEI-based cationic polyplex for enhanced systemic p53-mediated gene therapy. *Gene therapy*, 2006. 13(21): p. 1512-1523.

32. **Van der Aa, M., G. Koning, C. d'Oliveira, R. Oosting, K. Wilschut, W. Hennink, and D. Crommelin**, An NLS peptide covalently linked to linear DNA does not enhance transfection efficiency of cationic polymer based gene delivery systems. *The journal of gene medicine*, 2004. 7(2): p. 208-217.
33. **Davis, F.F.**, The origin of peganology. *Advanced drug delivery reviews*, 2002. 54(4): p. 457-458.
34. **Harris, J.M. and R.B. Chess**, Effect of pegylation on pharmaceuticals. *Nat Rev Drug Discov*, 2003. 2(3): p. 214-221.
35. **Roberts, M., M. Bentley, and J. Harris**, Chemistry for peptide and protein PEGylation. *Advanced drug delivery reviews*, 2012. 64: p. 116-127.
36. **Graham, M.L.**, Pegaspargase: a review of clinical studies. *Advanced drug delivery reviews*, 2003. 55(10): p. 1293-1302.
37. **Bailon, P., A. Palleroni, C.A. Schaffer, C.L. Spence, W.-J. Fung, J.E. Porter, G.K. Ehrlich, W. Pan, Z.-X. Xu, and M.W. Modi**, Rational design of a potent, long-lasting form of interferon: a 40 kDa branched polyethylene glycol-conjugated interferon α -2a for the treatment of hepatitis C. *Bioconjugate chemistry*, 2001. 12(2): p. 195-202.
38. **Levy, Y., M.S. Hershfield, C. Fernandez-Mejia, S.H. Polmar, D. Scudiery, M. Berger, and R.U. Sorensen**, Adenosine deaminase deficiency with late onset of recurrent infections: response to treatment with polyethylene glycol-modified adenosine deaminase. *The Journal of pediatrics*, 1988. 113(2): p. 312-317.
39. **Laga, R., Č. Koňák, V. Šubr, and K. Ulbrich**, New, Hydrophilic, HPMa-Based Polymers for Bioresponsive Shielding of Gene-Delivery Vectors. *Macromolecular Chemistry and Physics*, 2009. 210(13-14): p. 1138-1148.
40. **Jäger, E., A. Jäger, T. Etrych, F.C. Giacomelli, P. Chytil, A. Jigounov, J.-L. Putaux, B. Říhová, K. Ulbrich, and P. Štěpánek**, Self-assembly of biodegradable copolyester and reactive HPMa-based polymers into nanoparticles as an alternative stealth drug delivery system. *Soft Matter*, 2012. 8(37): p. 9563-9575.
41. **Šubr, V., C. Konák, R. Laga, and K. Ulbrich**, Coating of DNA/poly (L-lysine) complexes by covalent attachment of poly [N-(2-hydroxypropyl) methacrylamide]. *Biomacromolecules*, 2006. 7(1): p. 122-130.
42. **Maruyama, K., S. Okuizumi, O. Ishida, H. Yamauchi, H. Kikuchi, and M. Iwatsuru**, Phosphatidyl polyglycerols prolong liposome circulation in vivo. *International journal of pharmaceuticals*, 1994. 111(1): p. 103-107.
43. **Weber, T., Y. Gies, and A. Terfort**, Bacteria-Repulsive Polyglycerol Surfaces by Grafting Polymerization onto Aminopropylated Surfaces. *Langmuir*, 2012. 28(45): p. 15916-15921.
44. **Sheng, Y., C. Liu, Y. Yuan, X. Tao, F. Yang, X. Shan, H. Zhou, and F. Xu**, Long-circulating polymeric nanoparticles bearing a combinatorial coating of PEG and water-soluble chitosan. *Biomaterials*, 2009. 30(12): p. 2340-2348.
45. **Lemarchand, C., R. Gref, C. Passirani, E. Garcion, B. Petri, R. Müller, D. Costantini, and P. Couvreur**, Influence of polysaccharide coating on the interactions of nanoparticles with biological systems. *Biomaterials*, 2006. 27(1): p. 108-118.
46. **He, M., Z. Zhao, L. Yin, C. Tang, and C. Yin**, Hyaluronic acid coated poly (butyl cyanoacrylate) nanoparticles as anticancer drug carriers. *International journal of pharmaceuticals*, 2009. 373(1): p. 165-173.
47. **Luxenhofer, R., Y. Han, A. Schulz, J. Tong, Z. He, A.V. Kabanov, and R. Jordan**, Poly (2-oxazoline)s as Polymer Therapeutics. *Macromolecular rapid communications*, 2012. 33(19): p. 1613-1631.
48. **Romberg, B., F.M. Flesch, W.E. Hennink, and G. Storm**, Enzyme-induced shedding of a poly (amino acid)-coating triggers contents release from dioleoyl

- phosphatidylethanolamine liposomes. *International journal of pharmaceutics*, 2008. 355(1): p. 108-113.
49. **Tanisaka, H., S. Kizaka-Kondoh, A. Makino, S. Tanaka, M. Hiraoka, and S. Kimura**, Near-infrared fluorescent labeled peptosome for application to cancer imaging. *Bioconjugate chemistry*, 2007. 19(1): p. 109-117.
 50. **Wu, J., T. Akaike, K. Hayashida, T. Okamoto, A. Okuyama, and H. Maeda**, Enhanced vascular permeability in solid tumor involving peroxynitrite and matrix metalloproteinases. *Cancer Science*, 2001. 92(4): p. 439-451.
 51. **Wu, J., T. Akaike, and H. Maeda**, Modulation of enhanced vascular permeability in tumors by a bradykinin antagonist, a cyclooxygenase inhibitor, and a nitric oxide scavenger. *Cancer research*, 1998. 58(1): p. 159-165.
 52. **Iyer, A.K., G. Khaled, J. Fang, and H. Maeda**, Exploiting the enhanced permeability and retention effect for tumor targeting. *Drug Discovery Today*, 2006. 11(17-18): p. 812-818.
 53. **Maeda, H., J. Wu, T. Sawa, Y. Matsumura, and K. Hori**, Tumor vascular permeability and the EPR effect in macromolecular therapeutics: a review. *Journal of Controlled Release*, 2000. 65(1): p. 271-284.
 54. **Torchilin, V.**, Tumor delivery of macromolecular drugs based on the EPR effect. *Advanced drug delivery reviews*, 2011. 63(3): p. 131-135.
 55. **Fahrmeir, J., M. Gunther, N. Tietze, E. Wagner, and M. Ogris**, Electrophoretic purification of tumor-targeted polyethylenimine-based polyplexes reduces toxic side effects in vivo. *Journal of Controlled Release*, 2007. 122(3): p. 236-245.
 56. **Wightman, L., R. Kircheis, V. Rössler, S. Carotta, R. Ruzicka, M. Kurs, and E. Wagner**, Different behavior of branched and linear polyethylenimine for gene delivery in vitro and in vivo. *The journal of gene medicine*, 2001. 3(4): p. 362-372.
 57. **Coll, J.-L., P. Chollet, E. Brambilla, D. Desplanques, J.-P. Behr, and M. Favrot**, In vivo delivery to tumors of DNA complexed with linear polyethylenimine. *Human gene therapy*, 1999. 10(10): p. 1659-1666.
 58. **Hatakeyama, H., H. Akita, K. Kogure, M. Oishi, Y. Nagasaki, Y. Kihira, M. Ueno, H. Kobayashi, H. Kikuchi, and H. Harashima**, Development of a novel systemic gene delivery system for cancer therapy with a tumor-specific cleavable PEG-lipid. *Gene Therapy*, 2006. 14(1): p. 68-77.
 59. **Ishida, T., X. Wang, T. Shimizu, K. Nawata, and H. Kiwada**, PEGylated liposomes elicit an anti-PEG IgM response in a T cell-independent manner. *Journal of Controlled Release*, 2007. 122(3): p. 349-355.
 60. **Ishida, T., M. Ichihara, X. Wang, K. Yamamoto, J. Kimura, E. Majima, and H. Kiwada**, Injection of PEGylated liposomes in rats elicits PEG-specific IgM, which is responsible for rapid elimination of a second dose of PEGylated liposomes. *Journal of controlled release*, 2006. 112(1): p. 15-25.
 61. **Dams, E.T.M., P. Laverman, W.J.G. Oyen, G. Storm, G.L. Scherphof, J.W.M. van der Meer, F.H.M. Corstens, and O.C. Boerman**, Accelerated blood clearance and altered biodistribution of repeated injections of sterically stabilized liposomes. *Journal of Pharmacology and Experimental Therapeutics*, 2000. 292(3): p. 1071-1079.
 62. **Chan, C.L., R.N. Majzoub, R.S. Shirazi, K.K. Ewert, Y.J. Chen, K.S. Liang, and C.R. Safinya**, Endosomal escape and transfection efficiency of PEGylated cationic liposome-DNA complexes prepared with an acid-labile PEG-lipid. *Biomaterials*, 2012. 33(19): p. 4928-4935.
 63. **Nie, Y., M. Günther, Z. Gu, and E. Wagner**, Pyridylhydrazone-based PEGylation for pH-reversible lipopolyplex shielding. *Biomaterials*, 2011. 32(3): p. 858-869.

64. **Kim, T.H., Y. Chen, C.W. Mount, W.R. Gombotz, X. Li, and S.H. Pun**, Evaluation of temperature-sensitive, indocyanine green-encapsulating micelles for noninvasive near-infrared tumor imaging. *Pharmaceutical research*, 2010. 27(9): p. 1900-1913.
65. **He, Y., G. Cheng, L. Xie, Y. Nie, B. He, and Z. Gu**, Polyethyleneimine/DNA polyplexes with reduction-sensitive hyaluronic acid derivatives shielding for targeted gene delivery. *Biomaterials*, 2012. 34(4): p. 1235-1245.
66. **Meyer, M., C. Dohmen, A. Philipp, D. Kiener, G. Maiwald, C. Scheu, M. Ogris, and E. Wagner**, Synthesis and Biological Evaluation of a Bioresponsive and Endosomolytic siRNA–Polymer Conjugate. *Molecular Pharmaceutics*, 2009. 6(3): p. 752-762.
67. **Zhu, C., M. Zheng, F. Meng, F.M. Mickler, N. Ruthardt, X. Zhu, and Z. Zhong**, Reversibly shielded DNA polyplexes based on bioreducible PDMAEMA-SS-PEG-SS-PDMAEMA triblock copolymers mediate markedly enhanced nonviral gene transfection. *Biomacromolecules*, 2012. 13(3): p. 769-778.
68. **Gao, W., R. Langer, and O.C. Farokhzad**, Poly (ethylene glycol) with Observable Shedding. *Angewandte Chemie International Edition*, 2010. 49(37): p. 6567-6571.
69. **Gao, Z.G., H.D. Fain, and N. Rapoport**, Controlled and targeted tumor chemotherapy by micellar-encapsulated drug and ultrasound. *Journal of controlled release*, 2005. 102(1): p. 203-222.
70. **Romberg, B., W. Hennink, and G. Storm**, Sheddable Coatings for Long-Circulating Nanoparticles. *Pharmaceutical Research*, 2008. 25(1): p. 55-71.
71. **Walker, G.F., C. Fella, J. Pelisek, J. Fahrmeir, S. Boeckle, M. Ogris, and E. Wagner**, Toward Synthetic Viruses: Endosomal pH-Triggered Deshielding of Targeted Polyplexes Greatly Enhances Gene Transfer in vitro and in vivo. *Mol Ther*, 2005. 11(3): p. 418-425.
72. **von Maltzahn, G., T.J. Harris, J.H. Park, D.H. Min, A.J. Schmidt, M.J. Sailor, and S.N. Bhatia**, Nanoparticle self-assembly gated by logical proteolytic triggers. *Journal of the American Chemical Society*, 2007. 129(19): p. 6064.
73. **Harris, T.J., G. von Maltzahn, M.E. Lord, J.H. Park, A. Agrawal, D.H. Min, M.J. Sailor, and S.N. Bhatia**, Protease-Triggered Unveiling of Bioactive Nanoparticles. *small*, 2008. 4(9): p. 1307-1312.
74. **Mok, H., K.H. Bae, C.H. Ahn, and T.G. Park**, PEGylated and MMP-2 specifically dePEGylated quantum dots: comparative evaluation of cellular uptake. *Langmuir*, 2008. 25(3): p. 1645-1650.
75. **Singh, N., A. Karambelkar, L. Gu, K. Lin, J.S. Miller, C.S. Chen, M.J. Sailor, and S.N. Bhatia**, Bioresponsive Mesoporous Silica Nanoparticles for Triggered Drug Release. *Journal of the American Chemical Society*, 2011. 133(49): p. 19582-19585.
76. **Hatakeyama, H., H. Akita, and H. Harashima**, A multifunctional envelope type nano device (MEND) for gene delivery to tumours based on the EPR effect: A strategy for overcoming the PEG dilemma. *Advanced Drug Delivery Reviews*, 2011. 63(3): p. 152-160.
77. **Yingyuad, P., M. Mével, C. Prata, S. Furegati, C. Kontogiorgis, M. Thanou, and A.D. Miller**, Enzyme-Triggered PEGylated pDNA-Nanoparticles for Controlled Release of pDNA in Tumours. *Bioconjugate Chemistry*, 2013. 24(3): p. 343-362.
78. **Liu, Q., R.T. Li, H.Q. Qian, M. Yang, Z.S. Zhu, W. Wu, X.P. Qian, L.X. Yu, X.Q. Jiang, and B.R. Liu**, Gelatinase-stimuli strategy enhances the tumor delivery and therapeutic efficacy of docetaxel-loaded poly (ethylene glycol)-poly (ϵ -caprolactone) nanoparticles. *International journal of nanomedicine*, 2012. 7: p. 281.
79. **Zhang, J.X., S. Zalipsky, N. Mullah, M. Pechar, and T.M. Allen**, Pharmacological attributes of dioleoylphosphatidylethanolamine/cholesterylhemisuccinate liposomes

- containing different types of cleavable lipopolymers. *Pharmacological research*, 2004. 49(2): p. 185-198.
80. **Xu, H., Y. Deng, D. Chen, W. Hong, Y. Lu, and X. Dong**, Esterase-catalyzed dePEGylation of pH-sensitive vesicles modified with cleavable PEG-lipid derivatives. *Journal of Controlled Release*, 2008. 130(3): p. 238-245.
 81. **Xu, H., K.Q. Wang, Y.H. Deng, and D.W. Chen**, Effects of cleavable PEG-cholesterol derivatives on the accelerated blood clearance of PEGylated liposomes. *Biomaterials*, 2010. 31(17): p. 4757-4763.
 82. **Wang, S., H. Xu, J. Xu, Y. Zhang, Y. Liu, Y. Deng, and D. Chen**, Sustained liver targeting and improved antiproliferative effect of doxorubicin liposomes modified with galactosylated lipid and PEG-Lipid. *AAPS PharmSciTech*, 2010. 11(2): p. 870-877.
 83. **Chen, D., W. Liu, Y. Shen, H. Mu, Y. Zhang, R. Liang, A. Wang, K. Sun, and F. Fu**, Effects of a novel pH-sensitive liposome with cleavable esterase-catalyzed and pH-responsive double smart mPEG lipid derivative on ABC phenomenon. *International journal of nanomedicine*, 2011. 6: p. 2053.
 84. **Grosse, S.M., A.D. Tagalakakis, M.F.M. Mustapa, M. Elbs, Q.H. Meng, A. Mohammadi, A.B. Tabor, H.C. Hailes, and S.L. Hart**, Tumor-specific gene transfer with receptor-mediated nanocomplexes modified by polyethylene glycol shielding and endosomally cleavable lipid and peptide linkers. *The FASEB Journal*, 2010. 24(7): p. 2301-2313.
 85. **Zhao, Y., C. Wang, L. Wang, Q. Yang, W. Tang, Z. She, and Y. Deng**, A frustrating problem: Accelerated blood clearance of PEGylated solid lipid nanoparticles following subcutaneous injection in rats. *European Journal of Pharmaceutics and Biopharmaceutics*, 2012. 81(3): p. 506-513.
 86. **Howard, M.D., X. Lu, J.J. Rinehart, T. Dziubla, and M. Jay**, Carboxylesterase-Triggered Hydrolysis of Nanoparticle PEGylating Agents. *Langmuir*, 2012. 28(33): p. 12030-12037.
 87. **Nagase, H. and J.F. Woessner Jr**, Matrix metalloproteinases. *Journal of Biological Chemistry*, 1999. 274(31): p. 21491-21494.
 88. **Egeblad, M. and Z. Werb**, New functions for the matrix metalloproteinases in cancer progression. *Nature Reviews Cancer*, 2002. 2(3): p. 161-174.
 89. **Sternlicht, M.D. and Z. Werb**, How matrix metalloproteinases regulate cell behavior. *Annual review of cell and developmental biology*, 2001. 17: p. 463.
 90. **Ishihara, T., M. Takeda, H. Sakamoto, A. Kimoto, C. Kobayashi, N. Takasaki, K. Yuki, K.-i. Tanaka, M. Takenaga, and R. Igarashi**, Accelerated blood clearance phenomenon upon repeated injection of PEG-modified PLA-nanoparticles. *Pharmaceutical research*, 2009. 26(10): p. 2270-2279.
 91. **Yang, H.M., C.W. Park, T. Ahn, B. Jung, B.K. Seo, J.H. Park, and J.D. Kim**, A direct surface modification of iron oxide nanoparticles with various poly (amino acid)s for use as magnetic resonance probes. *Journal of Colloid and Interface Science*, 2012. 391: p. 158-167.
 92. **Park, S.-I., E.-O. Lee, J.W. Kim, Y.J. Kim, S.H. Han, and J.-D. Kim**, Polymer-hybridized liposomes anchored with alkyl grafted poly (asparagine). *Journal of colloid and interface science*, 2011. 364(1): p. 31-38.
 93. **Romberg, B., J.M. Metselaar, L. Baranyi, C.J. Snel, R. Bünger, W.E. Hennink, J. Szebeni, and G. Storm**, Poly (amino acid)s: promising enzymatically degradable stealth coatings for liposomes. *International journal of pharmaceutics*, 2007. 331(2): p. 186-189.
 94. **Makino, A., S. Kizaka-Kondoh, R. Yamahara, I. Hara, T. Kanzaki, E. Ozeki, M. Hiraoka, and S. Kimura**, Near-infrared fluorescence tumor imaging using

- nanocarrier composed of poly (l-lactic acid)-*block*-poly (sarcosine) amphiphilic polydepsipeptide. *Biomaterials*, 2009. 30(28): p. 5156-5160.
95. **Ferguson, E.L. and R. Duncan**, Dextrin– Phospholipase A2: Synthesis and Evaluation as a Bioresponsive Anticancer Conjugate. *Biomacromolecules*, 2009. 10(6): p. 1358-1364.
 96. **Hardwicke, J., R. Moseley, P. Stephens, K. Harding, R. Duncan, and D.W. Thomas**, Bioresponsive Dextrin– rhEGF Conjugates: In Vitro Evaluation in Models Relevant to Its Proposed Use as a Treatment for Chronic Wounds. *Molecular Pharmaceutics*, 2010. 7(3): p. 699-707.
 97. **Hardwicke, J.T., J. Hart, A. Bell, R. Duncan, D.W. Thomas, and R. Moseley**, The effect of dextrin–rhEGF on the healing of full-thickness, excisional wounds in the (db/db) diabetic mouse. *Journal of Controlled Release*, 2011. 152(3): p. 411-417.
 98. **Ferguson, E.L., A.M. Alshame, and D.W. Thomas**, Evaluation of hyaluronic acid–protein conjugates for polymer masked–unmasked protein therapy. *International journal of pharmaceutics*, 2010. 402(1): p. 95-102.
 99. **Bernardos, A., L. Mondragón, E. Aznar, M.D. Marcos, R.n. Martínez-Máñez, F.I. Sancenón, J. Soto, J.M. Barat, E. Pérez-Payá, and C. Guillem**, Enzyme-responsive intracellular controlled release using nanometric silica mesoporous supports capped with “saccharides”. *Acs Nano*, 2010. 4(11): p. 6353-6368.
 100. **Lau, K.H.A., C. Ren, T.S. Sileika, S.H. Park, I. Szleifer, and P.B. Messersmith**, Surface-Grafted Polysarcosine as a Peptoid Antifouling Polymer Brush. *Langmuir*, 2012. 28(46): p. 16099-16107.
 101. **Hey, T., H. Knoller, and P. Vorstheim**, Half-Life Extension through HESylation®. *Therapeutic Proteins: Strategies to Modulate Their Plasma Half-lives*, 2012.
 102. **Treib, J., J.-F. Baron, M. Grauer, and R. Strauss**, An international view of hydroxyethyl starches. *Intensive care medicine*, 1999. 25(3): p. 258-268.
 103. **Jungheinrich, C. and T.A. Neff**, Pharmacokinetics of hydroxyethyl starch. *Clinical pharmacokinetics*, 2005. 44(7): p. 681-699.
 104. **Lemarchand, C., R. Gref, and P. Couvreur**, Polysaccharide-decorated nanoparticles. *European journal of pharmaceutics and biopharmaceutics*, 2004. 58(2): p. 327-341.
 105. **Besheer, A., G. Hause, J. Kressler, and K. Mader**, Hydrophobically Modified Hydroxyethyl Starch: Synthesis, Characterization and Aqueous Self-Assembly into Nano-Sized Polymeric Micelles and Vesicles. *Biomacromolecules*, 2007. 8(6): p. 2045-2045.
 106. **Orlando, M.**, Modification of proteins and low molecular weight substances with hydroxyethyl starch (HES). in *Institut Biologie, Chemie und Geowissenschaften*. 2003, Justus Liebig Universität Giessen: Giessen.
 107. **Kontermann, R.E.**, Strategies to extend plasma half-lives of recombinant antibodies. *BioDrugs*, 2009. 23(2): p. 93-109.
 108. **Besheer, A., J.r. Vogel, D. Glanz, J.r. Kressler, T. Groth, and K. Mäder**, Characterization of PLGA Nanospheres Stabilized with Amphiphilic Polymers: Hydrophobically Modified Hydroxyethyl Starch vs Pluronics. *Molecular Pharmaceutics*, 2009. 6(2): p. 407-415.
 109. **Yoshida, M. and T. Kishikawa**, A Study of Hydroxyethyl Starch. Part II. Degradation-Sites of Hydroxyethyl Starch by Pig Pancreas alpha-Amylase. *Starch - Stärke*, 1984. 36(5): p. 167-169.
 110. **Yoshida, M., T. Yamashita, J. Matsuo, and T. Kishikawa**, Enzymic Degradation of Hydroxyethyl Starch. Part I. Influence of the Distribution of Hydroxyethyl Groups on the Enzymic Degradation of Hydroxyethyl Starch. *Starch - Stärke*, 1973. 25(11): p. 373-376.

111. **Inaji, H., H. Koyama, M. Higashiyama, S. Noguchi, H. Yamamoto, O. Ishikawa, K. Omichi, T. Iwanaga, and A. Wada**, Immunohistochemical, ultrastructural and biochemical studies of an amylase-producing breast carcinoma. *Virchows Archiv*, 1991. 419(1): p. 29-33.
112. **Weitzel, J., P. Pooler, R. Mohammed, M. Levitt, and J. Eckfeldt**, A unique case of breast carcinoma producing pancreatic-type isoamylase. *Gastroenterology*, 1988. 94(2): p. 519.
113. **Lenler-Petersen, P., A. Grove, A. Brock, and R. Jelnes**, Alpha-amylase in resectable lung cancer. *European Respiratory Journal*, 1994. 7(5): p. 941-945.
114. **Sandiford, J. and S. Chiknas**, Hyperamylasemia and ovarian carcinoma. *Clinical chemistry*, 1979. 25(6): p. 948-950.
115. **Shimamura, J., L. Fridhandler, and J.E. Berk**, Nonpancreatic-type hyperamylasemia associated with pancreatic cancer. *Digestive Diseases and Sciences*, 1976. 21(4): p. 340-345.
116. **Caldwell, M.L. and J.-f.T. Kung**, A Study of the Influence of a Number of Factors upon the Stability and upon the Activity of Pancreatic Amylase¹. *Journal of the American Chemical Society*, 1953. 75(13): p. 3132-3135.
117. **Speckmann, H.-D., B. Kottwitz, K.-H. Maurer, and C. Nitsch**, Detergents containing amylase and protease. 2002, Google Patents.
118. **Agreda-Vásquez, G.P., I. Espinosa-Poblano, S.A. Sánchez-Guerrero, E. Crespo-Solís, S. Cabrera-Vásquez, J. López-Salmorán, J. Barajas, P. Peñaloza-Ramírez, N. Tirado-Cárdenas, and A. Velázquez**, Starch and albumin mixture as replacement fluid in therapeutic plasma exchange is safe and effective. *Journal of clinical apheresis*, 2008. 23(5): p. 163-167.
119. **Warren, B.B. and M.E. Durieux**, Hydroxyethyl starch: safe or not? *Anesthesia Analgesia*, 1997. 84(1): p. 206-212.
120. **Wilkes, M.M., R.J. Navickis, and W.J. Sibbald**, Albumin versus hydroxyethyl starch in cardiopulmonary bypass surgery: a meta-analysis of postoperative bleeding. *The Annals of thoracic surgery*, 2001. 72(2): p. 527-533.
121. **Navickis, R.J., G.R. Haynes, and M.M. Wilkes**, Effect of hydroxyethyl starch on bleeding after cardiopulmonary bypass: a meta-analysis of randomized trials. *The Journal of Thoracic and Cardiovascular Surgery*, 2012. 144(1): p. 223-230.
122. **Treib, J., J.F. Baron, M.T. Grauer, and R.G. Strauss**, An international view of hydroxyethyl starches. *Intensive Care Medicine*, 1999. 25(3): p. 258-268.
123. **Laxenaire, M., C. Charpentier, and L. Feldman**, Anaphylactoid reactions to colloid plasma substitutes: incidence, risk factors, mechanisms. A French multicenter prospective study. in *Annales francaises d'anesthesie et de reanimation*. 1994.
124. **Greindl, A., C. Kessler, B. Breuer, U. Haberl, A. Rybka, M. Emgenbroich, A.J. Pötgens, and H.-G. Frank**, AGEM400 (HES), a novel erythropoietin mimetic peptide conjugated to hydroxyethyl starch with excellent in vitro efficacy. *Open Hematology Journal*, 2010. 4: p. 1-14.
125. **Luo, Q., P. Wang, Y. Miao, H. He, and X. Tang**, A novel 5-fluorouracil prodrug using hydroxyethyl starch as a macromolecular carrier for sustained release. *Carbohydrate Polymers*, 2011. 87(4): p. 2642-2647.
126. **Besheer, A., H. Caysa, H. Metz, T. Mueller, J. Kressler, and K. Mäder**, Benchtop-MRI for in vivo imaging using a macromolecular contrast agent based on hydroxyethyl starch (HES). *International Journal of Pharmaceutics*, 2011. 417(1-2): p. 196-203.
127. **Harling, S., A. Schwoerer, K. Scheibe, R. Daniels, and H. Menzel**, A new hydrogel drug delivery system based on Hydroxyethylstarch derivatives. *Journal of microencapsulation*, 2010. 27(5): p. 400-408.

128. **Wöhl-Bruhn, S., A. Bertz, S. Harling, H. Menzel, and H. Bunjes,** Hydroxyethylstarch-based polymers for the controlled release of biomacromolecules from hydrogel microspheres. *European Journal of Pharmaceutics and Biopharmaceutics*, 2012. 81(3): p. 573-581.
129. **T'Joel, V., L. De Grande, H. Declercq, and M. Cornelissen.** HESC cryopreservation: use of dimethylsulfoxide and hydroxyethylstarch in an adapted protocol for efficient hESC banking. in 17th Annual ISCT meeting (ISCT-2011). 2011.
130. **Stoll, C., J.L. Holovati, J.P. Acker, and W.F. Wolkers,** Synergistic effects of liposomes, trehalose, and hydroxyethyl starch for cryopreservation of human erythrocytes. *Biotechnology progress*, 2012. 28(2): p. 364-371.
131. **Baier, G., D. Baumann, J.r.M. Siebert, A. Musyanovych, V. Mailänder, and K. Landfester,** Suppressing unspecific cell uptake for targeted delivery using hydroxyethyl starch nanocapsules. *Biomacromolecules*, 2012. 13(9): p. 2704-2715.

II Controlled shielding and deshielding of gene delivery polyplexes using hydroxyethyl starch and alpha-amylase

This chapter has been published in the *Journal of Controlled Release*:

Noga M*, Edinger D, Rödl W, Wagner E, Winter G, Besheer A**. Controlled shielding and deshielding of gene delivery polyplexes using hydroxyethyl starch (HES) and alpha-amylase. *Journal of Controlled Release* 2012;159(1):92-103.

* First author

** Corresponding author

The following study would not have been possible without our engaged cooperation partners Prof. Dr. Ernst Wagner and his group members Daniel Edinger and Wolfgang Rödl. All cell culture experiments, namely studies of the luciferase reporter gene expression, the metabolic activity of transfected cells, as well as flow cytometry experiments were performed together with Daniel Edinger under his guidance. Wolfgang Rödl provided purified LPEI material.

Abstract

The non-viral delivery of nucleic acids faces many extracellular and intracellular hurdles on the way from injection site to the site of action. Among these, aggregation in the blood stream and rapid elimination by the mononuclear phagocytic system (MPS) represent strong obstacles towards successful development of these promising therapeutic modalities. Even the state-of-the-art solutions using PEGylation show low transfection efficiency due to limited uptake and hindered endosomal escape. Engineering the carriers with sheddable coats reduces aggregation and phagocytosis due to the effective shielding, while the controlled deshielding at the desired site of action enhances the uptake and intracellular release. This work reports for the first time the use of hydroxyethyl starch (HES) for the controlled shielding/deshielding of polyplexes. HES, with different molar masses, was grafted to polyethylenimine (PEI) and characterized using ^1H NMR, colorimetric copper-assay, and SEC. HES-PEI conjugates were used to generate polyplexes with the luciferase-expressing plasmid DNA pCMVluc, and were characterized by DLS and zeta potential measurements. Deshielding was tested *in vitro* by zeta potential measurements and, erythrocyte aggregation assay upon addition of α -amylase (AA) to the HES-decorated particles. The addition of AA led to gradual increase in the zeta potential of the nanoparticles over 0.5 to 1 h and to a higher aggregation tendency for erythrocytes due to the degradation of the HES-coat and exposure of the polyplexes' positive charge. *In vitro* transfection experiments were conducted in 2 cell-lines \pm AA in the culture medium. The amylase-treated HES-decorated complexes showed up to 2 orders of magnitude higher transfection levels compared to the untreated HES-shielded particles, while AA had no effect on the transfection of PEG-coated or uncoated polyplexes. Finally, flow cytometry showed that the addition of AA increased the amount of delivered DNA per cell for HES-shielded polyplexes. This study shows that decorating nanoparticles with HES can be a promising tool for the controlled shielding/deshielding of polyplexes.

Keywords

Hydroxyethyl starch (HES), shielding and deshielding, bioreversible coats, nucleic acid delivery, polyplexes

1 Introduction

Non-viral gene delivery to specific tissues and organs is a promising treatment modality for many diseases that are currently difficult to cure, most notably cancer. Since the seminal work of Theodore Friedmann in 1972 [1], the development of safe and efficient gene delivery systems has been the focus of many research groups, particularly the lipid- and polymer-mediated nucleic acid transfection. They employ cationic lipids or polycations to condense the DNA into lipoplexes or polyplexes, respectively, and overcome many extracellular and intracellular hurdles on the way from the application site to the desired site of action. Among these hurdles, the nucleic acid complexes are prone to *in vivo* aggregation and rapid removal from the systemic circulation. This is because of the non-specific binding of cationic complexes to the anionic plasma proteins and erythrocytes, leading to aggregation and accumulation in the lungs. Additionally, they are rapidly eliminated by the mononuclear phagocytic system (MPS), and thus have a short systemic half-life. This is detrimental to targeted-tumor-therapy, since sufficiently long residence time in the bloodstream is indispensable to allow passive gene targeting through the leaky vasculature of tumors or inflammatory foci by the enhanced permeability and retention (EPR) effect [2, 3].

PEGylation of nanomedicines is the state-of-the-art technology to overcome the aforementioned problems. Incorporating the hydrophilic polymer poly(ethylene glycol) (PEG) onto the surface of polyplexes [4, 5], and lipoplexes [6, 7] prevents aggregation by masking the surface charges and decreasing the non-specific electrostatic interactions. Additionally, PEGylation prolongs the *in vivo* circulation time [8] - an effect coined “stealth” effect - by a mechanism not yet fully known [9], however the effect might be due to 1) reducing protein adsorption and opsonization, 2) selective adsorption of dysopsonins [10, 11] or 3) due to influencing the rates of adsorption of different opsonization/desopsonization proteins [12].

However, the PEG coat reduces transfection efficiency *in vitro* and *in vivo*, in what is known as the “PEG-dilemma” [13]. This is because it may 1) reduce the cellular interaction and uptake, 2) interfere with endosomal escape and 3) interfere with DNA release from the complexes [13, 14]. Different groups have addressed these problems by developing sheddable PEG coatings, which shield the DNA complexes in the bloodstream and are shed down gradually or at the target site (deshielding). For instance, PEG-lipids can be spontaneously extracted out of lipoplexes for DNA delivery, and the rate of extraction can be controlled by tuning the hydrophobicity of the lipid part [15]. Additionally, the linker between PEG and the delivery vector can be a stimuli-sensitive bond, which cleaves upon a drop of the pH [16-19],

presence in a reductive environment [20], or by the action of proteases on biodegradable peptide linkers [21, 22].

Contrary to PEG, shields composed of biodegradable polymers can get deshielded by degradation of the protective coat itself. There are however very few reports on this approach [23, 24]. For instance, Romberg *et al.* used a protease-cleavable poly(hydroxyethyl-L-asparagine) to impart stealth properties to liposomes [25, 26]. The latter polymer is then deshielded extra- or intracellularly by the action of proteases. Duncan's group used dextrin for shielding and deshielding of proteins rather than nanoparticles, in what they dubbed as "polymer masked-unmasked protein therapy" (PMUPT) [27-29]. For instance, they coupled dextrin to rhEGF to stabilize it in wound environment, and slowly activate it by the action of amylase on dextrin [29]. To the best of our knowledge, no similar approach was tested with polyplexes. In this work, we describe the use of a biodegradable polysaccharide, namely hydroxyethyl starch (HES), for the controlled shielding/deshielding of polyplexes for nucleic acid delivery.

HES is a semisynthetic biodegradable polymer widely used as plasma volume expander [30-32]. It is degraded *in vivo* by serum α -amylase (AA) [33, 34]. Contrary to the above mentioned biodegradable polymers, it offers the advantage of controllable biodegradation, where the rate and extent of degradation can be regulated by fine-tuning the molar mass and degree of hydroxyethylation. Additionally, it has a high water solubility, low hypersensitivity [35], and protein repellent characteristics [36]. These favourable properties raised interest in HES as a biomedical material, where it was tested as a macromolecular MRI contrast agent [37], and as a substitute for PEG in the half-life extension of peptides and proteins [38, 39].

In this paper, the biodegradation of HES is integrated in the design of DNA complexes to serve a smart function, namely, the controlled shielding/deshielding of DNA complexes. To this end, HES with different molar masses was coupled to polyethylenimine (PEI) by Schiff's base formation and reductive amination [40]. The HES-PEI copolymer was characterized by ^1H NMR, colorimetric copper assay, and SEC. Biophysical characterization of the polyplexes included particle size and zeta potential measurements. Deshielding was tested *in vitro* by zeta potential measurements and erythrocyte aggregation assay upon addition of AA. The effect of shielding/deshielding on *in vitro* gene transfection was examined using Neuro2A as well as HUH7 cells in cell culture medium \pm AA. Unmodified PEI polyplexes (unshielded) and PEG-PEI polyplexes (shielded) were used as controls in most of the experiments.

2 Experimental Section

2.1 Materials

Hydroxyethyl starch (HES) with an average molar mass (M_w) of 70 kDa and a molar substitution of 0.5 (MS; the mean number of hydroxyethyl groups per glucose unit) was kindly provided by Serumwerk Bernburg, Germany. Sodium cyanoborohydride (NaBH_3CN) was purchased from Merck Schuchardt OHG (Hohenbrunn, Germany). Linear polyethylenimine with an average molar mass of 22 kDa (PEI22) and the PEI22 – PEG20 conjugate (PEG20: polyethylene glycol with the average molecular weight of 20 kDa) were synthesized as described in [41]. α -amylase (AA) from porcine pancreas (with 30 units amylase per mg), Triton-X 100, and citrated human plasma were bought from Sigma-Aldrich (Steinheim, Germany). Blood from C57BL/6 mice was obtained from the Institute of Pharmacology, Department of Pharmacy, Munich. Plasmid pCMVluc [42] was prepared by PlasmidFactory, Bielefeld, Germany. Phadebas® Amylase Test was purchased from Magle AB, Lund, Sweden. Label IT® CyTM 5 Labeling kit was obtained from Mirus Bio Corporation (Madison, USA). Other solvents and chemicals were reagent grade and were used as received.

2.2 Methods

2.2.1 Acid hydrolysis of HES70

The acid hydrolysis was performed according to the starch degradation process of Nitsch [43] with some modifications. Briefly, 5 g HES70 were dissolved in 100 mL HCl (0.05 M) and heated up to 100°C on oil bath (with reflux condensation). The reaction was stopped after 2 h by the addition of 1 M sodium hydroxide (NaOH) solution, and adjusting the pH to neutrality. The resulting solution was dialyzed against highly purified water for 48 hours (Cellu Sep T1, nominal MWCO 3500 Da, Membrane Filtration Products Inc, Seguin, TX, USA). The product was then lyophilized and stored in a desiccator at room temperature.

2.2.2 Determination of the molar mass of acid-hydrolyzed HES using asymmetric flow field flow fractionation (AF4)

The AF4 instrument used for the characterization of the hydrolyzed HES products consisted of an Eclipse 2 separation system (Wyatt Technology Corp., Santa Barbara, CA) that was coupled to an 18 angle multi-angle light scattering (MALS) detector (DAWN EOS MALS,

Wyatt Technology Corp.) with a laser of wavelength 690 nm. The Agilent HPLC system 1100 Series was used (Agilent Technologies, Palo Alto, CA). It was equipped with a degasser, isopump, autosampler, and a refractive index (RI) detector. Samples were prepared at a sample concentration of 5 mg/mL in filtered 50 mM NaCl solution (0.1 μ m cellulose nitrate filter, Whatman GmbH Dassel, Germany) with 0.02 % w/v NaN_3 preservative. 100 μ L sample volume was injected into the standard separation channel system (25 cm), with channel thickness of 350 μ m and equipped with a 5 kDa cutoff regenerated cellulose ultrafiltration membrane (Wyatt Technology Europe, Dernbach, Germany). The separation was performed with an applied channel flow of 2 mL/min coupled to a linearly decreasing cross flow gradient (from 2 mL/min to 0 mL/min over 30 minutes) [44]. Molecular weight was calculated using ASTRA software version 5.3.2.22 (Wyatt Technology Corp.) using the refractive index increment (dn/dc) of 0.1475 cm^3/g for HES [44].

2.2.3 Biodegradation of HES70 and HES20 with pancreatic α -amylase (AA)

The enzymatic activity of pancreatic AA was determined using the Phadebas Amylase Test according to the standard protocol provided by the manufacturer. Mixtures of HES70 or HES20 with AA were prepared at a HES concentration of 5 mg/mL in either HBG pH 6.0 or 7.1 (HEPES buffered glucose; 20 mM HEPES, 5 % glucose (w/v)) or PBS pH 7.4. 100 μ L sample volume was injected into the AF4 channel assembly, using a regenerated cellulose ultrafiltration membrane (Wyatt Technology, cut-off 5 kDa). All samples containing pancreatic AA were adjusted to an enzyme activity of 40 U/L. Mixtures were incubated at 25 or 37 $^{\circ}\text{C}$, and samples were withdrawn at time points 0, 0.5, 1, 2, 4, 6, and 24 h. To stop the enzymatic degradation of HES, samples were heated to 99 $^{\circ}\text{C}$ for 3 min. All samples and controls were treated under aseptic conditions with sterile filtration to prevent possible degradation caused by microbial contamination. The reduction in the molar mass of HES70 and HES20 was followed by the Wyatt Eclipse 2 AF4 system in combination with MALS- and RI-detection as explained earlier.

2.2.4 Synthesis and purification of HES-PEI conjugates

Conjugates of HES20 and HES70 with PEI22 were prepared in the molar ratio of 25:1 HES to PEI according to a modified procedure of PEI modification described by Kircheis *et al.* [45]. PEI was attached to HES via Schiff's base formation and reductive amination. An amount of 50 mg linear PEI22 was added to HES20 or HES70 in 150 mM PBS buffer (pH 7.4), and was

shaken at room temperature. After 2 hours 59.8 mg of the reducing agent NaBH_3CN was added and reductive amination was performed for 20 hours. Ion exchange chromatography was carried out to remove unbound HES, where HES-PEI mixtures were loaded onto a cation-exchange column (Bio-Rad Macro-Prep high S HR 10/10, Hercules, CA, USA) and fractionated using a sodium chloride gradient from 0.5 M to 3.0 M salt concentration in 20 mM HEPES, pH 7.3. PEI-containing fractions were detected by UV-spectroscopy at 280 nm. The collected fractions were dialyzed against highly purified water (Cellu Sep T1, nominal MWCO 3500 Da, Membrane Filtration Products Inc, Seguin, TX, USA), then lyophilized.

2.2.5 Nuclear magnetic resonance spectroscopy

For the ^1H -NMR measurements, 10 mg samples of both polymer conjugates were dissolved in D_2O , and the spectra were obtained by using Jeol JNMR-GX500 (500 MHz) spectrometer.

2.2.6 Copper assay

In accordance to Ungaro *et al.* [46], a calibration curve for PEI was created over the concentration range 5.0 to 50.0 $\mu\text{g/mL}$ in 150 mM PBS, pH 7.4, and measured spectrophotometrically at 285 nm. An amount of 23 mg $\text{CuSO}_4 \cdot 5 \text{H}_2\text{O}$ were dissolved in 100 ml 0.1 M sodium acetate buffer solution (pH 5.4), added to solutions of PEI or HES-PEI conjugate, and incubated at room temperature for 15 minutes. Photometric analysis was performed on an Agilent 8453 UV-vis Spectroscopy System (Agilent Technologies, Waldbronn, Germany).

2.2.7 Size exclusion chromatography

The characterization of the HES-PEI conjugates was performed using a combination of SEC with MALS at 18 angles using the Eclipse 2 separation system (Wyatt Technology Corp.) and the 1100 Series Agilent HPLC system (Agilent Technologies, Palo Alto, CA). Detection was carried out via MALS (DAWN EOS, Wyatt Technology Corp.). SEC experiments were performed with a TSKgel G5000PWXL-CP column (7.8 mm x 30.0 cm) that was kindly provided by Tosoh Bioscience GmbH, Stuttgart, Germany. The HES-PEI conjugate samples were prepared at a concentration of 5 mg/mL, the control solutions (mixture of HES and PEI, free PEI) were made at a PEI concentration of 1 mg/mL in 50 mM NaCl. An amount of 100 μL sample was injected per SEC run, the fluid flow was 0.5 mL/min. ASTRA software (version 5.3.2.22, Wyatt Technology Corp.) was used for data analysis.

2.2.8 Preparation and characterization of polyplexes

Naked polyplexes (nPx) were prepared by the rapid addition and mixing of PEI to the plasmid pCLuc (pDNA), to a final DNA concentration of 20 µg/mL in HBG pH 7.1, at N/P ratios of 3.6, 4.8, 6.0, 7.2, or 8.4, then incubated at room temperature (RT) for 30 minutes prior to analysis. The N/P ratio is defined as the molar ratio of PEI nitrogen atoms to plasmid nucleic acid phosphate atoms. For instance, PEI/DNA transfection particles at the N/P ratio of 6.0 were composed of 20 µg DNA and 16 µg PEI. HESylated polyplexes were produced in the same fashion as nPx, with the exception that pure PEI was partially replaced by HES-modified PEI, e.g. HES70-PEI/DNA complexes at N/P ratio 6.0 and a ratio of PEI to HES-modified PEI of 90:10 were made of 20 µg DNA, and a mixture of 14.4 µg PEI and 1.6 µg HES70-PEI22 (weigh of the PEI fraction). HES70-PEI/DNA (HES70Px) and HES20-PEI/DNA (HES20Px) polyplexes were generated with three varying ratios of PEI to HES-PEI conjugates; namely 95:5, 90:10, and 85:15. Polyplexes containing PEG20-PEI (PEG20Px) were prepared at 90:10, molar ratio of free PEI to PEG-PEI conjugates.

2.2.9 Particle size and zeta potential determination

Measurements of the particle size and surface charge of various polyplexes (nPx, HES70Px, HES20Px, and PEG20Px) were performed in HBG pH 6.0 and/or pH 7.1 using a Malvern Zetasizer Nano ZS (Malvern Instruments, Worcestershire, United Kingdom). The measurements were conducted in semi-micro PMMA disposable cuvettes (Brand, Wertheim, Germany) and in folded capillary cells (Malvern Instruments, Worcestershire, United Kingdom) at 25 or 37 °C. For data analysis, the employed values for the viscosity of the dispersant (water with 5% glucose (w/v)) were 1.0366 mPas at 25 °C, and 0.8359 mPas at 37 °C (viscosity values were already available in the MALVERN Zetasizer software V. 6.12). The resulting particle size data are the average of at least three measurements ($n \geq 3$), whereas every single measurement is composed of three serial runs of 15 subruns. Analysis of the particle surface charge was carried out in triplicates directly after particle size determination without further sample treatment. The performed voltage was set to 100 V, and the monomodal setup was applied. Malvern Zetasizer software version 6.12 (Malvern Instruments, Worcestershire, United Kingdom) was used for data acquisition and analysis.

2.2.10 Treatment of polyplexes with pancreatic α -amylase (AA)

The effect of pancreatic AA (40 U/L and 100 U/L) on biophysical properties of HES-decorated polyplexes was investigated. nPx and HES70Px were generated at the DNA concentration of 20 $\mu\text{g/mL}$ in HBG pH 6.0, and at an N/P ratio of 6.0. HESylated polyplexes were prepared with varying ratios of PEI to PEI-conjugates (95:5, 90:10, 85:15). After 30 min incubation of the polyplexes at room temperature, AA stock solution (amylase activity 1000 U/L) was added to the polyplex solution to give a final AA activity of 40 or 100 U/L, mixed intensively, and the resulting AA-polyplex mixture was analyzed using a Malvern Zetasizer Nano ZS instantly after combination of the enzyme and substrate. Analysis of particle size and zeta potential of PEI/DNA complexes was performed at time point 0, 0.25, 0.5, 1, 2, 4, and 6 h holding the polyplexes at 37 °C.

2.2.11 Erythrocyte aggregation assay

Fresh blood from 3 months old male C57BL/6 mice (Department of Pharmacy, Institute of Pharmacology, Munich) was collected, spiked with 3.2 % (m/v) sodium citrate to prevent coagulation, and washed by six centrifugation steps (2500 \times g, 10 min, 4 °C) with PBS pH 7.4 until a colorless supernatant was obtained. The resuspension of erythrocytes was carried out in phosphate-buffered saline at a concentration of 2% (V/V). An amount of 50 μL of HES70Px and HES20Px (95:5, 90:10, and 85:15 molar ratio of free PEI to modified PEI, respectively) in HBG pH 7.1 was mixed with 100 μL erythrocyte suspension in PBS pH 7.4 \pm AA with 40 U/L final concentration. Buffer, buffer + AA, nPx, and PEG20Px (90:10) were used as controls. The solutions were incubated in 24-well plates (Costar) for 90 min at 37 °C under constant gentle agitation. For microscopic analysis, pictures were taken with a Keyence VHX-500F digital microscope (Keyence Corporation, Osaka, Japan) with a 1000-fold magnification.

2.2.12 Cell culture experiments

Cell culture media, antibiotics and fetal calf serum (FCS) were purchased from Life Technologies (Karlsruhe, Germany). All cultured cells were grown at 37 °C in 5% CO₂ humidified atmosphere. Murine neuroblastoma, Neuro2A (ATCC CCI-131, purchased from DSMZ, Braunschweig, Germany) were cultured in Dulbecco's Modified Eagle Medium (DMEM). Human hepatoma cells HUH7 (JCRB 0403, Tokyo, Japan) were cultured in

DMEM/HAM's F12 medium (1:1). All media were supplemented with 10% FCS, 4 mM stable glutamine, 100 U/mL penicillin, and 100 μ g/mL streptomycin.

2.2.13 Luciferase reporter gene expression studies

In vitro pDNA transfection efficiency was evaluated in murine Neuro2A and human HUH7 cell lines. Experiments were performed in 96 well plates by seeding 1×10^4 cells per well in 100 μ L medium 24 h prior to transfection. Directly before transfection, the medium was exchanged against fresh medium with/without pancreatic AA (40 U/L). An amount of 10 μ L polyplex solution (N/P 6.0, 20 μ g/mL DNA concentration) was added to the cells. 4 h after transfection, the medium was replaced by fresh medium with/without AA. 24 h after pDNA transfection, the cells were treated with 100 μ L cell lysis buffer (25 mM Tris pH 7.8, 2 mM EDTA, 2 mM DTT, 10% glycerol, 1% Triton X-100). Luciferase activity in 35 μ L cell lysate was measured in white 96 well plates using a luciferase assay kit (100 μ L Luciferase Assay buffer, Promega, Mannheim, Germany) on a luminometer for 10 s (Centro LB 960 instrument, Berthold, Bad Wildbad, Germany). The effect of using higher AA concentration on transfection efficiency in Neuro2A cells was tested by using the same procedure as above, but with 100 U/L of AA instead of 40 U/L.

2.2.14 Metabolic activity of transfected cells

The cellular metabolic activity after pDNA transfection was evaluated using MTT assay. Cells were seeded and transfected as explained above. 24 h after transfection, MTT (3-(4,5-dimethylthiazol-2-yl)-2,5-diphenyltetrazolium bromide) (Sigma-Aldrich, Germany) was dissolved in phosphate buffered saline at 5 mg/mL, and 10 μ L aliquots were added to each well reaching a final concentration of 0.5 mg MTT/mL. After an incubation time of 2 h, unreacted dye with medium was removed and the cells were lysed by incubation at -80 °C for 30 min. The formazan product was dissolved in 100 μ L/well dimethyl sulfoxide and quantified by a plate reader (Tecan, Groedig, Austria) at 590 nm with background correction at 630 nm. The metabolic activity (%) relative to control wells containing HBG treated cells was calculated as follows ($\text{Metabolic activity} = A_{\text{test}}/A_{\text{control}} \times 100$).

2.2.15 Flow cytometry experiment

Uptake and binding of HES-decorated polyplexes and control particles, under the effect of AA (40 U/L), was studied in a murine Neuro2A cell line. Cells were seeded in 24 well plates

at a density of 1×10^5 cells per well in 500 μL medium 24 h prior to transfection. Directly before transfection, the medium was exchanged against fresh medium with/without pancreatic AA (40 U/L). An amount of 50 μL polyplex solution (N/P 6.0, 20 $\mu\text{g/mL}$ final pDNA concentration) was added to the cells, where particles contained 10% Cy5-labeled pDNA. In the case of binding studies treated cells were kept at 4 °C for 30 min, washed with PBS (phosphate buffered saline), trypsinized (1x Trypsin/EDTA solution Biochrom AG, Berlin, Germany) and transferred to Eppendorf tubes. For uptake studies treated cells were kept at 37 °C for 60 min incubated with heparin (1000 I.E./mL) to disassemble the polyplexes, washed, trypsinized and transferred to Eppendorf tubes. After 2 washing steps the amount of Cy5 positive cells and mean fluorescence intensity was detected using a Flow cytometer (CyAn ADP; Dako Cytomation Fort Collins USA). Results were analyzed using Flow Jo software (Treestar, Inc., San Carlos, USA).

3 Results

3.1 Acid-induced fragmentation of HES70

In order to test the effect of molar mass on the concept of shielding/deshielding, HES70 was degraded by acid hydrolysis to produce smaller fractions. Preliminary experiments using 1 M and 0.1 M HCl for cleavage of HES70 resulted in very rapid degradation and problems in controlling the molar mass of the product. Carrying out the hydrolysis reaction using 0.05 M hydrochloric acid yielded (after 2 h) a HES product of around 20 kDa molecular weight and a low polydispersity of 1.15 (vs. 1.96 for HES70) as determined by AF4-MALS. The yield was 62 % w/w.

3.2 HES degradation experiments with pancreatic α -amylase

Figure II. 1 shows the degradation of HES70 and HES20 as a function of time in different buffers, pH and temperatures. Control samples lacking AA did not show any degradation, while in the presence of the enzyme, the degradation at 37 °C seems to be rapid at the beginning, levelling-off after approximately 2 h, whereas the degradation at 25 °C is slower at the beginning, but ultimately results in a degraded product of similar molar mass to the one degraded at 37 °C after 6 h. HES70 loses approximately 50 % of its molar mass after 6 h,

while HES20 loses approximately 20%. It seems that the pH has no effect on degradation rate as can be seen for HBG buffer at pH 7.1 and 6.0 (Figure II. 1 E), while degradation is clearly faster in PBS pH 7.4 compared to HBG pH 6. This is probably due to the fact that α -amylase is more active and stable in the presence of chloride ions [47].

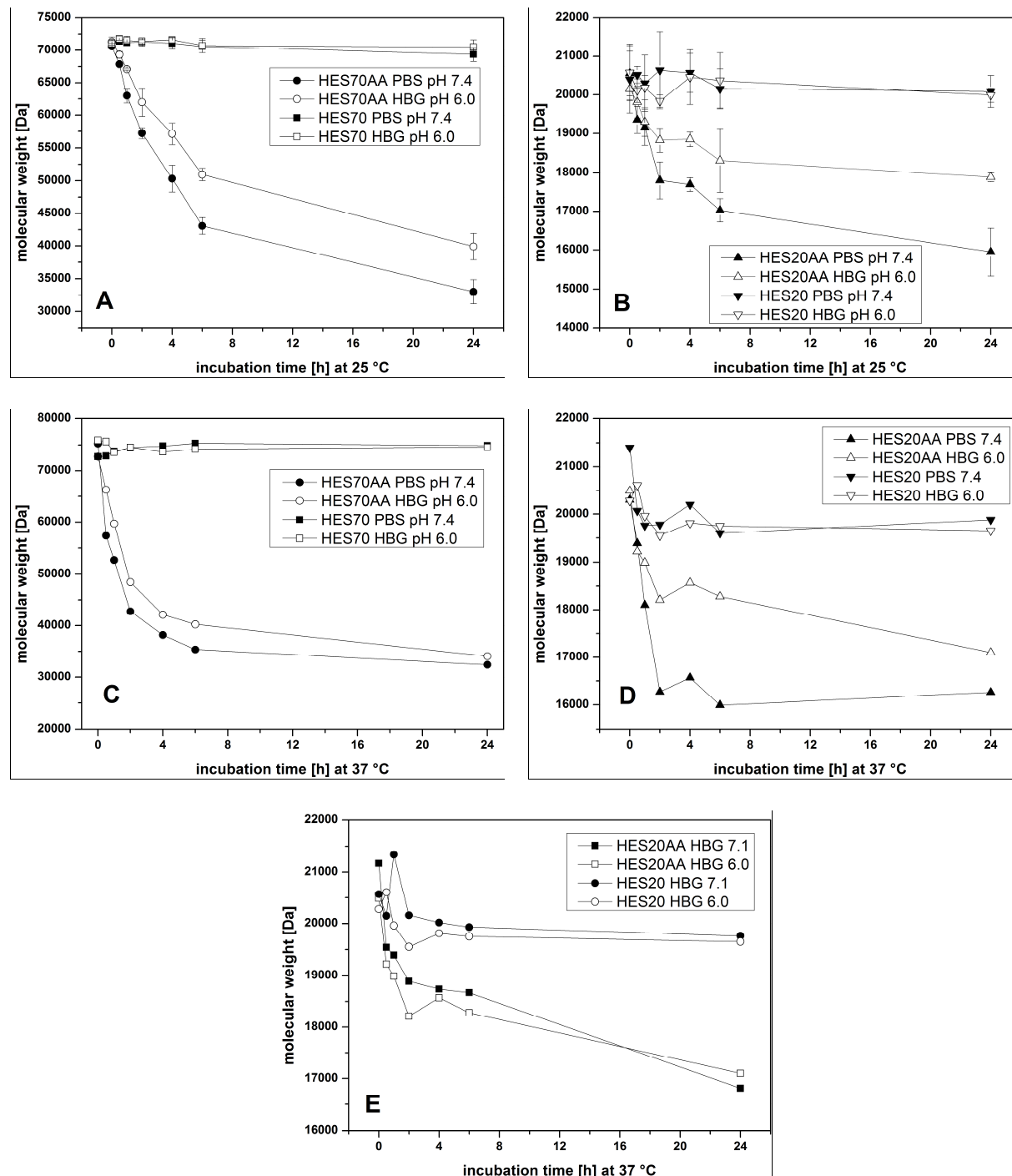
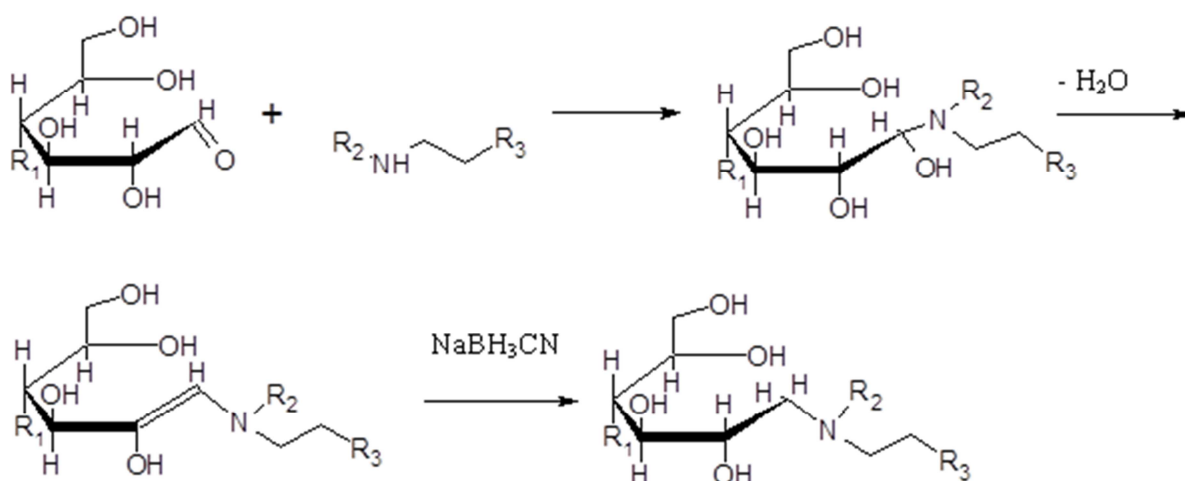


Figure II. 1. Biodegradation of HES70 at 25°C (A), and 37°C (C) as well as HES20 at 25°C(B), and 37°C (D) with pancreatic α -amylase as a function of time. The effect of the pH on the biodegradation of HES20 (E) was also investigated.

3.3 Polycation modification: HES-conjugation to PEI22

The graft copolymer was prepared by coupling HES20 and HES70 with the linear polyamine PEI22 in PBS pH 7.4 using a large excess of HES (molar ratio 25:1) to ensure Schiff's base formation between the one single terminal aldehyde function of HES and the amine groups in PEI. The synthesis of modified PEI polymers proceeded in a two step reaction [48], as shown in Scheme II. 1. In the first step, HES-PEI copolymers were generated by grafting HES onto linear PEI by a condensation reaction via an unstable aminol intermediate that immediately rearranged to an enamine function. In the second step, the reducing agent sodium cyanoborohydride was added 2 h after the beginning of the reaction to reduce the enamine to secondary (or tertiary) amine groups. Ion exchange chromatography was used to purify the conjugates, which were then characterized using ^1H NMR, UV spectroscopy (copper assay), and SEC.



Scheme II. 1. PEI modification by Schiff's base formation with HES and subsequent reductive amination. (scheme adapted from [48])

3.4 Characterization of polymeric HES-PEI conjugates

^1H NMR measurements were carried out for HES20-g-PEI22 and HES70-g-PEI22 to get information regarding the coupling efficiency and ratio of HES to PEI in the generated products. Figure II. 2 shows the NMR spectra of both polymer conjugates, where the peaks between 5.3 and 5.7 ppm belong to the proton at position C1 of the anhydroglucose unit (AGU) of HES, and the peaks between 2.8 and 3.1 ppm belong to the four protons of the

ethylene structure of PEI. Results show the following molar ratios, HES20:PEI22 1.44:1, and HES70:PEI22 2.35:1 (see Table II. 1).

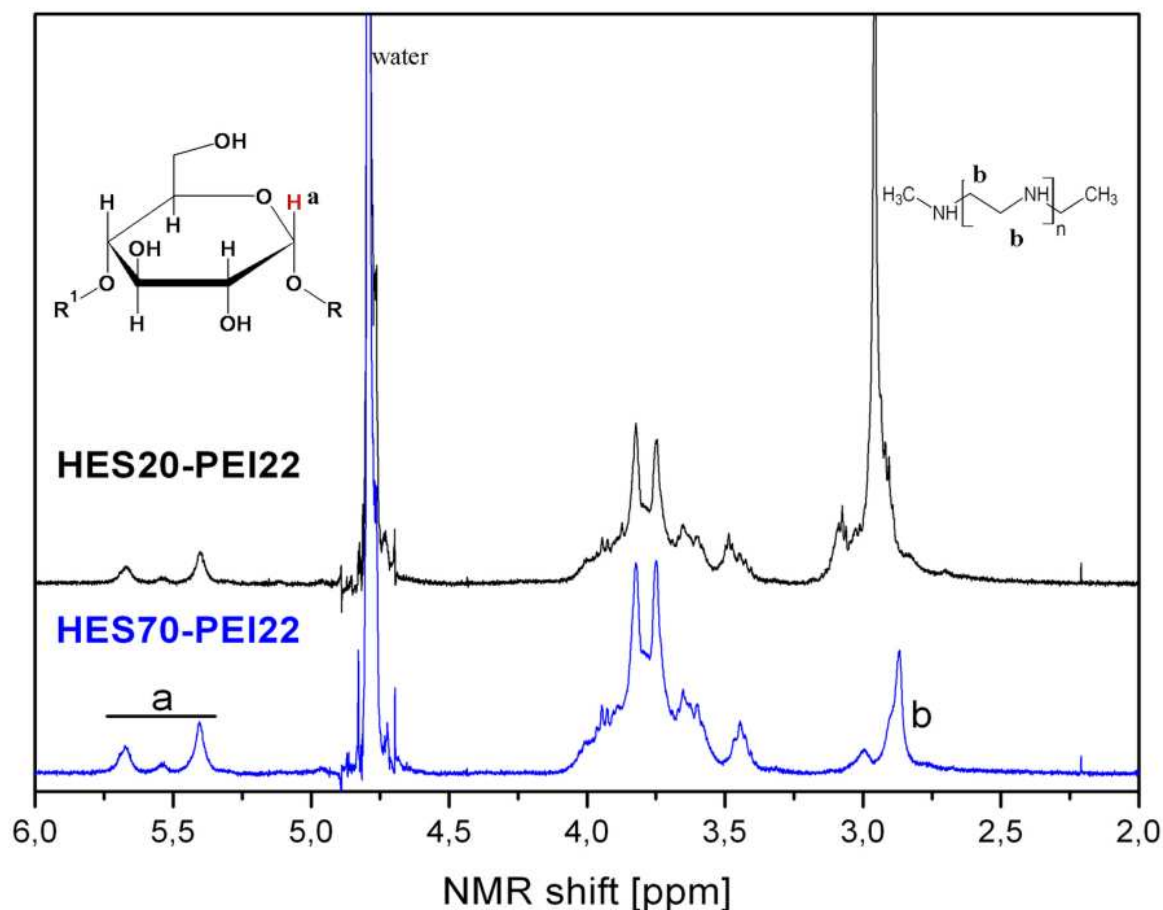


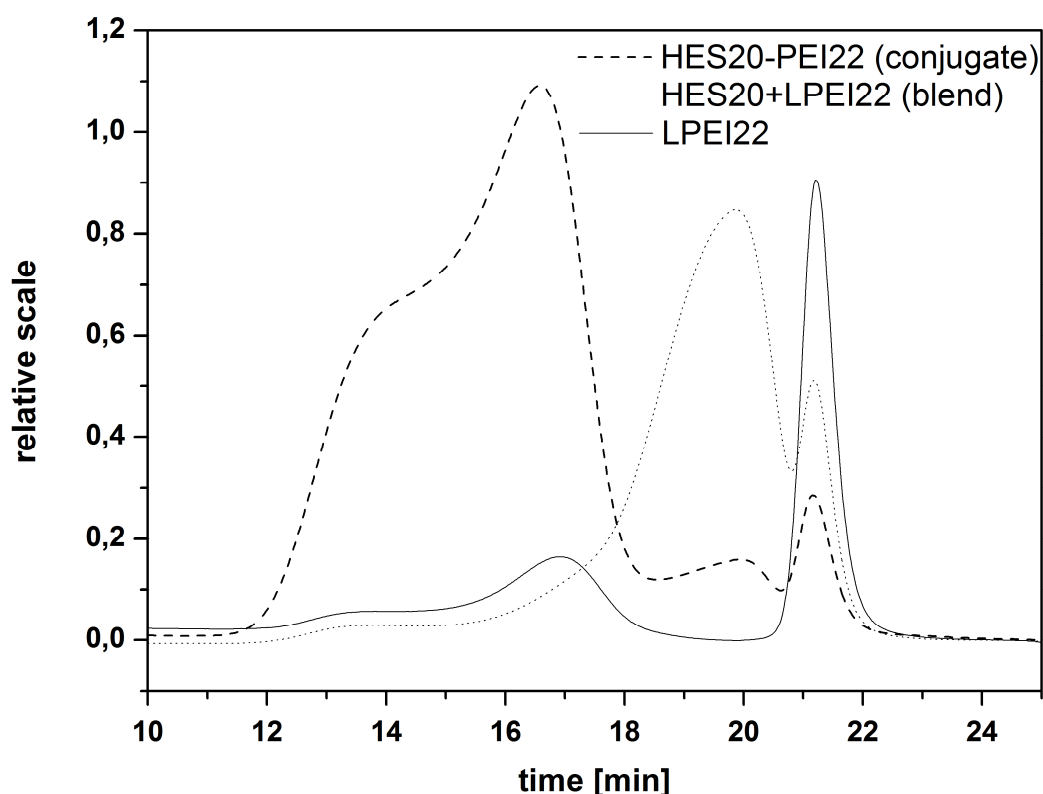
Figure II. 2. ^1H NMR spectra of HES20-PEI22 (top) and HES70-PEI22 (bottom) in D_2O with peak assignment.

To confirm the results of ^1H NMR spectroscopy, *Copper Assay* was performed to evaluate the quantity of PEI within the generated HES20-PEI22 and HES70-PEI22 conjugates. The photometric copper complex assay is based on the formation of a bluish complex, consisting of copper (II) ions and PEI, which can be detected by UV-vis spectroscopy at λ_{max} 285nm [46]. A negative control using a mixture of pure HES and pure PEI was measured and showed no interference for HES in the measurements. The obtained results were in excellent agreement with the findings of the NMR measurements (see Table II. 1).

Table II. 1. Mass ratios and molar ratios for HES20-PEI22 and HES70-PEI22 as determined by ^1H -NMR and the photometric copper complex assay.

	Amount of HES20 in generated HES-PEI conjugates		Amount of HES70 in generated HES-PEI conjugates	
	Mass ratio [%]	Molar ratio	Mass ratio [%]	Molar ratio
		HES20 : PEI22		HES70 : PEI22
^1H -NMR	56.7	1.44 : 1	88.2	2.35 : 1
Copper assay	56.7 ± 8.83	1.44 : 1	$88,31 \pm 1.49$	2.37 : 1

SEC-MALS, the combination of size exclusion chromatography with multi-angle light scattering is a common mean for the characterization of polymers. The SEC chromatograms (see Figure II. 3) verified the successful conjugation of HES20 and HES70 to the linear polyamine PEI22, where the HES-PEI conjugates eluted earlier than the blends of HES and PEI. Additionally, only a low amount of unbound PEI22 appeared in the chromatogram.



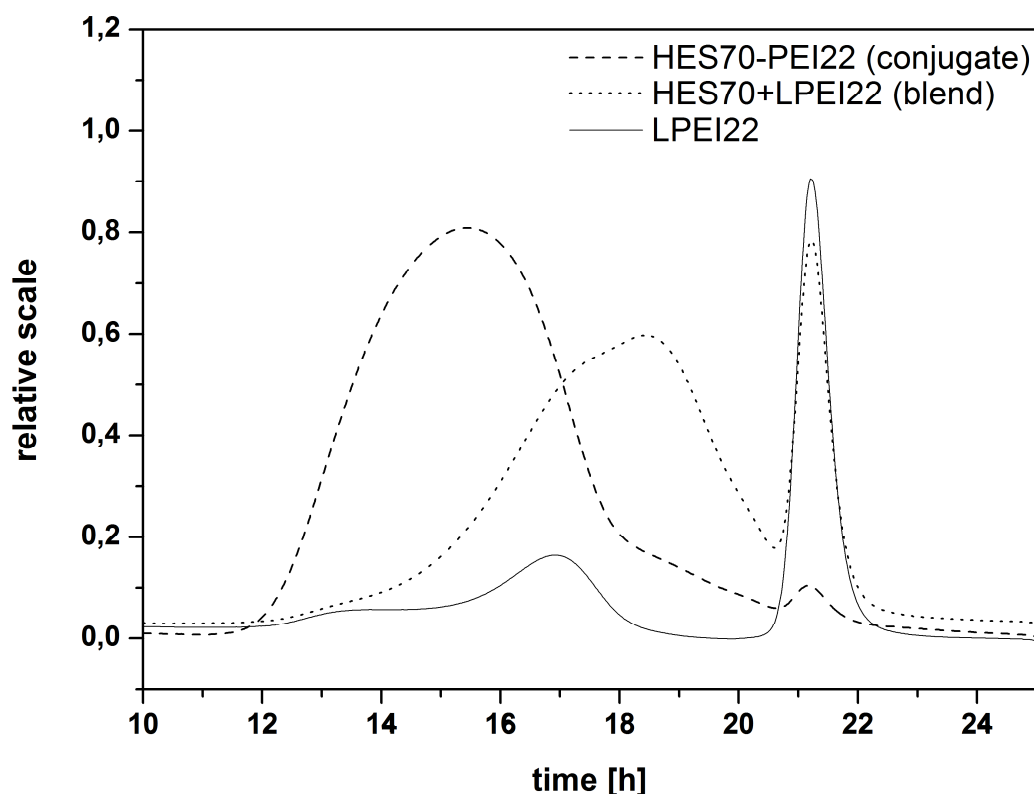


Figure II. 3. Size exclusion chromatograms of HES20-PEI22 (top) and HES70-PEI22 (bottom) copolymers. Blends of free HES and PEI, as well as uncoupled PEI were used as controls.

3.5 Biophysical characterization of the generated polyplexes

The effect of different N/P ratios and various ratios of free PEI to HES-PEI on the formation of polyplexes and their properties, namely the particle size and zeta potential, was evaluated. For these studies, naked polyplexes and PEG-PEI complexes served as controls. By increasing the N/P ratio, the particle size of the polyplexes tends to decrease, but then levels off at approximately 70 nm at N/P ratio ≥ 6.0 (Figure II. 4, top). At lower values, nPx tend to aggregate since there are not enough excess charges for particle stabilization, while the HES- and PEG-modifications impart additional steric stabilization and prevent aggregation. It is worth noting that the HES70-PEI conjugate produced smaller particles at N/P ratio of 3.6 compared to nPx and PEG-PEI polyplexes. This might point to the possibility of producing more stable polyplexes using HES conjugates, which can thus be used to administer lesser amounts of PEI and reduce the toxicity.

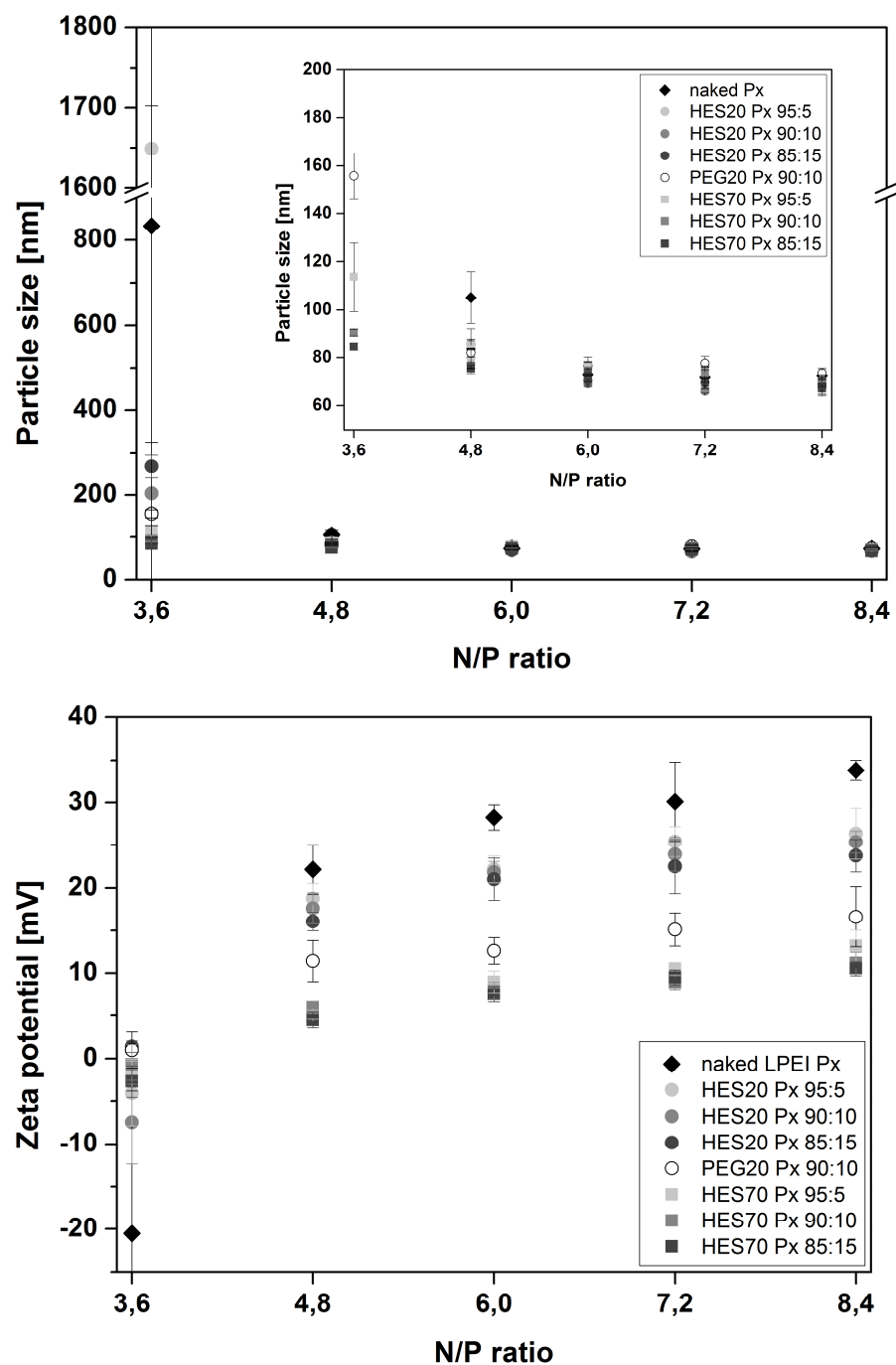
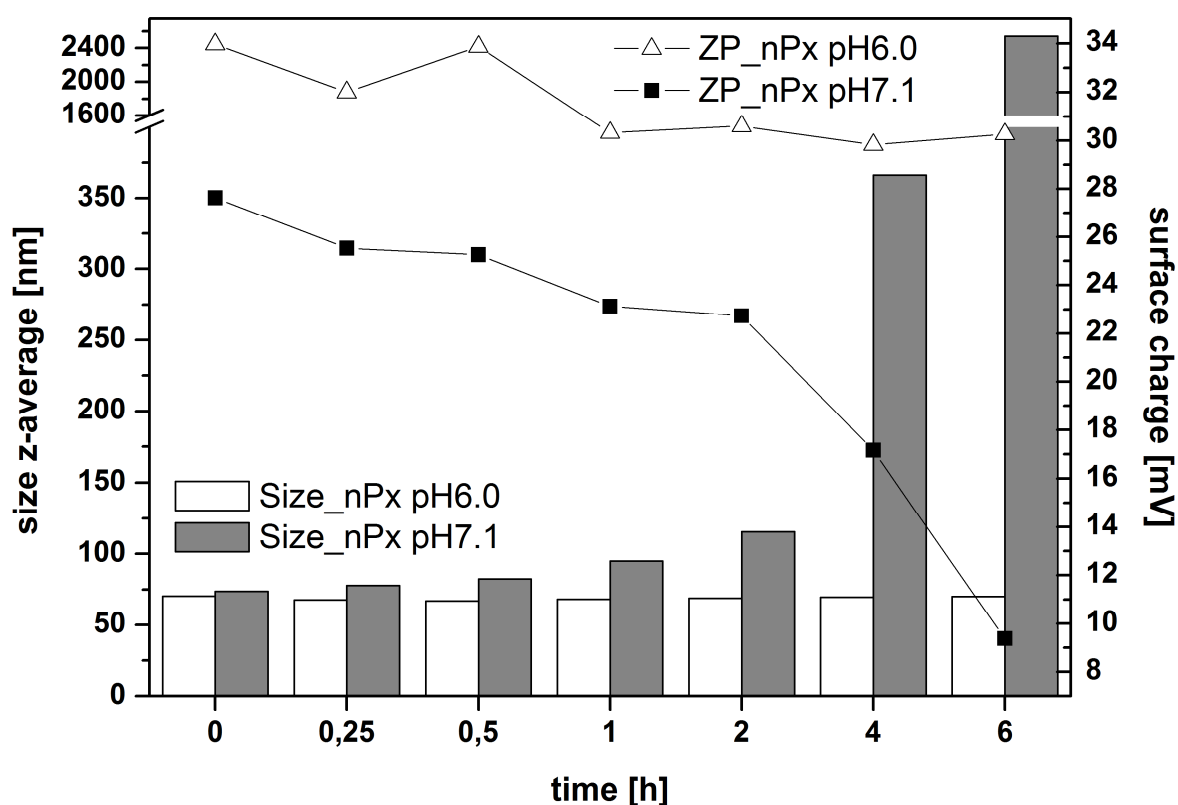


Figure II. 4. (Top) Particle size of different polyplexes as a function of increasing N/P ratio. Insert shows a magnification of the smaller particle size region. (Bottom) Zeta potential of different polyplexes as a function of increasing N/P ratio.

3.6 Treatment of polyplexes with pancreatic α -amylase

To establish an *in vitro* model for the enzymatically-catalyzed deshielding, we planned to monitor the effect of AA on the zeta potential and size of the HES-decorated polyplexes over

6 hours. Accordingly, we tested the stability of naked polyplexes and HES70-PEI polyplexes in HBG buffer at pH 7.1 and 6 as seen in Figure II. 5. Results show that the polyplexes were not stable at pH 7.1 for the required test period of 6 h, where the zeta potential decreased, while the particle size increased. Meanwhile, the zeta potential and particle size of the polyplexes in pH 6 were much more stable over 6 h, probably due to the additional stability from the extra positive charges at this pH. Accordingly we decided to investigate the effect of AA on polyplexes at pH 6.



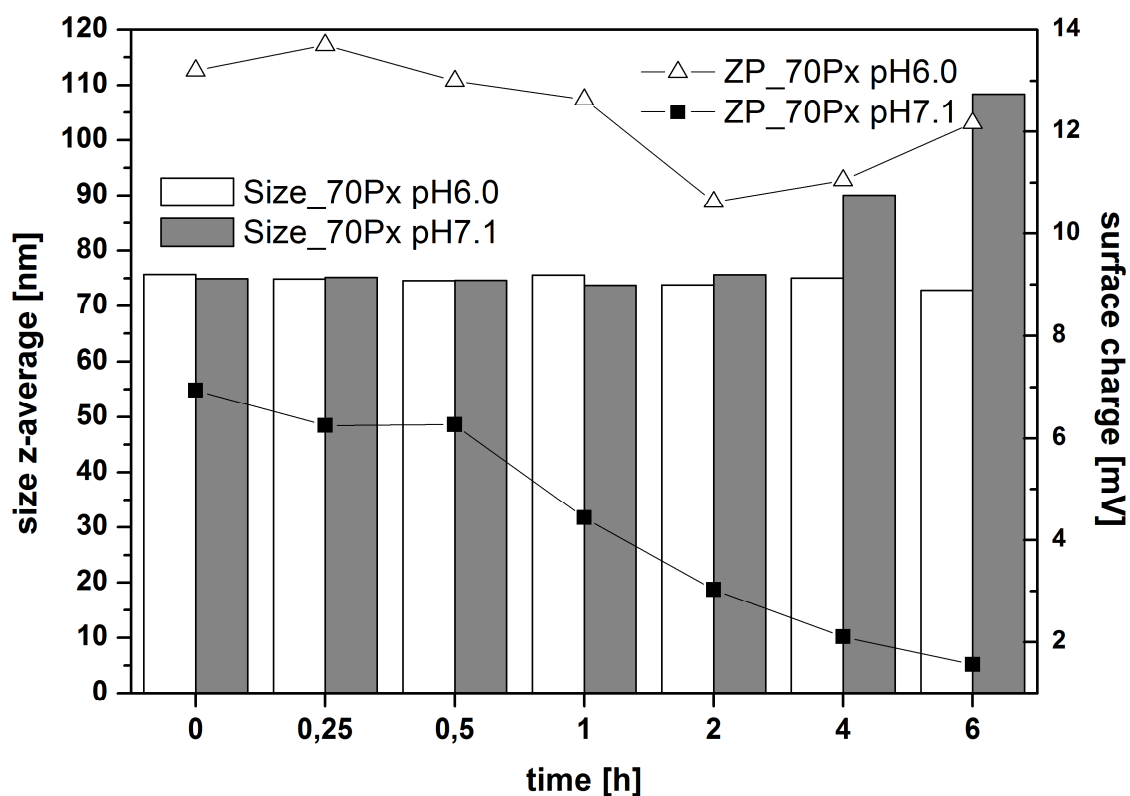


Figure II. 5. Particle size and zeta potential of naked polyplexes (top) and HES70-PEI polyplexes (bottom) in HBG buffer with pH 6 and pH 7.1 as a function of time. Particles were prepared with N/P ratio = 6.

The addition of AA to polyplexes of HES70-PEI with different ratios of free PEI to PEI-conjugate is shown in Figure II. 6. At low amount of HES70-PEI (5%), it is possible to see an increase in zeta potential, though not statistically significant. Using higher amounts of the conjugate (10 and 15%), the zeta potential increases gradually with time after addition of AA, and levels off after ca. 1 h at 37 °C, probably a second indication for the enzymatic deshielding. After 4-6 h, the polyplexes treated with AA increase in size. This might point to destabilization due to a reduction in steric stabilization as the HES coat is “eaten” up.

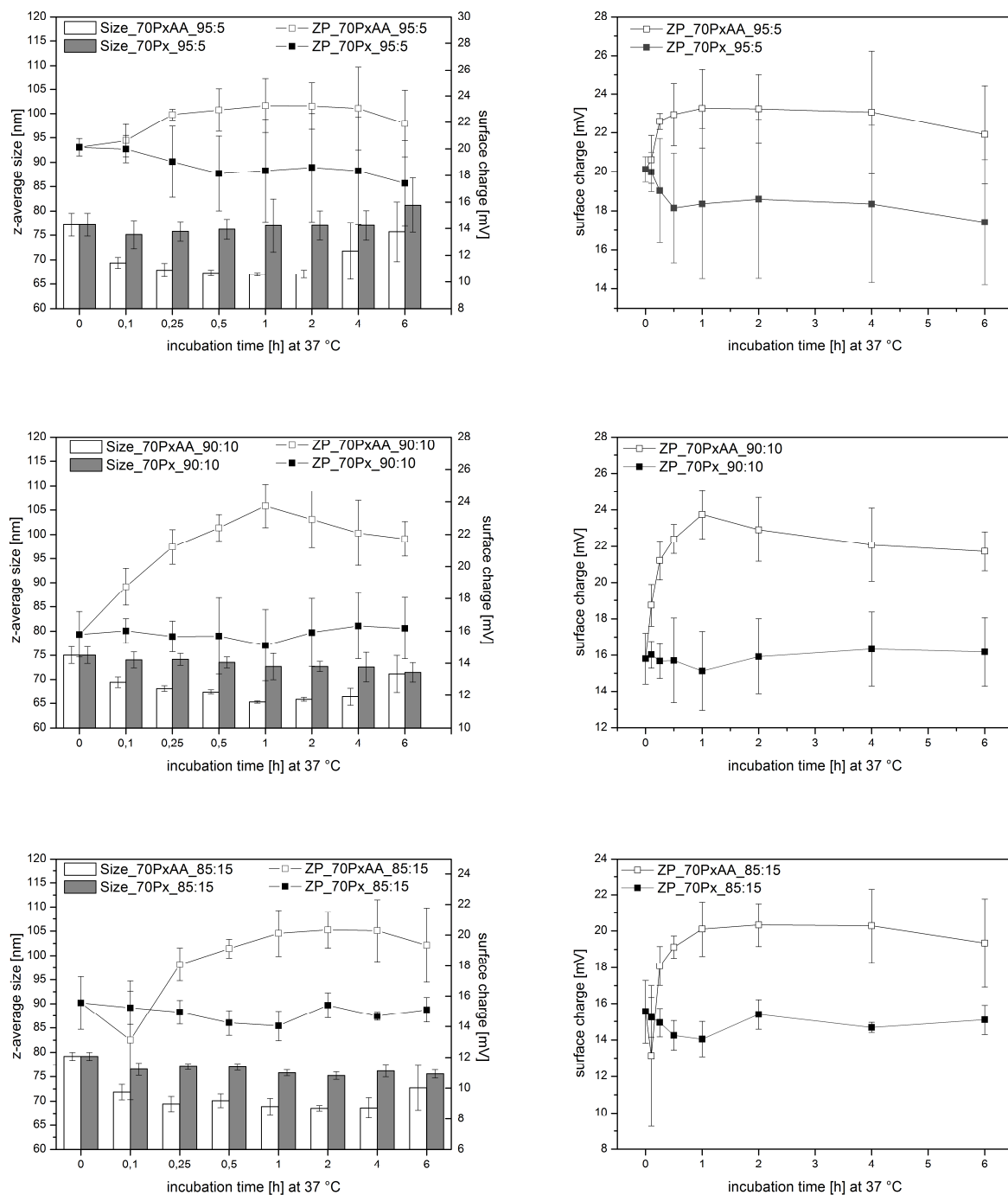


Figure II. 6. Particle size and zeta potential as a function of time (left) for polyplexes with different ratios of PEI:HES70-PEI (from top to bottom 95:5, 90:10 and 85:15) stored without AA (control) or with 40 U/L AA at 37 °C. Right graphs show the zeta potential alone for the same polyplexes with and without AA. Particles were prepared with N/P ratio = 6.

3.7 Erythrocyte aggregation assay

The shielding of HES-decorated polyplexes and deshielding using AA were additionally tested using erythrocyte aggregation assay. nPx cause considerable aggregation as seen in Figure II. 7 due to the electrostatic interaction between their positive charge and the negatively charged nPx. Meanwhile, the effective shielding with PEG or HES (HES70 or HES20 with different ratios of PEI:PEI-conjugate) prevented the formation of such aggregates. The addition of AA triggered enzymatic deshielding, which led to development of small erythrocyte aggregates. The latter seemed to depend on the molar mass and amount of HES on the surface of polyplexes as seen in Figure II. 7.

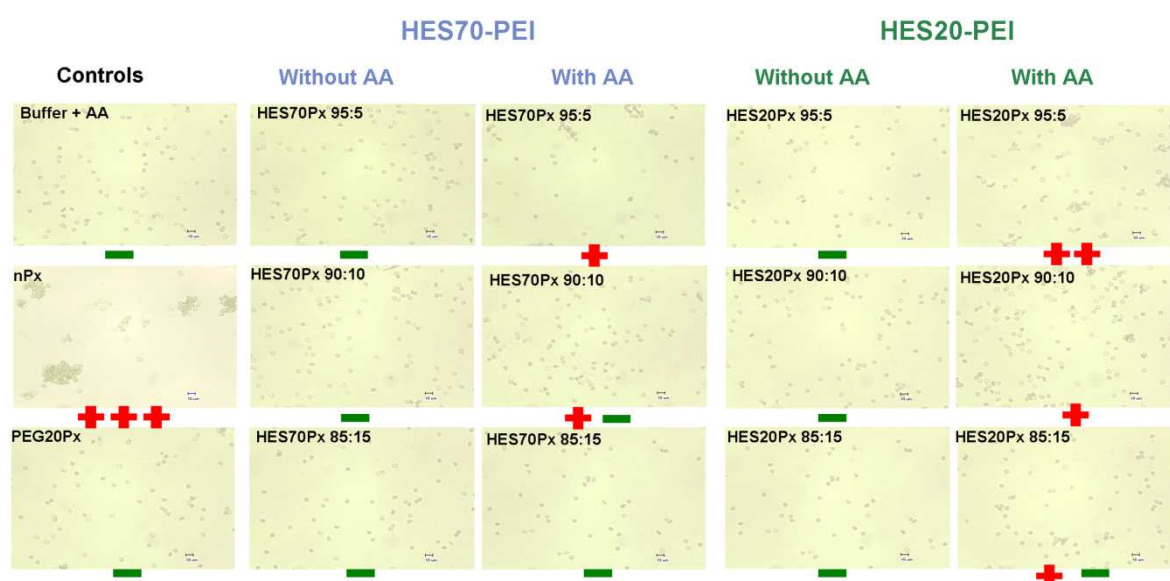


Figure II. 7. Erythrocyte aggregation assay for polyplexes prepared with different ratios of PEI:HES20-PEI or PEI:HES70-PEI \pm 40 U/L AA. Shielding the polyplexes with different amounts of HES20-PEI or HES70-PEI prevents erythrocyte aggregation, while deshielding under the effect of AA leads to the formation of small erythrocyte aggregates. Controls included PEG-decorated polyplexes (PEG20Px), naked polyplexes (nPx), and buffer + AA. Particles were prepared with N/P ratio = 6.

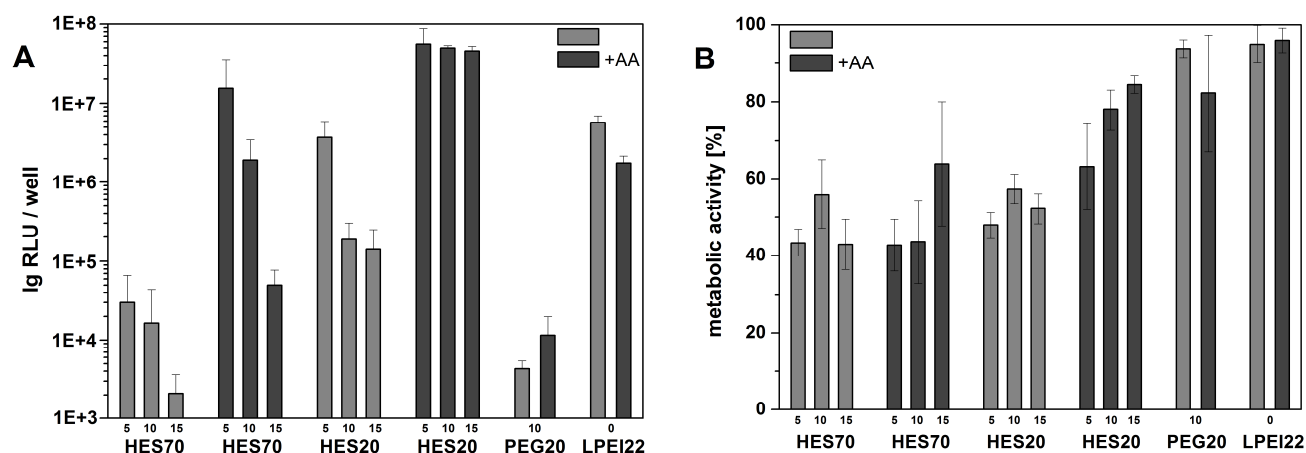
3.8 Cell culture experiments - Luciferase reporter gene transfection efficiency

In vitro transfection experiments were conducted on Neuro2A cells and HUH7 cells in cell culture medium with/without AA to study the effect of HES-shielding and enzymatic deshielding on transfection efficiencies.. The transfection of Neuro2A cells using HES70-

decorated polyplexes was similar to PEG polyplexes and was clearly less efficient compared to nPx. The shielding effect is additionally evidenced by the dependence on the polymer molar mass and amount in the nanoparticle shell. For instance, HES20 shows a higher transfection efficiency (and lower shielding) compared to HES70, while the transfection efficiency decreases by increasing the amount of HES in the nanoparticle shell (see Figure II. 8 A). Meanwhile, the addition of AA to the culture medium leads to a 2-3 orders of magnitude increase in transfection efficiency both for HES70 and HES20. Such an effect cannot be seen for nPx or PEG-polyplexes, indicating that the deshielding due to the specific action of AA on HES is responsible for this effect (Figure II. 8 A). It is worth noting that the HES20 polyplexes showed a higher efficiency compared to the nPx, a phenomenon that warrants further investigations to elucidate the possible reasons for this super-performance.

HUH7 cells showed a quite similar trend to Neuro2A cells regarding gene transfection. In general, the transfection using HES20-coated polyplexes was more efficient (i.e. lower shielding efficiency) compared to HES70, and the addition of AA led to an enhancement of 1-3 orders of magnitude in transfection (Figure II. 8 C).

The metabolic activity of Neuro2A cells treated with the polyplexes was lower for HES-PEI-containing particles than for PEG-PEI or PEI particles, while it was not affected in the case of HUH7 cells. Generally, HUH7 cells show slow proliferation rate, a less efficient transfection performance, and higher sensitivity to cytotoxicity compared to Neuro2A cells. It seems that HES-PEI interfered with the cell proliferation of Neuro2A cells (but not with cell viability) and thus led to the observed reduction in metabolic activity due to the smaller number of cells. This effect was not observed in the slowly proliferating HUH7 cells. The reason for the reduced metabolic activity with Neuro2A cells needs to be further investigated.



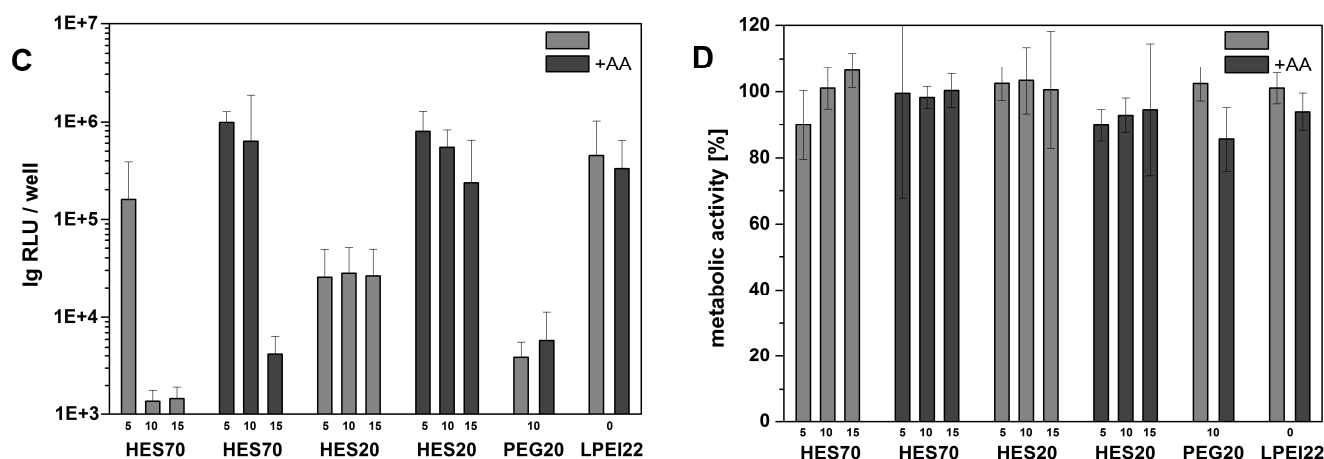


Figure II. 8. Luciferase gene expression in Neuro2A cells (A) and the corresponding metabolic activity (B), as well as in HUH7 cells (C) and the corresponding metabolic activity (D). Polyplexes with different HES-PEI content (numbers represent the percentage of HES-PEI content relative to PEI) were freshly prepared prior to transfection, and given directly to the cells in medium containing AA (+AA), or lacking it. The analysis of the transfection performance and metabolic activity was carried out 24h post transfection. Naked PEI- and PEGylated- polyplexes (10:90 PEG-PEI:PEI) served as controls. Particles were prepared with N/P ratio = 6.

3.9 Effect of AA activity

The effect of 2 levels of AA activity (40 and 100 U/L) on the biophysical properties of the polyplexes and transfection efficiency was investigated. Amylase activity was determined using Phadebas amylase test, for which a normal range of clinical serum activity between 60-310 U/L has been reported [49]. Tracking the zeta potential of the HES70-coated polyplexes (PEI:HES-PEI 90:10) incubated with 2 different amylase activities over 6 h show that increasing the AA activity from 40 to 100 U/L accelerates the increase in zeta potential, so that a plateau is reached after only 0.5 h rather than 1 h (Figure II. 9 A). Additionally, the higher amylase activity seems to increase the zeta potential to a higher level (though the difference in the plateau region is not statistically significant). The effect of amylase activity on the transfection efficiency of the HES70-decorated polyplexes in Neuro2A cells was also investigated. Results in Figure II. 9 B show that the polyplexes treated with the higher amylase activity show the same deshielding trend, reaching transfection efficiencies similar to nPx, while it had no effect on the controls (PEG-Px and nPx). These results show that the amylase activity has an effect on HES degradation and deshielding kinetics *in vitro*, but less influence on the extent of transfection.

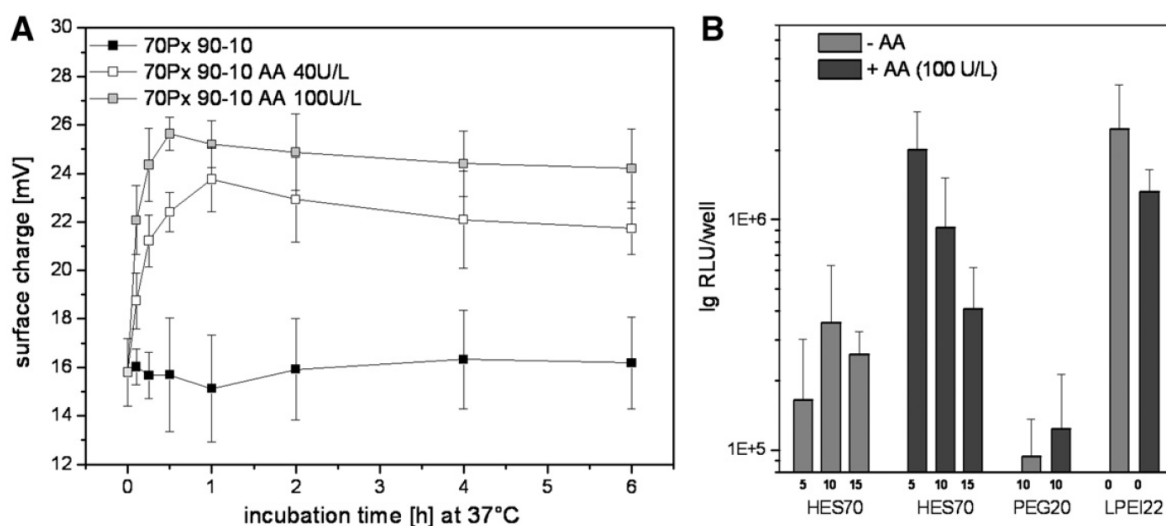


Figure II. 9. Effect of AA activity. The effect of 40 and 100 U/L of amylase on the zeta potential of HES70Px (90:10) as a function of time (A). Luciferase gene expression in Neuro2A cells \pm 100 U/L AA (C.f. **Fehler! Verweisquelle konnte nicht gefunden werden.**). Naked PEI- and PEGylated- polyplexes (10:90 PEG-PEI:PEI) served as controls (B).

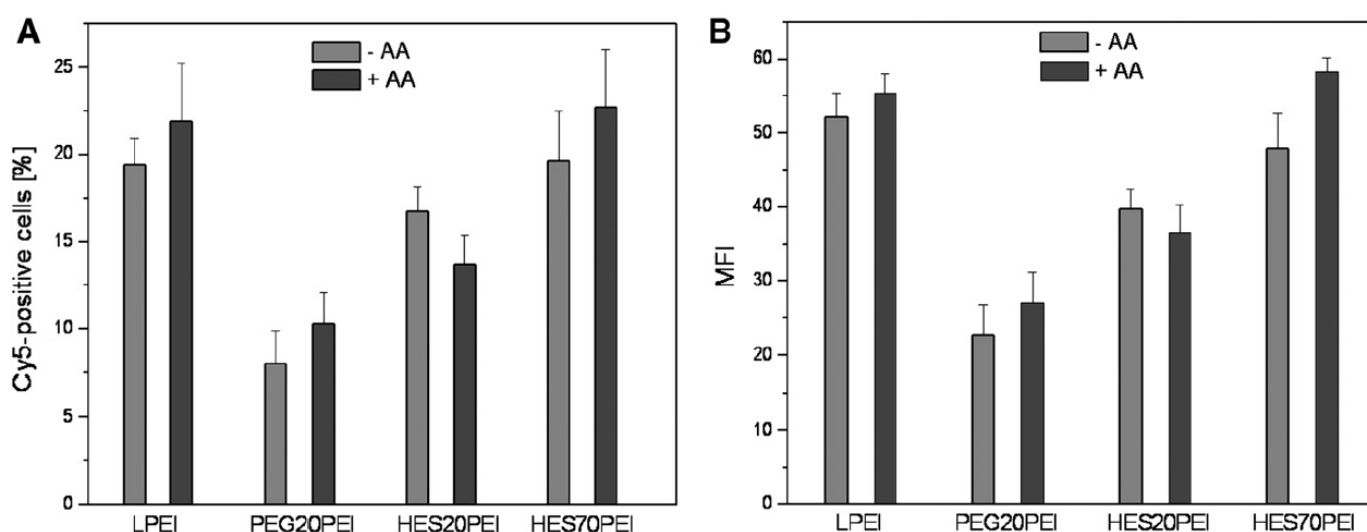
3.10 Binding and uptake experiments using flow cytometry

Nie et al. [18] used flow cytometry to determine the effect of cleavable and non-cleavable PEGylation on the binding and uptake of cationic lipopolyplexes for DNA transfection. They showed that both types of PEGylation reduced the cellular binding and association at 4°C but did not affect cellular uptake at 37°C. They concluded that endoplasmic escape was more crucial for transfection than cellular uptake, since the non-PEGylated lipopolyplexes, as well as lipopolyplexes PEGylated with non-cleavable or cleavable PEG had equal uptake at 37°C. However, lipopolyplexes with intracellularly-cleavable PEG showed higher transfection efficiency than those having non-cleavable PEG, because the former showed less interference with endoplasmic escape [18].

With these conclusions in mind, the *in vitro* binding and uptake of the HES-decorated polyplexes was investigated using flow cytometric analysis. Binding was performed at 4°C, where only non-specific adsorption to the cell-surface takes place, while the energy-dependent uptake is inhibited. Results in Figure II. 10 A and B show that PEG20 and HES20 were effective in inhibiting binding (compared to nPx), as it is illustrated in the percentage of cells associated with labelled-DNA as well as the mean fluorescence intensity (MFI, an indicator for the average amount of labelled DNA per cell). This shows the effective shielding

of PEG20 and HES20, and their ability to reduce non-specific adsorption. The apparent ineffectiveness of HES70 in preventing non-specific adsorption contradicts with results from transfection efficiency and erythrocyte aggregation assay, and is probably difficult to explain at this point. Finally, the addition of AA does not have a significant effect on binding, probably due to the low activity of AA at 4°C.

Results of the uptake at 37°C in Figure II. 10 C and D show that the percentage of Cy5 positive cells is much higher than at 4°C, but does not differ much between the different polyplexes before or after addition of AA, and lies between approximately 75-85 %. Meanwhile, MFI decreases for PEG20- and HES20-decorated polyplexes, in accordance with the binding experiments. Furthermore, the addition of AA leads to a significant increase in MFI by 28 % and 36 % for the HES20- and HES70-decorated polyplexes, respectively, without any significant effect on the nPx and PEG20 polyplexes. The above results are in agreement with those reported with Nie et al., where we show that HES can reduce nonspecific binding to the cells similar to PEG, but to a lesser extent. Meanwhile, although the addition of AA does not affect the percentage of cells which actively phagocytose the polyplexes, it can significantly increase the amount of delivered DNA per cell, which is an indication for effective degradation of the polymer shell. Results of the flow cytometry constitute an additional proof that HES-decorated polyplexes can be effectively deshielded by amylase, leading to an increase in the amount of DNA delivered per cell. This deshielding is also expected to reduce the interference with the endoplasmic escape and increase transfection efficiency as already observed with the luciferase transfection experiments.



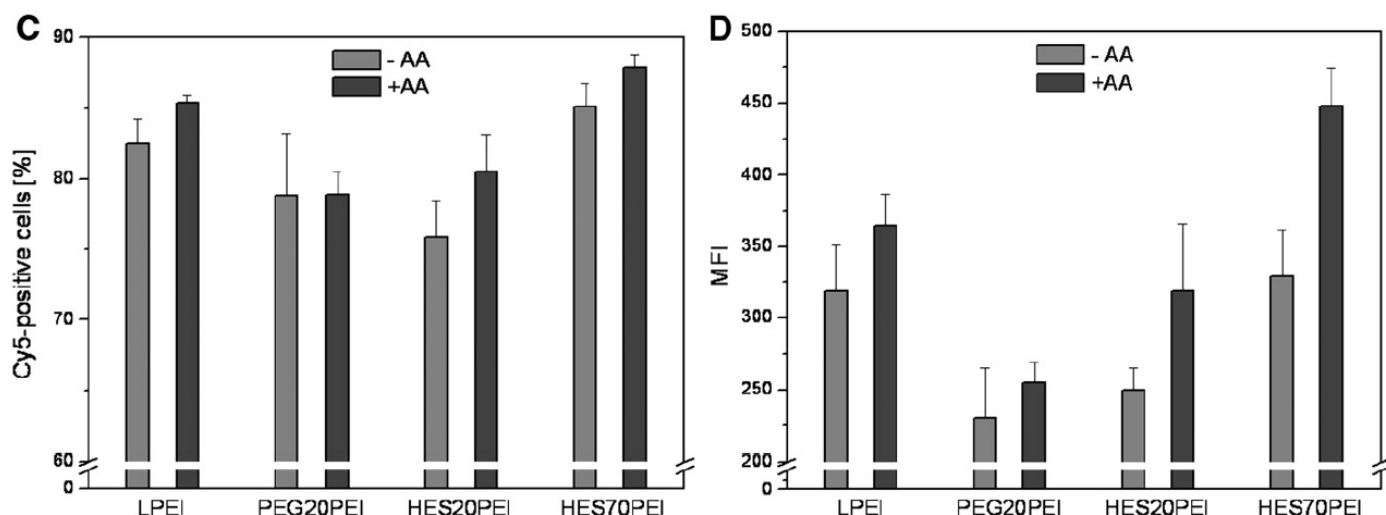


Figure II. 10. Binding (A and B) and uptake (C and D) of the polyplexes studied using flow cytometry. The percentage of Cy5 positive cells (A and C) and the mean fluorescence intensity (B and D) for Neuro2A cells incubated with HES20- or HES70-decorated polyplexes (10:90 HES-PEI:PEI) at 4°C for 30 min (Binding, A and B) or at 37°C for 1 h (Uptake C and D) with/without AA. Naked PEI- and PEGylated- polyplexes (10:90 PEG-PEI:PEI) served as controls.

4 Discussion

Li and Huang pointed out the importance of effective shielding and subsequent shedding of the PEG coat for successful tumor targeting [50]. However, due to the many disadvantages of PEG, there is a continuous search for better cleavable or biodegradable alternatives. For instance, Romberg *et al.* used a protease-cleavable poly(hydroxyethyl-L-asparagine) to impart stealth properties to liposomes [25, 26]. The latter polymer is then deshielded extra- or intracellularly by the action of proteases. “Polymer masked-unmasked protein therapy” (PMUPT) from Duncan’s lab [27-29] uses dextrin to screen the activity of proteins or enzymes, which is then regained by enzymatic cleavage of dextrin. In this work, we propose the use of hydroxyethyl starch (HES) for the controlled shielding/deshielding of polyplexes for nucleic acid delivery. HES is a biodegradable water soluble polymer with protein repellant activity, and was thus suggested as a possible substitute for PEG [44]. Compared to the aforementioned biodegradable polymers, it has the advantage of tunable biodegradation rate through changing its molar mass and degree of hydroxyethylation. This proof-of-concept study investigates the feasibility of capitalizing on the biodegradation of HES to regulate the shielding/deshielding and transfection of DNA polyplexes.

To carry out the *in vitro* deshielding experiments, the use of blood serum would have been the optimum choice, but it would greatly complicate this feasibility study. Accordingly, it was decided to use porcine α -amylase (AA) for HES deshielding. The ability of AA to cleave HES under different test conditions *in vitro* was evaluated. The concentration of AA was kept constant at 40 U/L. Results in Figure II. 1 show that indeed AA could cleave HES *in vitro*, and that the rate and extent of degradation depend on the molar mass, and to a lesser extent on the presence of chlorides in the buffer [47], but was not dependent on the pH.

The synthesis of the HES-PEI copolymers was carried out by reductive amination according to Kircheis *et al* [45]. Linear PEI contains only secondary amines, and the ends are not primary amines, where one end contains the electrophilic initiator in the oxazoline polymerization; usually mesylate, while the other end contains a terminating hydroxyl group [51]. Those secondary amines are less reactive towards reductive amination, necessitating a large excess of the polysaccharide (up to 25 times molar excess). The synthesized polymers were characterized using ^1H NMR, colorimetric copper assay (for the determination of PEI content in the conjugates) as well as SEC. The different characterization methods confirmed the successful conjugation, and the highly congruent results of the proton NMR and copper assay showed that the polymers were synthesized with molar ratios of 1.44:1 and 2.35:1 for HES20:PEI22 and HES70:PEI22, respectively (see Table II. 1).

A considerable part of the study was then dedicated to the investigation of the shielding of the polyplexes with HES and deshielding using AA. Shielding could be shown by the effect of HES coating on the zeta potential. The latter is the measure of electronic potential at the slip plane between the bound solvent layer at the particle's surface and the bulk solution. With the increase of this layer, for instance by adsorption or coupling of a nonionic hydrophilic polymer, the (absolute value of) zeta potential decreases [52]. This effect was observed for all the hydrophilic polymers tested, with the reduction in zeta potential (i.e. shielding) more pronounced for HES70>PEG20>HES20 (Figure II. 4). Additionally, the shielding effect could be shown by prevention of erythrocyte aggregation (Figure II. 7) as well as the reduction of transfection efficiency of the HES- and PEG-coated polyplexes in Neuro2A and HUH7 cells (Figure II. 8). In those transfection experiments, the increase in the amount of HES on the particle surface seemed to even reduce the transfection efficiency more effectively. Finally, the flow cytometry results show that HES and PEG could reduce the non-specific association both during binding and uptake. All these results show that HES can act

as a shielding polymer conferring some stealth characters to the nanoparticles. These results are in accordance with previously reported experiments, which showed that hydrophobically-modified HES adsorbed on PLGA nanoparticles, and could reduce protein adsorption and particle phagocytosis by murine macrophages [52].

Deshielding of HES-decorated polyplexes using AA was shown using a number of techniques. Addition of 40 U/L of AA to HES70-decorated polyplexes increased the zeta potential gradually over 1 h due to degradation of the HES coat and reduction of the bound polymer layer (Figure II. 6). The effect could be observed with different ratios of HES-PEI to PEI, where the higher amounts of HES-PEI show better shielding and lower plateau after degradation. Additionally, addition of AA to the HES70-shielded polyplexes led to decrease of the particle size by 5-7 nm (Figure II. 6). Incubation of RBCs with the HES70- or HES20-polyplexes in the presence of AA also led to an increased tendency in erythrocyte aggregation (Figure II. 7). Addition of AA to the culture media during cell transfection led to 2-3 orders of magnitude increase in the transfection of luciferase reporter gene, both in Neuro2A and HUH7 cells (Figure II. 8). Evaluation of the effect of amylase activity revealed that the higher amylase activity affects the kinetics of HES degradation and the rate of deshielding, but not the extent of cell transfection (Figure II. 9). The employed amylase activities in this study (40 and 100 U/L) are relevant to the clinical serum amylase levels (60 - 310 U/L) and show that indeed the deshielding of the polyplexes can occur at the serum amylase activities encountered *in vivo*, and that degradation kinetics can be an important factor for controlling delivery *in vitro* and *in vivo*. Finally, the uptake experiment using flow cytometry shed some light on the possible mechanisms of transfection after the action of amylase on the HES-shielded polyplexes (Figure II. 10). Results show that, although the addition of AA did not increase the percentage of transfected cells, the amount of delivered DNA per cell increased by 28 % and 36 % for HES20 and HES70, respectively. Additionally, an enhancement of the endoplasmic escape (in comparison to the non-degradable PEG) as reported by Nie *et al* [18] is quite probable. It is worth noting that, the deshielding effect of AA on the HES-decorated polyplexes was specific, since it did not have any statistically significant effect on the controls used, namely naked polyplexes or PEGylated polyplexes.

Having shown the feasibility of using HES and AA to regulate the shielding and deshielding of DNA polyplexes, future publications will present the *in vivo* behavior of HES-coated polyplexes, as well as the effect of molar mass, degree of hydroxyethylation and amount of polymer in the HES corona on the transfection efficiency.

5 Conclusions

The results presented in this work show, for the first time, the possibility of using HES for the shielding and controlled enzymatically-catalyzed deshielding of DNA polyplexes. HES20 and HES70 were grafted onto linear PEI22 via Schiff's base formation and reductive amination. The generated HES-g-PEI copolymers were characterized by ^1H NMR, copper-assay, and SEC, where all methods verified the successful coupling of HES to PEI, with molar ratios of 2.35:1 and 1.44:1 for HES70-g-PEI22 and HES20-g-PEI22, respectively. HES conjugates were used to form stable polyplexes with plasmid DNA, and their biophysical characterization at different N/P ratios revealed that both hydrodynamic diameter and surface charge were similar to PEGylated conjugates. The effect of amylase on zeta potential of HESylated nanoparticles was tested *in vitro*, showing a gradual increase in the surface charge of the nanoparticles over 1 h, indicating effective enzymatic deshielding. Furthermore, addition of amylase to mixtures of HESylated polyplexes and erythrocytes lead to erythrocyte aggregation, while aggregation did not occur in the absence of amylase. *In vitro* transfection experiments were performed on 2 cell-lines \pm AA in the culture medium. The proof-of-concept experiments revealed that addition of AA to the cell culture medium increased the transfection efficiency of HES-coated particles 2-3 orders of magnitude, while it had no effect on PEG-coated or the uncoated particles. Flow cytometry experiments showed that the addition of AA increased the amount of delivered DNA per cell. In brief, HES-PEI copolymers can be used for the controlled shielding/deshielding of polyplexes for gene delivery. The possibility to control the rate of HES biodegradation by varying its molecular weight and molar substitution offers a great potential for engineering the polyplexes and their site of degradation.

6 Acknowledgements

Funding by DFG Cluster of Excellence "Nanosystems Initiative Munich" (to E.W.) is gratefully acknowledged. The constructive comments and suggestions of the anonymous reviewers are highly appreciated.

7 References

1. **Friedmann, T. and R. Roblin**, Gene Therapy for Human Genetic Disease? *Science*, 1972. 175(4025): p. 949-955.
2. **Iyer, A.K., G. Khaled, J. Fang, and H. Maeda**, Exploiting the enhanced permeability and retention effect for tumor targeting. *Drug Discovery Today*, 2006. 11(17-18): p. 812-818.
3. **Maeda, H., T. Sawa, and T. Konno**, Mechanism of tumor-targeted delivery of macromolecular drugs, including the EPR effect in solid tumor and clinical overview of the prototype polymeric drug SMANCS. *Journal of Controlled Release*, 2001. 74(1-3): p. 47-61.
4. **Merdan, T., K. Kunath, H. Petersen, U. Bakowsky, K.H. Voigt, J. Kopecek, and T. Kissel**, PEGylation of Poly(ethylene imine) Affects Stability of Complexes with Plasmid DNA under in Vivo Conditions in a Dose-Dependent Manner after Intravenous Injection into Mice. *Bioconjugate Chemistry*, 2005. 16(4): p. 785-792.
5. **Kursa, M., G.F. Walker, V. Roessler, M. Ogris, W. Roedel, R. Kircheis, and E. Wagner**, Novel Shielded Transferrin–Polyethylene Glycol–Polyethylenimine/DNA Complexes for Systemic Tumor-Targeted Gene Transfer. *Bioconjugate Chemistry*, 2003. 14(1): p. 222-231.
6. **Nicolazzi, C., N. Mignet, N. de la Figuera, M. Cadet, R.T. Ibad, J. Seguin, D. Scherman, and M. Bessodes**, Anionic polyethyleneglycol lipids added to cationic lipoplexes increase their plasmatic circulation time. *Journal of Controlled Release*, 2003. 88(3): p. 429-443.
7. **Santel, A., M. Aleku, O. Keil, J. Endruschat, V. Esche, G. Fisch, S. Dames, K. Löffler, M. Fechtner, W. Arnold, K. Giese, A. Klippel, and J. Kaufmann**, A novel siRNA-lipoplex technology for RNA interference in the mouse vascular endothelium. *Gene Ther*, 2006. 13(16): p. 1222-1234.
8. **Harris, J.M. and R.B. Chess**, Effect of PEGylation on Pharmaceuticals. *Nature Reviews Drug Discovery*, 2003. 2: p. 214-221.
9. **Xu, L. and T. Anchordoquy**, Drug delivery trends in clinical trials and translational medicine: Challenges and opportunities in the delivery of nucleic acid-based therapeutics. *J Pharm Sci*, 2011. 100(1): p. 38-52.
10. **Müller, R.H., C. Jacobs, and O. Kayser**, Nanosuspensions as particulate drug formulations in therapy: Rationale for development and what we can expect for the future. *Advanced Drug Delivery Reviews*, 2001. 47: p. 3-19.
11. **Park, Y.S. and L. Huang**, Effect of Chemically Modified G(M1) and Neoglycolipid Analogs of G(M1) on Liposome Circulation Time - Evidence Supporting the Dysopsonin Hypothesis. *Biochimica et Biophysica Acta*, 1993. 1166(1): p. 105-114.
12. **Lynch, I. and K.A. Dawson**, Protein-nanoparticle interactions. *Nano Today*, 2008. 3(1-2): p. 40-47.
13. **Hatakeyama, H., H. Akita, and H. Harashima**, A multifunctional envelope type nano device (MEND) for gene delivery to tumours based on the EPR effect: A strategy for overcoming the PEG dilemma. *Advanced Drug Delivery Reviews*, 2011. 63(3): p. 152-160.
14. **Mishra, S., P. Webster, and M.E. Davis**, PEGylation significantly affects cellular uptake and intracellular trafficking of non-viral gene delivery particles. *European Journal of Cell Biology*, 2004. 83(3): p. 97-111.
15. **dlakha-Hutcheon, G., M.B. Bally, C.R. Shew, and T.D. Madden**, Controlled destabilization of a liposomal drug delivery system enhances mitoxantrone antitumor activity. *Nature Biotechnology*, 1999. 17(8): p. 775-779.

16. **Knorr, V., M. Ogris, and E. Wagner**, An Acid Sensitive Ketal-Based Polyethylene Glycol-Oligoethylenimine Copolymer Mediates Improved Transfection Efficiency at Reduced Toxicity. *Pharmaceutical Research*, 2008. 25(12): p. 2937-2945.
17. **Knorr, V., V. Russ, L. Allmendinger, M. Ogris, and E. Wagner**, Acetal linked oligoethylenimines for use as pH-sensitive gene carriers. *Bioconjugate Chemistry*, 2008. 19(8): p. 1625-1634.
18. **Nie, Y., M. Gunther, Z.W. Gu, and E. Wagner**, Pyridylhydrazone-based PEGylation for pH-reversible lipopolyplex shielding. *Biomaterials*, 2011. 32(3): p. 858-869.
19. **Walker, G.F., C. Fella, J. Pelisek, J. Fahrmeir, S. Boeckle, M. Ogris, and E. Wagner**, Toward Synthetic Viruses: Endosomal pH-Triggered Deshielding of Targeted Polyplexes Greatly Enhances Gene Transfer in vitro and in vivo. *Mol Ther*, 2005. 11(3): p. 418-425.
20. **Takae, S., K. Miyata, M. Oba, T. Ishii, N. Nishiyama, K. Itaka, Y. Yamasaki, H. Koyama, and K. Kataoka**, PEG-Detachable Polyplex Micelles Based on Disulfide-Linked Block Cationomers as Bioresponsive Nonviral Gene Vectors. *Journal of the American Chemical Society*, 2008. 130(18): p. 6001-6009.
21. **Hatakeyama, H., H. Akita, K. Kogure, M. Oishi, Y. Nagasaki, Y. Kihira, M. Ueno, H. Kobayashi, H. Kikuchi, and H. Harashima**, Development of a novel systemic gene delivery system for cancer therapy with a tumor-specific cleavable PEG-lipid. *Gene Ther*, 2006. 14(1): p. 68-77.
22. **Zhang, J.X., S. Zalipsky, N. Mullah, M. Pechar, and T.M. Allen**, Pharmacological attributes of dioleoylphosphatidylethanolamine/cholesterylhemisuccinate liposomes containing different types of cleavable lipopolymers. *Pharmacological Research*, 2004. 49(2): p. 185-198.
23. **Romberg, B., W.E. Hennink, and G. Storm**, Sheddable coatings for long-circulating nanoparticles. *Pharm.Res.*, 2008. 25(1): p. 55-71.
24. **Lee, Y., H. Koo, G.W. Jin, H.J. Mo, M.Y. Cho, J.Y. Park, J.S. Choi, and J.S. Park**, Poly(ethylene oxide sulfide): New poly(ethylene glycol) derivatives degradable in reductive conditions. *Biomacromolecules*, 2005. 6(1): p. 24-26.
25. **Romberg, B., F.M. Flesch, W.E. Hennink, and G. Storm**, Enzyme-induced shedding of a poly(amino acid)-coating triggers contents release from dioleoyl phosphatidylethanolamine liposomes. *International Journal of Pharmaceutics*, 2008. 355(1-2): p. 108-113.
26. **Romberg, B., C. Oussoren, C.J. Snel, M.G. Carstens, W.E. Hennink, and G. Storm**, Pharmacokinetics of poly(hydroxyethyl-L-asparagine)-coated liposomes is superior over that of PEG-coated liposomes at low lipid dose and upon repeated administration. *Biochimica et Biophysica Acta-Biomembranes*, 2007. 1768(3): p. 737-743.
27. **Duncan, R., H.R.P. Gilbert, R.J. Carbajo, and M.J. Vicent**, Polymer masked-unmasked protein therapy. 1. Bioresponsive dextrin-trypsin and -melanocyte stimulating hormone conjugates designed for alpha-amylase activation. *Biomacromolecules*, 2008. 9(4): p. 1146-1154.
28. **Ferguson, E.L. and R. Duncan**, Dextrin-Phospholipase A(2): Synthesis and Evaluation as a Bioresponsive Anticancer Conjugate. *Biomacromolecules*, 2009. 10(6): p. 1358-1364.
29. **Hardwicke, J., E.L. Ferguson, R. Moseley, P. Stephens, D.W. Thomas, and R. Duncan**, Dextrin-rhEGF conjugates as bioresponsive nanomedicines for wound repair. *Journal of Controlled Release*, 2008. 130(3): p. 275-283.

30. **Audibert, G., M. Dormer, J.C. Lefèvre, J.F. Stoltz, and M.C. Laxenaire**, Rheologic Effects of Plasma Substitutes Used for Preoperative Hemodilution. *Anesthesia & Analgesia*, 1994. 78(4): p. 740-745.
31. **Sakr, Y., D. Payen, K. Reinhart, F.S. Sipmann, E. Zavala, J. Bewley, G. Marx, and J.-L. Vincent**, Effects of hydroxyethyl starch administration on renal function in critically ill patients. *British Journal of Anaesthesia*, 2007. 98(2): p. 216-224.
32. **Warren, B.B. and M.E. Durieux**, Hydroxyethyl starch: safe or not? *Anesthesia Analgesia*, 1997. 84(1): p. 206-212.
33. **Yoshida, M. and T. Kishikawa**, A Study of Hydroxyethyl Starch. Part II. Degradation-Sites of Hydroxyethyl Starch by Pig Pancreas alpha-Amylase. *Starch - Stärke*, 1984. 36(5): p. 167-169.
34. **Yoshida, M., T. Yamashita, J. Matsuo, and T. Kishikawa**, Enzymic Degradation of Hydroxyethyl Starch. Part I. Influence of the Distribution of Hydroxyethyl Groups on the Enzymic Degradation of Hydroxyethyl Starch. *Starch - Stärke*, 1973. 25(11): p. 373-376.
35. **Treib, J., J.F. Baron, M.T. Grauer, and R.G. Strauss**, An international view of hydroxyethyl starches. *Intensive Care Med*, 1999. 25(3): p. 258-68.
36. **Besheer, A., G. Hause, J. Kressler, and K. Mader**, Hydrophobically modified hydroxyethyl starch: synthesis, characterization, and aqueous self-assembly into nano-sized polymeric micelles and vesicles. *Biomacromolecules*, 2007. 8(2): p. 359-367.
37. **Besheer, A., H. Caysa, H. Metz, T. Mueller, J. Kressler, and K. Mäder**, Benchtop-MRI for in vivo imaging using a macromolecular contrast agent based on hydroxyethyl starch (HES). *International Journal of Pharmaceutics*, 2011. 417(1-2): p. 196-203.
38. **Besheer, A., T.C. Hertel, J. Kressler, K. Mader, and M. Pietzsch**, Enzymatically catalyzed HES conjugation using microbial transglutaminase: Proof of feasibility. *J Pharm Sci*, 2009. 98(11): p. 4420-4428.
39. **Orlando, M.**, Modification of proteins and low molecular weight substances with hydroxyethyl starch (HES). 2003, Justus Liebig Universität Giessen.
40. **Oupicky, D., M. Ogris, K.A. Howard, P.R. Dash, K. Ulbrich, and L.W. Seymour**, Importance of lateral and steric stabilization of polyelectrolyte gene delivery vectors for extended systemic circulation. *Mol Ther*, 2002. 5(4): p. 463-72.
41. **Schaffert, D., M. Kiss, W. Rodl, A. Shir, A. Levitzki, M. Ogris, and E. Wagner**, Poly(I:C)-mediated tumor growth suppression in EGF-receptor overexpressing tumors using EGF-polyethylene glycol-linear polyethylenimine as carrier. *Pharm Res*, 2011. 28(4): p. 731-41.
42. **Plank, C., K. Zatloukal, M. Cotten, K. Mechtler, and E. Wagner**, Gene transfer into hepatocytes using asialoglycoprotein receptor mediated endocytosis of DNA complexed with an artificial tetra-antennary galactose ligand. *Bioconjug Chem*, 1992. 3(6): p. 533-9.
43. **Nitsch, E.**, Process for the production of starch degradation products with a narrow molecular weight distribution. 1995, (Laevosan-Gesellschaft mbH, Austria). Application: US
44. **Besheer, A.**, Nanomedicines based on modified hydroxyethyl starch: From synthesis to in vivo evaluation, in *Naturwissenschaftliche Fakultät I, Biowissenschaften*. 2009, Martin-Luther-Universität, Halle-Wittenberg: Halle-Wittenberg.
45. **Kirchheis, R., L. Wightman, A. Schreiber, B. Robitza, V. Rossler, M. Kurs, and E. Wagner**, Polyethylenimine/DNA complexes shielded by transferrin target gene expression to tumors after systemic application. *Gene Therapy*, 2001. 8(1): p. 28-40.
46. **Ungaro, F., G. De Rosa, A. Miro, and F. Quaglia**, Spectrophotometric determination of polyethylenimine in the presence of an oligonucleotide for the

- characterization of controlled release formulations. *Journal of Pharmaceutical and Biomedical Analysis*, 2003. 31(1): p. 143-149.
47. **Caldwell, M.L. and J.-f.T. Kung**, A Study of the Influence of a Number of Factors upon the Stability and upon the Activity of Pancreatic Amylase¹. *Journal of the American Chemical Society*, 1953. 75(13): p. 3132-3135.
48. **Wollrab, A.**, *Organische Chemie*, Springer-Verlag, Editor. 2009: Berlin Heidelberg. p. 495, 496.
49. **Bretoniere, J.P., R. Rej, P. Drake, A. Vassault, and M. Bailly**, Suitability of control materials for determination of alpha-amylase activity. *Clin.Chem*, 1981. 27(6): p. 806-815.
50. **Li, S.D. and L. Huang**, Stealth nanoparticles: High density but sheddable PEG is a key for tumor targeting. *Journal of Controlled Release*, 2010. 145(3): p. 178-181.
51. **Hoogenboom, R., M.W. Fijten, C. Br.,ndli, J. Schroer, and U.S. Schubert**, Automated Parallel Temperature Optimization and Determination of Activation Energy for the Living Cationic Polymerization of 2-Ethyl-2-oxazoline. *Macromolecular Rapid Communications*, 2003. 24: p. 98-103.
52. **Besheer, A., J. Vogel, D. Glanz, J. Kressler, T. Groth, and K. Mader**, Characterization of PLGA Nanospheres Stabilized with Amphiphilic Polymers: Hydrophobically Modified Hydroxyethyl Starch vs Pluronic. *Mol.Pharm*, 2009. 6 (2): p. 407-415.

III The effect of molar mass and degree of hydroxyethylation on the controlled shielding and deshielding of hydroxyethyl starch-coated polyplexes

This chapter has been published in *Biomaterials*:

Noga M*, Edinger D, Kläger R, Wegner SV, Spatz JP, Wagner E, Winter G, Besheer A**.

The effect of molar mass and degree of hydroxyethylation on the controlled shielding and deshielding of hydroxyethyl starch-coated polyplexes. *Biomaterials* 2013; 34(10):2530-2538.

* First author

** Corresponding author

The following work published in *Biomaterials* would not have been possible without our engaged cooperation partners:

Prof. Dr. Joachim P. Spatz and Dr. Seraphine V. Wegner are acknowledged for making possible my research stay in Heidelberg and for using their QCM device (Q-Sense) for studying the enzymatic biocleavage of HES-PEI copolymers.

Prof. Dr. Ernst Wagner is kindly acknowledged for the brilliant scientific advice and for the access to cell culture and animal studies and to all other required analytical tools in the research field of polymeric delivery of nucleic acids. All cell culture experiments, namely studies of the luciferase reporter gene expression and the metabolic activity of transfected cells were performed together with Daniel Edinger under his guidance. All veterinary work associated with the animal studies were conducted by Raphaela Kläger and Daniel Edinger, subsequent organ preparation and luciferase reporter gene expression studies were performed together with Raphaela Kläger and Daniel Edinger.

Abstract

PEGylation is currently the gold standard in shielding cationic DNA-polyplexes against non-specific interaction with blood components. However, it reduces cellular uptake and transfection, in what is known as the “PEG dilemma”. In an approach to solve this problem we developed nano-dandelions: hydroxyethyl starch (HES)-shielded polyplexes which get deshielded under the action of alpha amylase (AA). In this study, the effect of molar mass and degree of hydroxyethylation on the shielding and deshielding of the polyplexes as well as their *in vivo* performance were investigated. For this purpose, a battery of HES-polyethylenimine (PEI) conjugates was synthesized, and their rate and extent of biodegradation was investigated using asymmetric flow-field flow fractionation (AF4) and quartz-crystal microbalance with dissipation (QCM-D). Additionally, the transfection efficiency of the polyplexes was tested in Neuro2A cells and tumor-bearing mice. AF4 and QCM results show a rapid degradation for HES with lower degrees of hydroxyethylation. Meanwhile, *in vitro* transfection experiments showed a better shielding for higher HES molar masses, as well as deshielding with a significant boost in transfection upon addition of AA. Finally, *in vivo* experiments showed that the biodegradable HES markedly reduced the non-specific lung transcription of the polyplexes, but maintained gene expression in the tumor, contrary to the non-degradable HES and PEG controls, which reduced both tumor and lung expression. This study shows that by controlling the molecular characteristics of HES it is possible to engineer the shielding and deshielding properties of the polyplexes for more efficient gene delivery.

Keywords

Hydroxyethyl starch (HES), linear polyethylenimine (LPEI), gene delivery, biodegradable coating, amylase, quartz crystal microbalance (QCM-D)

1 Introduction

Designing carriers for safe and efficient delivery of therapeutic genes offers great potential for the treatment of many difficult-to-cure diseases, such as metastatic cancer. Although the use of viral carriers shows very high efficiency in gene transfection, their application is limited due to several safety concerns, most importantly the potential for flawed insertion of the virally-carried genetic material into the human genome, associated with the risk of developing cancer [1, 2], as well as the high incidence of immunogenic responses to recombinant viruses [3-5] possibly leading to death [6]. Meanwhile, polymeric carriers are extensively studied as possible alternatives to viral carriers, with poly(ethylene imine) (PEI) as the gold-standard, since it shows a high nucleic acid transfection efficiency [7]. The latter efficiency is due to 1) its high ability to compact DNA into nano-sized particles, 2) the high PEI-mediated cellular uptake due to its high surface charge, and 3) its capacity for endosomal release [7-9]. However, PEI-based polyplexes show non-specific interactions with blood components and cells, leading to aggregation and accumulation in the lung [10]. Despite the successful use of polyethylene glycol (PEG) to reduce these effects [11, 12], PEGylation compromises the cellular uptake and endosomal release, leading to lowered transfection efficiency *in vitro* and *in vivo* [13], in what is known as the “PEG-dilemma” [14]. Accordingly, several groups developed sheddable PEG-coats by incorporating labile linkers, which lead to shedding the disturbing PEG molecules in response to several stimuli, such as temperature, pH, reducing environment or tumor-specific enzymes [15-22].

We previously described an alternative approach for the controlled shielding and enzymatically-catalyzed deshielding of polyplexes using hydroxyethyl starch (HES) and α -amylase (AA) [23]. In the later proof-of-concept study, the developed HES-decorated core-shell nanoparticles showed effective shielding and reduced transfection *in vitro*, as well as deshielding and activation after partial cleavage of the HES-coat by AA. In the current study, we investigate the effect of HES' molecular characteristics, namely molar mass and degree of molar substitution of hydroxyethyl groups on the rate and extent of biodegradation, as well as the shielding and deshielding characteristics of the polyplexes. Additionally, gene expression was evaluated in tumor-bearing mice to show the feasibility of this approach *in vivo*. LPEI and PEG20-PEI polymers served as controls in most of the experiments.

2 Experimental Section

2.1 Materials

HES70[0.5] with an average molar mass (M_w , nominal value as provided by supplier, number after HES) of 70 kDa and a molar substitution (MS = the mean number of hydroxyethyl groups per glucose unit; nominal value as provided by supplier, number in square brackets) of 0.5 was kindly provided by Serumwerk Bernburg, Germany [23]. HES10[1.0], HES30[0.4], HES30[1.0], HES60[0.7], HES60[1.0] and HES60[1.3] were kindly provided by Fresenius Kabi, Friedberg, Germany. Linear polyethylenimine (LPEI) with an average molar mass of 22 kDa and the PEG20-PEI conjugate (PEG20: polyethylene glycol with an average molar mass of 20 kDa) were synthesized as described in Ref. [24]. α -amylase (AA) from porcine pancreas was bought from Sigma-Aldrich (Steinheim, Germany, catalogue number A3176). Plasmid pCMVluc [25] was prepared by PlasmidFactory, Bielefeld, Germany. Phadebas[®] Amylase Test was purchased from Magle AB, Lund, Sweden. Other solvents and chemicals were reagent grade and were used as received.

2.1.1 Synthesis and characterization of HES-PEI conjugates.

The different HES molecules were used to synthesize a library of HES-PEI conjugates, which were characterized according to Ref. [23]. PEI was attached to HES via Schiff's base formation between HES' reducing ending group and PEI's amino groups, followed by reductive amination. Briefly, 50 mg linear PEI were mixed with HES in 150 mM PBS buffer (pH 7.4). After 2 h, 59.8 mg of NaBH₃CN were added for reductive amination over 20 h. Ion exchange chromatography was carried out to remove unbound HES using a cation-exchange column (Bio-Rad Macro-Prep high S HR 10/10, Hercules, CA, USA) and fractionated using a sodium chloride gradient from 0.5 M to 3.0 M NaCl concentration in 20 mM HEPES, pH 7.3. The collected fractions were dialyzed against highly purified water (Cellu Sep T1, nominal MWCO 3500 Da, Membrane Filtration Products Inc, Seguin, TX, USA), then lyophilized. HES-PEI copolymers were characterized by ¹H NMR, colorimetry (using copper assay), and SEC as previously described [23].

2.1.2 Investigation of the biodegradation of HES homopolymers with AA using AF4-MALS

Several HES homopolymers differing in their molar mass and molar substitution were dissolved at a concentration of 5 mg/mL in PBS pH 7.4. 100 μ L sample volume was injected into the AF4 channel assembly, with a regenerated cellulose ultrafiltration membrane (Wyatt Technology, cut-off 5 kDa). All samples containing pancreatic AA were adjusted to an enzyme activity of 100 U/L using the Phadebas[®] Amylase Test. Mixtures were incubated at 25 °C, and samples were withdrawn at time points 0, 0.5, 1, 2, 4, 6, and 24 h. To stop the enzymatic degradation of HES, samples were heated to 99°C for 3 min. All samples and controls (without AA) were treated under aseptic conditions with sterile filtration to prevent possible degradation caused by microbial contamination. The reduction in the molar mass of HES was followed by the Wyatt Eclipse 2 AF4 system (Wyatt Technology Corp., Santa Barbara, CA) in combination with MALS (DAWN EOS MALS, Wyatt Technology Corp.)- and RI-detection (Agilent Technologies, Palo Alto, CA).

2.1.3 Quartz crystal microbalance with dissipation (QCM-D)

The Q-Sense E4 instrument (Q-Sense, Gothenburg, Sweden) was used for the investigations on the enzymatic degradation of HES in the different HES-PEI conjugates. Prior to each measurement, the silica-coated QCM-D sensor crystals (Qsx 303, Q-Sense) were washed with 2% SDS solution and treated with oxygen plasma (0.4 mbar, 150 W) for 45 minutes (TePla 100 System, Feldkirchen, Germany) to decontaminate the crystal surface. The system was operated at 25°C in the flow mode, interrupted by phases of no flow. A single QCM-D run comprised the following five steps: 1) System rinsing with buffer (15 min.), 2) polymer adsorption onto the SiO₂ sensor (5 min. sample flow, 10 min. no flow), 3) system rinsing with buffer under flow (15 min.), 4) start of enzymatic degradation by supplementation of α -amylase (5 min. sample flow, 55 min. no flow), and 5) system rinsing with buffer under flow (15 min.). A battery of HES-PEI copolymers was tested with the special focus on HES' molar mass and degree of hydroxyethylation (HES30[0.4]-PEI, HES30[1.0]-PEI, HES60[0.7]-PEI, HES60[1.0]-PEI, HES60[1.3]-PEI and HES70[0.5]-PEI). LPEI and PEG20-PEI served as controls. All polymers were applied at a concentration of 100 μ g/mL (based on LPEI) in HBG pH 7.1. The enzyme activity was set to 100 and 300 U/L (according to Phadebas[®] Amylase Test). To rule out polymer desorption, and to prove the enzyme-specific degradation, bovine serum albumin (BSA) was applied instead of AA as a negative control. The Sauerbrey

equation [26] was used to follow the adsorbed and desorbed mass onto the silica-coated quartz crystal. Changes in the mass Δm [ng/cm²] on the quartz surface are defined as:

$$\Delta m = \frac{-C \times \Delta f}{n}$$

whereas C is the mass-sensitivity constant (17.7 ng Hz⁻¹ cm⁻² for the 5 MHz quartz crystal), Δf [Hz] is the resonance frequency and n = 1, 3, 5, 7 is the overtone number. In the present analysis, the low overtone number 3 was used to avoid underestimation of the mass. QSoft 4.01 software was used for data acquisition, QTools for data analysis (both from Q-Sense, Sweden).

2.1.4 Preparation of HESylated polyplexes

Naked LPEI polyplexes (nPx) were prepared by mixing of PEI to the plasmid pCMVluc (pDNA) to a final DNA concentration of 20 µg/mL in HBG pH 7.4 at N/P ratio of 6.0, then incubated at room temperature (RT) for 30 minutes prior to analysis. For instance, naked polyplexes (nPx) were composed of 20 µg DNA and 16 µg PEI. HESylated polyplexes (and PEGylated control particles) were produced in the same fashion as nPx, with the exception that the unmodified PEI was partially replaced by HES-PEI or PEG-PEI, e.g. HES70[0.5]-PEI complexes with DNA at the molar ratio of HES-PEI to free PEI of 10:90 were made of 20 µg DNA, and a mixture of 14.4 µg free PEI and an amount of 8.475 µg HES70[0.5]-PEI equivalent 1.6 µg PEI. Similarly, polyplexes for *in vivo* experiments were made at a final DNA concentration of 200 µg/mL and N/P ratio 6.0.

2.1.5 Treatment of polyplexes with pancreatic α -amylase (AA)

The effect of pancreatic AA on the biophysical properties of polyplexes with HES60 decoration was investigated. HES60-decorated polyplexes were generated at the DNA concentration of 20 µg/mL in HBG pH 6.0, and at the N/P ratio of 6.0. HESylated polyplexes were prepared at the molar ratio 10:90 of PEI-conjugates to free PEI. After 30 min incubation of the polyplexes at room temperature, 100 µL of AA stock solution (amylase activity 1000 U/L) was added to 900 µL polyplex solution to give a final AA activity of 100 U/L, mixed intensively, and the resulting AA-polyplex mixture was analyzed using a Malvern Zetasizer Nano ZS (Malvern Instruments, Worcestershire, United Kingdom) instantly after combination of the enzyme and substrate. Analysis of particle size and zeta potential of PEI/DNA complexes was performed at time points 0, 0.25, 0.5, 1, 2, 4, and 6 h holding the polyplexes at

37 °C. Measurements of the particle size and the zeta potential were conducted in semi-micro PMMA disposable cuvettes (Brand, Wertheim, Germany) and in folded capillary cells (Malvern Instruments, Worcestershire, United Kingdom), respectively.

2.1.6 Cell culture experiments

Cell culture media, antibiotics and fetal calf serum (FCS) were purchased from Life Technologies (Karlsruhe, Germany). Cultured cells were grown at 37 °C in 5% CO₂ humidified atmosphere. Murine neuroblastoma, Neuro2A (ATCC CCL-131, purchased from DSMZ, Braunschweig, Germany) were cultured in Dulbecco's Modified Eagle Medium (DMEM). DMEM was supplemented with 10% FCS, 4 mM stable glutamine, 100 U/mL penicillin, and 100 µg/mL streptomycin.

2.1.7 *In vitro* luciferase reporter gene expression studies

In vitro pDNA transfection efficiency was evaluated in murine Neuro2A cells. Experiments were performed in 96 well plates by seeding 1×10^4 cells per well in 100 µL medium 24 h prior to transfection. Directly before transfection, the medium was exchanged against 90 µL fresh medium with/without pancreatic AA (100 U/L). An amount of 10 µL polyplex solution (N/P 6.0, 20 µg/mL DNA concentration, 10% and 25% molar ratio of conjugate to free PEI) was added to the cells. 4 h after transfection, the medium was replaced by fresh medium with/without AA. 24 h after pDNA transfection, the cells were treated with 100 µL cell lysis buffer (25 mM Tris pH 7.8, 2 mM EDTA, 2 mM DTT, 10% glycerol, 1% Triton X-100). Luciferase activity in 35 µL cell lysate was measured in white 96 well plates using a luciferase assay kit (100 µL Luciferase Assay buffer, Promega, Mannheim, Germany) on a luminometer for 10 s (Centro LB 960 instrument, Berthold, Bad Wildbad, Germany).

2.1.8 Metabolic activity of transfected cells

The cellular metabolic activity after pDNA transfection was evaluated using MTT assay. Cells were seeded and transfected as explained above. 24 h after transfection, MTT (3-(4,5-dimethylthiazol-2-yl)-2,5-diphenyltetrazolium bromide) (Sigma-Aldrich, Germany) was dissolved in phosphate buffered saline at 5 mg/mL, and 10 µL aliquots were added to each well reaching a final concentration of 0.5 mg MTT/mL. After an incubation time of 2 h, unreacted dye with medium was removed and the cells were lysed by incubation at -80 °C for

30 min. The formazan product was dissolved in 100 μ L/well dimethyl sulfoxide and quantified by a plate reader (Tecan, Groedig, Austria) at 590 nm with background correction at 630 nm. The metabolic activity (%) relative to control wells containing HBG treated cells was calculated as follows (Metabolic activity = $A_{\text{test}}/A_{\text{control}} \times 100$).

2.1.9 *In vivo* transfection with HESylated polyplexes in tumor-bearing mice

In vivo pDNA expression studies were evaluated in Neuro2A tumor-bearing A/J mice (6-8 weeks, female, Harlan Winkelmann). A number of 1×10^6 Neuro2A cells in 100 μ l PBS was inoculated subcutaneously into the flank of each mouse. Once the tumors reached the desired size of approximately 100 mm³, 250 μ L of polyplexes' solution were systemically administered via the tail vein. Two *in vivo* experiments were performed, where in the first one, the impact of the degradability of HES on gene expression in the lung and tumor was studied (n=5). For this purpose, nPx as well as polyplexes coated with HES70[0.5], HES60[1.3] and PEG20 were utilized. All polyplexes were generated at N/P ratio of 6.0 with a pCMVluc concentration of 200 μ g/mL in HBG, pH 7.4. Particles decorated with HES70[0.5], HES60[1.3], and PEG20 were prepared in the same molar ratio of HES or PEG to total PEI (i.e. free PEI plus conjugated PEI) (see Table III. 1), so as to rule out differences in the number of HES or PEG molecules attached per PEI molecule.

Table III. 1. Composition of various LPEI-based transfection particles used for the investigation of the effect of polymer biodegradability on *in vivo* transfection. It is expressed as the molar ratio of HES or PEG : total PEI as well as the molar ratio of HES-PEI or PEG-PEI : free PEI.

	Molar ratio of HES-PEI (or PEG-PEI) : free PEI	Molar ratio of HES (or PEG) : total PEI
LPEI	---	---
HES70-PEI[0.5]	10:90	0.27:1
HES60-PEI[1.3]	15:85	0.27:1
PEG20-PEI	20:80	0.27:1

In the second experiment, the effect of different HES amounts on the luciferase gene expression in the lung and tumor (n=4) was investigated using HES70[0.5]-PEI. HES70[0.5]-decorated polyplexes were prepared in the molar ratio of HES70[0.5]-PEI to free PEI of 10:90, 30:70 or 50:50 (i.e. 10, 30 or 50%, see Table III. 2). Naked and PEGylated polyplexes served as controls.

Table III. 2. *Composition of various LPEI-based transfection particles used for the investigation of the effect of amount of HES70[0.5]-PEI in the polyplexes on the in vivo transfection. It is expressed as the molar ratio of HES or PEG : total PEI as well as the molar ratio of HES-PEI or PEG-PEI : free PEI.*

	Molar ratio of HES-PEI (or PEG-PEI) to free PEI	Molar ratio of HES (or PEG) to total PEI
LPEI	---	---
HES70-PEI[0.5]	10:90	0.27:1
HES70-PEI[0.5]	30:70	0.81:1
HES70-PEI[0.5]	50:50	1.35:1
PEG20-PEI	30:70	0.81:1

In all experiments, animals were sacrificed 24 h after polyplex-injection, and the lung and tumor tissues were resected and stored at -80°C. Tissues were homogenized in cell culture lysis reagent (25 mM Tris, pH 7.8, 2 mM EDTA, 2 mM DTT, 10% glycerol, 1% Triton X-100) using a tissue and cell homogenizer (MP, FastPrep[®]-24, Solon, OH, United States), followed by a centrifugation step at 3000 g at 4°C for 10 min to separate insoluble cell components. 50 µl of the supernatants were transferred to white 96 well plates (TPP, Trasadingen, Switzerland) and luciferase activity was determined using a luciferase assay kit (100 µL Luciferase Assay buffer, Promega, Mannheim, Germany) and a Centro LB 960 luminometer (Berthold, Bad Wildbad, Germany). Luciferase transfection performance is expressed as relative light units (RLU) per mg organ.

3 Results

To study the effect of HES' molecular characteristics, namely its molar mass and degree of molar substitution on the shielding and deshielding of HES-decorated polyplexes, we synthesized a battery of HES-PEI conjugates, where the HES fraction covers a broad range of molar masses (ranging from 10-70 kDa) and molar substitutions (MS, from 0.4-1.3) (see Table III. 3).

Table III. 3. *HES-PEI conjugates and the amounts of HES coupled to PEI as determined by ^1H NMR and the colorimetric copper assay, using the methods described previously [23]. " M_w " represents the weight average molar mass as reported by the producer (in kDa), and "MS" is the degree of molar substitution.*

M_w (kDa)	MS	Amount of HES in HES-PEI		Amount of HES in HES-PEI	
		conjugates (^1H NMR)		conjugates (UV λ 285nm)	
		<i>Mass ratio [%]</i>	<i>Molar ratio</i>	<i>Mass ratio [%]</i>	<i>Molar ratio</i>
			<i>HES : PEI</i>		<i>HES : PEI</i>
10	1.0	35.12	1.36 : 1	28.04 ± 2.29	0.98 : 1
30	0.4	74.74	2.47 : 1	72.83 ± 1.06	2.24 : 1
30	1.0	50.39	0.85 : 1	51.01 ± 3.44	0.87 : 1
60	0.7	79.97	1.67 : 1	79.62 ± 1.44	1.63 : 1
60	1.0	75.40	1.28 : 1	76.01 ± 0.71	1.32 : 1
60	1.3	79.97	1.67 : 1	77.17 ± 4.51	1.41 : 1
70	0.5	88.20	2.68 : 1	88.31 ± 1.49	2.71 : 1

3.1 Biodegradation studies

Studying the AA-catalyzed degradation of the unmodified HES was performed using asymmetric flow field flow fractionation coupled to multi-angle light scattering (AF4-MALS), where the biodegradation experiments were performed using 100 U/L AA activity

(the normal activity of serum AA using the Phadebas[®] amylase test is between 60-310 U/L [27]). The absolute and relative degradation of various HES polymers as a function of incubation time in PBS pH 7.4 at 25 °C is illustrated in Figure III. 1. Control samples lacking the enzyme did not show any degradation (data not shown), while in the presence of AA, the degradation seemed to be rapid at the beginning, levelling-off after approximately 4-6 h. MS of HES had a clear impact on the rate and extent of the biodegradation, since polymers with the same molar mass but different MS showed higher degradation rates with lower MS. For instance, HES60[1.0] and HES30[1.0] lost approximately 5-10 % of their original molar mass after 6 h of treatment with the enzyme, while HES60[0.7] and HES30[0.4] lost around 25 % of their initial molar mass. Regarding the effect of molar mass on biodegradation, one observes that the rate and extent of degradation of HES70[0.5] is greater than HES30[0.4], despite their close MS. That might be an indication for better accessibility of α -1,4-glycosidic bonds of HES for AA in the case of the larger HES molecule.

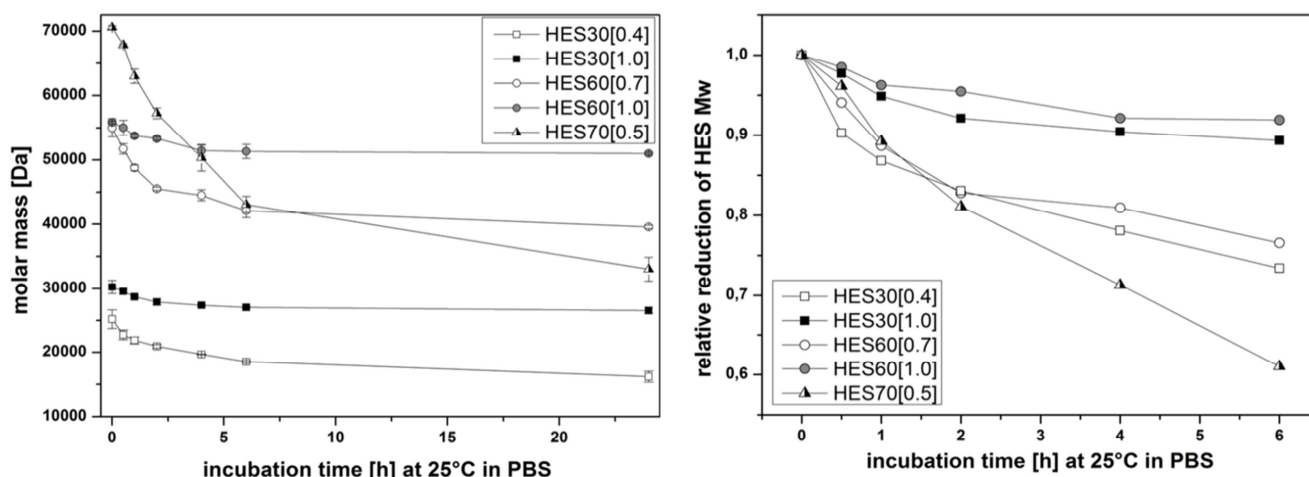


Figure III. 1. Enzymatic biodegradation of HES using 100 U/L of AA as a function of time, with the decrease in HES' molar mass as a function of incubation time (left), and the relative reduction in weight average molar mass as a function of incubation time (right).

In order to study the kinetics and extent of degradation of HES in the different HES-PEI polymers, quartz crystal microbalance with dissipation (QCM-D) was used. In this setup, the positively charged PEI residues adsorb to the negatively charged SiO₂-coated quartz crystal, while the HES molecules extend into the aqueous buffer, simulating the situation of the thin brush layer of HES at the surface of the polyplexes. The experiments involved 1) system

rinsing with buffer, 2) adsorption of HES-PEI conjugates on the SiO₂-coated quartz crystals, 3) washing off any unadsorbed polymers, 4) introducing AA solution into the chamber and incubation for 60 min, and finally 5) washing off of the AA solution. The changes in adsorbed mass were calculated using the changes in the frequency according to the Sauerbrey equation [26]. As can be seen in Figure III. 2, all HES-PEI conjugates are adsorbed to the SiO₂ crystals and are not washed away by the buffer after step 3. As illustrated in Figure III. 2 A and B, MS has a considerable impact on HES' degradation profile, with higher extent and rate of cleavage of the α -1,4-glycosidic bonds of HES with lower MS. For instance, HES30[0.4]-PEI showed rapid degradation at the beginning, followed by a phase of slower loss of mass. Meanwhile, the higher substituted HES30[1.0]-PEI copolymer was degraded very slowly. After 1 h treatment with 100 U/L α -amylase, HES30[0.4]-PEI lost about 35% of its initial mass, while HES30[1.0]-PEI lost only 5.5%. Similarly, HES60-PEI conjugates were degraded by AA in the following order with respect to the degree of molar substitution: $0.7 > 1.0 > 1.3$ (loss of mass about 15.5%, 5.8%, and 0%, respectively). Accordingly, HES60[1.3] is considered to be practically non-cleavable by AA. Increasing the enzyme activity to 300 U/L resulted in a more distinctive degradation (faster and higher extent of degradation), especially in the case of lower hydroxyethylated polymers. Regarding the effect of molar mass, HES70[0.5]-PEI showed a faster and stronger degradation compared to HES30[0.4]-PEI, in a manner similar to AF4-MALS results. This indicates that, beside the MS of HES and AA activity, HES' molar mass probably has an impact on the extent and kinetics of the biodegradation too (Figure III. 2 C). Finally, a number of control experiments were performed to validate the observed results. The stability of AA was followed over time using the Phadebas[®] Amylase Test, where the assay proved full maintenance of the amylase activity for at least 2h. Additionally, the effect of AA on adsorbed LPEI22 and PEG20-PEI, both representing non-degradable polymers, as well as the use of bovine serum albumin instead of AA, did not show any changes in the mass (data not shown), confirming that the observed changes in mass were not due to desorption, but due to the enzyme-specific degradation of HES.

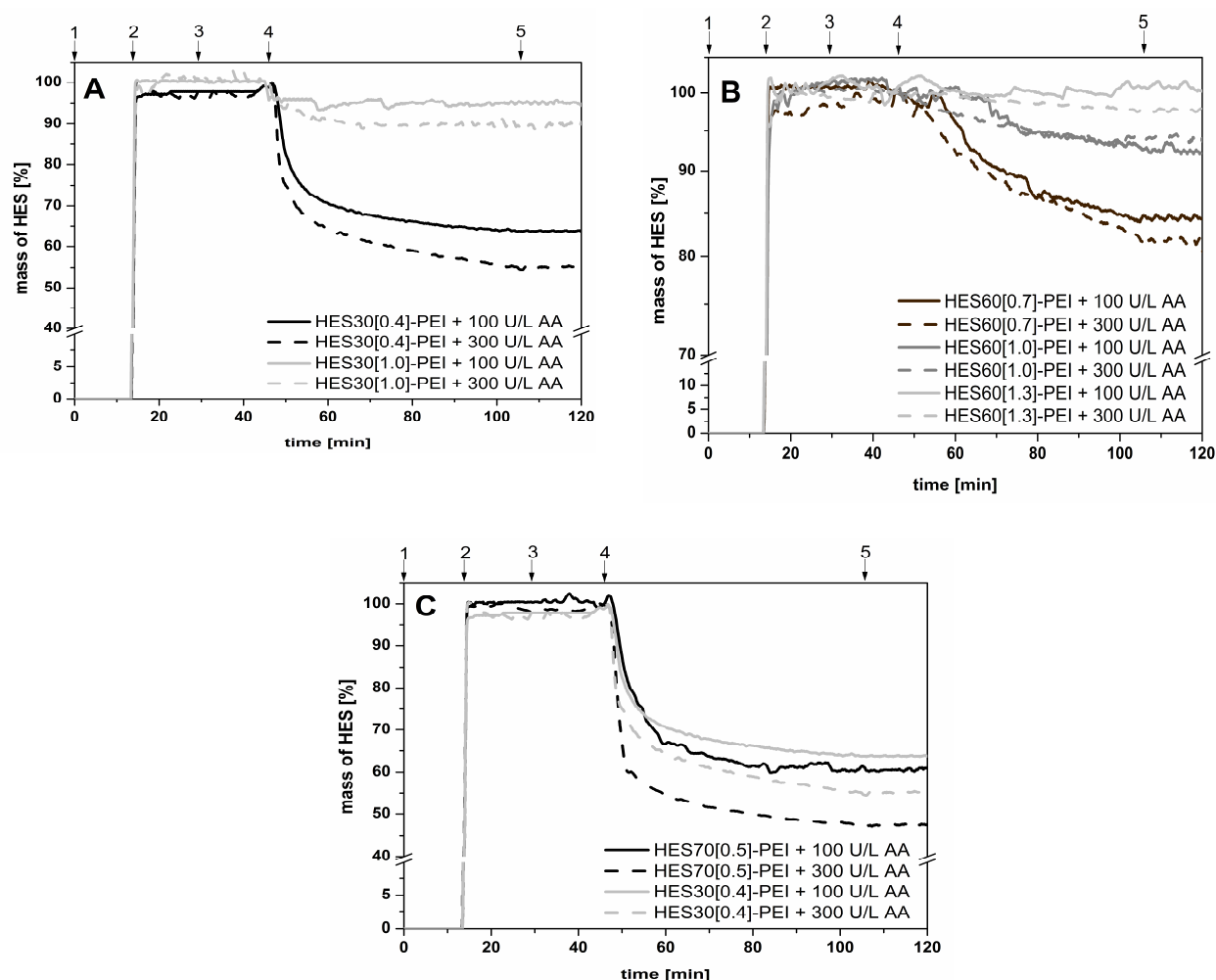


Figure III. 2. QCM-D measurements. Enzymatic degradation of HES30[0.4]-PEI and HES30[1.0]-PEI conjugates (A), HES60[0.7]-PEI, HES60[1.0]-PEI and HES60[1.3]-PEI conjugates (B) as well as HES70[0.5]-PEI in comparison to HES30[0.4]-PEI (C) as a function of time in the presence of α -amylase with 100 and 300U/L activity. Numbered arrows above the graphs highlight the 5 steps of the QCM-run; namely 1) system rinsing with buffer (15 min), 2) polymer adsorption onto SiO_2 sensor (15 min), 3) system rinsing with buffer (15 min), 4) introducing α -amylase solution into the chamber and incubation for 60 min, and 5) system rinsing with buffer (15 min).

The influence of HES' degradation on the biophysical properties of the polyplexes was investigated by monitoring the changes in the measured surface charge upon addition of AA as seen in Figure III. 3. Polyplexes formed using HES60[0.7]-PEI or HES60[1.0]-PEI, with the molar ratio of 10:90 HES-PEI to free PEI, were incubated with AA (activity of 100 U/L) for 6 h at 37°C and the zeta potential was measured. The zeta potential of HES60[0.7]-coated polyplexes increased gradually with time after addition of AA, and levelled-off after approximately 1-2 h (Figure III. 3, left). Meanwhile, HES60-decorated particles with MS of 1.0 (Figure III. 3, right) showed no increase of the surface charge over time. Similarly, no

effect of AA was observed on the zeta-potential of HES30-decorated particles (data not shown).

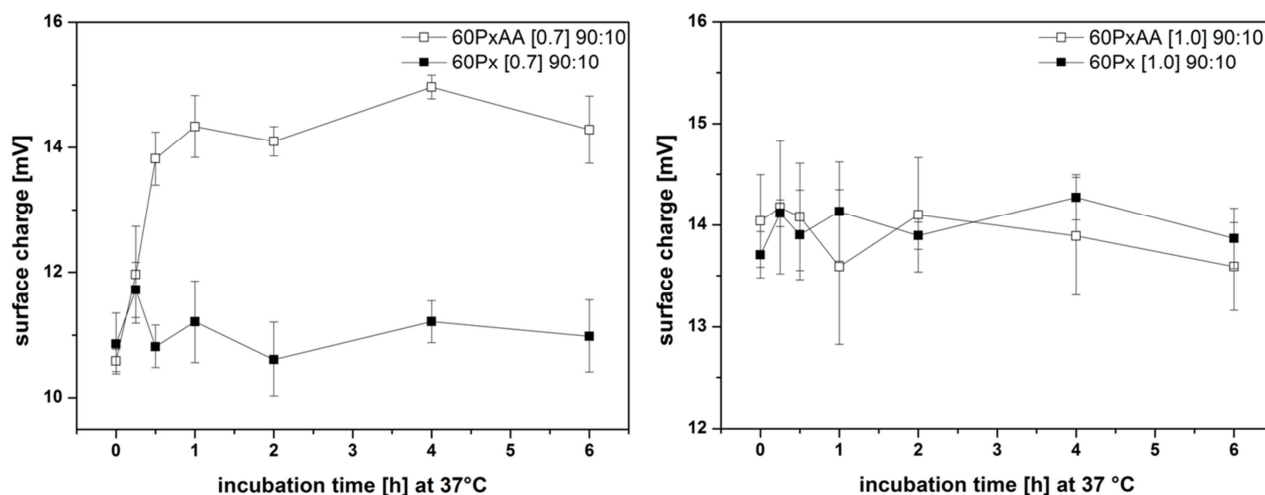


Figure III. 3. The effect of AA on biophysical characteristics of HESylated polyplexes. The surface charge of HES60[0.7]- (left) and HES60[1.0]-shielded (right) DNA polyplexes under the effect of AA as a function of time at 37 °C.

3.2 Effect of molar mass and degree of hydroxyethylation on the luciferase reporter gene transfection efficiency *in vitro*

The *in vitro* transfection efficiency of HES-decorated polyplexes was studied in Neuro2A cells incubated with DMEM in the presence or absence of 100 U/L AA. Results in Figure III. 4 A provide clues for the effect of molar mass and amount of HES on the particle shielding, as evidenced by the transfection efficiency in the absence of AA (light grey bars). One notices that the expression of the luciferase reporter gene decreases with the increase in molar mass and in the amount of HES-PEI, with a decrease of 1-3 orders of magnitude compared to the nPx in the case of 25% HES60- and HES70-coated polyplexes, while a lower shielding effect was observed for the low amounts of low molar mass HES (namely HES10-PEI and HES30-PEI with 10% HES-PEI:PEI) (see Figure III. 4 A). These results show that the molar mass and the amount of HES in the shell are indeed important parameters controlling the shielding of the polyplexes. Upon supplementation of AA, the HES-coat was degraded and the particles were “activated”, leading to an increase in luciferase gene expression by 1-3 orders of magnitude, whereas no effect could be observed for AA on the naked particles, as well as the particles shielded with non-degradable polymers, namely HES60[1.3] and PEG (Figure III. 4 A). Similarly, the polymers with a low extent of biodegradation as evidenced by AF4 and QCM-D, i.e. HES30[1.0] and HES60[1.0], show no effect on transfection upon addition of

AA. Meanwhile, the most prominent effect of AA-addition is clear for polyplexes having higher amounts of the large molar mass HES with low MS (i.e. those strongly shielded polyplexes with long, highly biodegradable polymer chains, namely HES60[0.7] and HES70[0.5]). These polyplexes showed the highest shielding effect, and accordingly the addition of AA and elimination of the HES coat effectively deshielded the particles to reach a transfection level similar to that of nPx. The HES30[0.4]-coated polyplexes, having short highly biodegradable HES molecules, showed an intermediate shielding as well as an intermediate effect of the deshielding enzyme on the transfection efficiency. These results are a clear indication for selective particle activation of HESylated nanoparticles using AA, as well as the important effect of molar mass, MS and amount of HES in the nanoparticle corona on both the effective shielding and deshielding of the particles. Finally, the viability of Neuro2A cells was not affected by incubation with the polyplexes, independent of the presence of the enzyme, indicating the relative safety of these polyplexes (Figure III. 4 B&C).

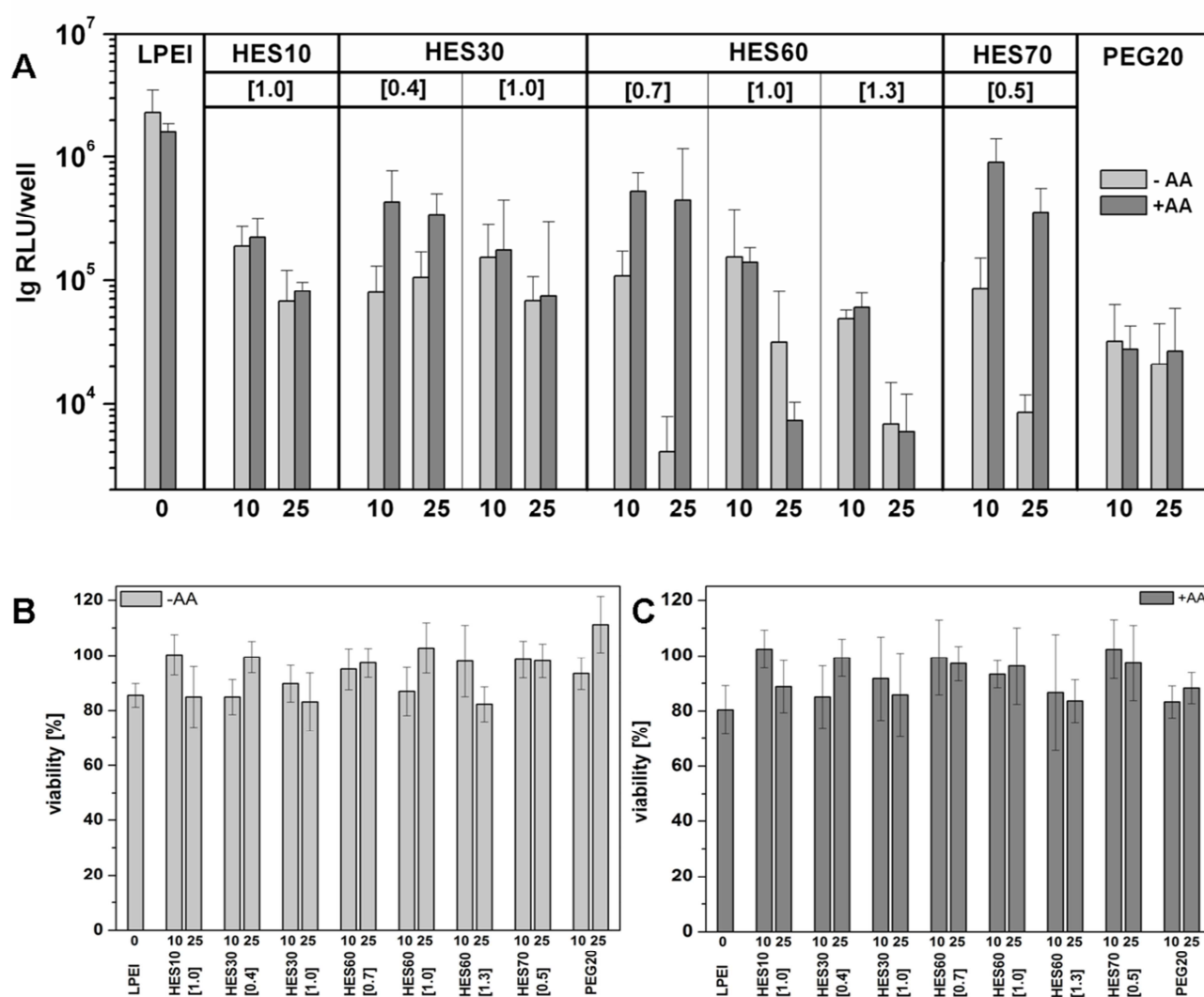


Figure III. 4. *Cell culture experiments – Luciferase reporter gene expression (A) and metabolic activity (B, C) in Neuro2A cells. Surface shielding and deshielding studies were performed in cell culture medium without AA (-AA) and with the enzyme (+AA) (A). The metabolic activity was determined for cells incubated with the polyplexes without AA (B) and with the enzyme (C). Analysis of the reporter gene expression and the corresponding metabolic activity was carried out 24h after polyplex treatment. (Numbers after HES represent the nominal molar mass of HES as provided by supplier, numbers in brackets are the nominal values for MS, while those numbers on the X-axis represent the mixing ratio of HES-PEI (or PEG-PEI) to free PEI in percentage, where 10% stands for 10:90 conjugate to free PEI).*

3.3 Gene transfer studies of HES-PEI polyplexes *in vivo*

To prove the *in vivo* feasibility of the shielding and deshielding concept, we compared polyplexes coated with HES70[0.5], a polymer that shows effective shielding and AA-catalyzed deshielding, against polyplexes coated with non-degradable polymers, namely HES60[1.3] and PEG20, as well as naked polyplexes. The naked polyplexes showed a high transfection efficiency in the lungs, indicating the formation of aggregates upon injection, which rapidly accumulate in the lungs (see Figure III. 5). Meanwhile, the incorporation of HES or PEG onto the polyplex surface reduced the gene expression in the lungs 2 to 4 orders of magnitude by surface shielding as illustrated in Figure III. 5. Meanwhile, by examining the tumor delivery of the different polyplexes, shielding the DNA polyplexes with the non-degradable HES60[1.3] or PEG20 resulted in a very low to complete loss of gene expression at the tumor site, while the use of the biodegradable HES70[0.5] showed a generally higher transfection efficiency compared to the naked polyplexes (with the exception of one animal which showed an exceptionally high tumor expression with the naked polyplexes, and accordingly an increase in the mean expression value).

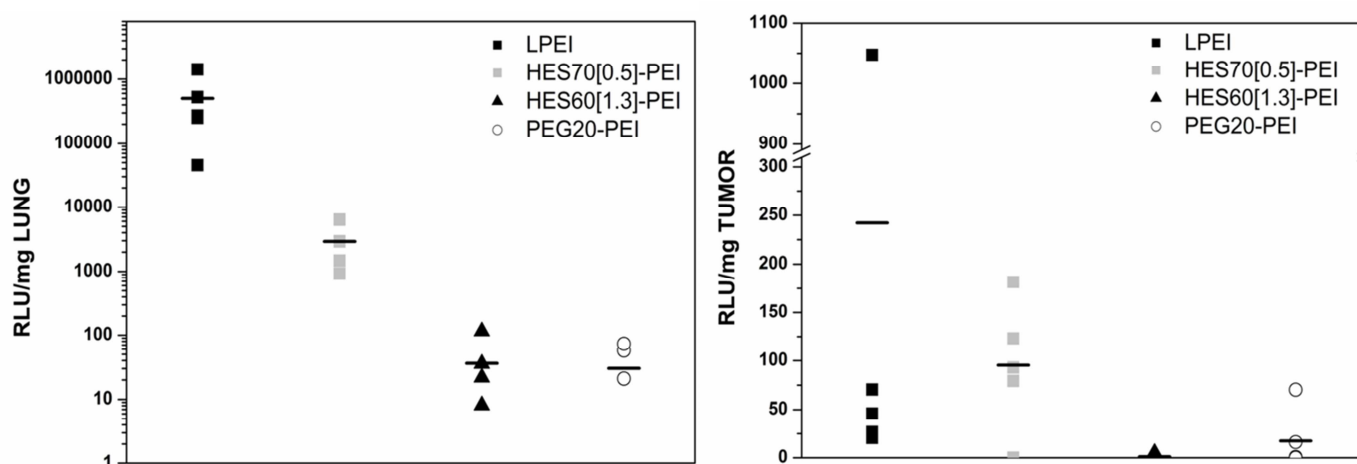


Figure III. 5. Gene expression in the lungs (left) and tumor tissue (right) in Neuro2A-tumor-bearing A/J mice after systemic administration of naked polyplexes, as well as polyplexes coated with HES70[0.5], HES60[1.3] and PEG20. The luciferase expression is presented as relative light units (RLU) per mg organ ($n=5$ per group), and the mean is represented as a short horizontal line.

Another *in vivo* experiment was performed with HES70[0.5]-coated polyplexes to investigate the effect of the amount of the biodegradable polymer on the transfection efficiency in the lung and the tumor. Results in Figure III. 6 show that, similar to the previous experiment, the naked LPEI-based DNA complexes strongly accumulated in the lung, while the HES- or PEG-decorated particles resulted in a strong decrease in lung expression by 3 to 4 orders of magnitude (see Figure III. 6), almost entirely blocking the luciferase gene expression in the lung. Polyplexes with the lowest investigated amount of HES70-PEI resulted in an almost 2-fold increase in luciferase expression in the tumor (illustrated in Figure III. 6, right) compared to nPx. Increasing the amount of HES70[0.5]-PEI three- or fivefold drastically reduced gene expression in the tumor, probably due to an incomplete deshielding of the higher amount of polymer in the particle corona, reaching expression level similar to the non-degradable PEG-coated polyplexes. To summarize, the best results were obtained using a low degree of HES70[0.5]-decoration. This lead-candidate reduced the luciferase gene expression in the lungs 3 orders of magnitude, while maintaining good expression-levels in the tumor compared to the unmodified particles.

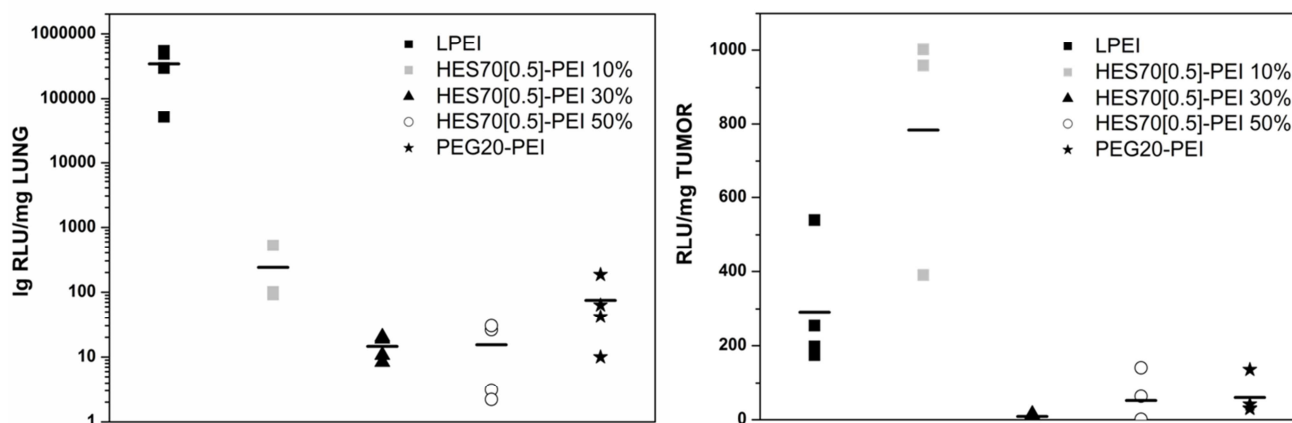


Figure III. 6. *In vivo* luciferase expression in the lung (left) and tumor (right) tissue in Neuro2A-tumor-bearing mice. An amount of 50 μ g pDNA (N/P ratio 6.0, with ratios of 10:90 (10%), 30:70 (30%) and 50:50 (50%) HES70[0.5]-PEI to free PEI, and 30:70 PEG20-PEI to free PEI was injected into the tail vein of A/J mice. Naked LPEI and PEGylated particles served as controls. The luciferase expression is presented as relative light units (RLU) per mg organ ($n=4$ animals per group), and the mean is represented as a short horizontal line.

4 Discussion

PEGylation of nanomedicines is the state-of-the-art-technique for imparting stealth character to nanocarriers and facilitating passive tumor targeting via the enhanced permeability and retention (EPR) effect [28, 29]. Similarly, the incorporation of the hydrophilic polymer PEG onto the surface of DNA-polyplexes increases their stability in the bloodstream and reduces the nonspecific interaction with blood components by the effect of surface charge shielding [11, 30, 31]. However, PEGylation of polymeric carriers for the delivery of nucleic acids reduces the gene expression by interfering with cellular uptake and endosomal release [13], both *in vitro* and *in vivo*. To overcome this PEG dilemma, many researchers have equipped PEGylated-systems with diverse labile bonds that enable shedding the disturbing PEG coat under the effect of various triggers [15-18, 20-22]. In a proof-of-concept study, we reported earlier on a novel molecular tool for tailored polyplex shielding and controlled enzymatic deshielding and activation using HES and α -amylase [23]. Building on our previous results, and in order to fine-tune the rate and extent of HES biodegradation and to harness this property for developing optimally designed polyplexes, we investigated the effect of molar mass and molar substitution on the shielding and deshielding of the polyplexes *in vitro* and *in vivo*.

Initially, the degradation rate and extent of different HES polymers under the effect of AA was studied in the case of the homopolymer using AF4-MALS, using QCM-D in the case of HES-PEI conjugates, and finally using zeta-potential measurements for the HES-coated polyplexes. AF4-MALS results show that the MS plays an important role in the kinetics and extent of the enzymatic cleavage of the α -1,4-glycosidic bonds of HES. These results were corroborated by the QCM experiments for the degradation of the different HES grades in the HES-PEI conjugates, where the polymers were adsorbed as a thin layer onto a SiO₂-coated quartz crystal, simulating the situation at the surface of the shielded polyplexes. Both analytical methods showed that the biodegradation of HES under the effect of AA was faster and to a greater extent for the low substituted HES polymers, MS 0.4, 0.5 and 0.7, getting slower and less efficient with increasing MS to 1.0, and totally blocked with an MS of 1.3. In some cases (such as HES30[0.4] and HES70[0.5]), a rapid initial degradation, followed by slower HES cleavage was observed, indicating that the easier accessible α -1,4-glycosidic bonds of HES were cleaved at the beginning, whereas the less accessible bonds were degraded slower (Figure III. 1 and Figure III. 2). In a further experiment, the impact of the MS on the enzymatically-catalyzed degradation of HES in case of the polyplexes was indirectly studied by monitoring the zeta potential of HES60-decorated polyplexes. Addition of AA led to a gradual increase of the zeta potential in case of HES60[0.7] similar to our previous results with HES70[0.5] coatings [23], but had no effect for the HES60[1.0] coating, indicating that indeed the lower MS facilitates significant cleavage of the glycosidic bonds and reduction in the molar mass of HES leading to increase in the zeta potential, while in case of HES60[1.0], and although the polymer is relatively biodegradable, the lower extent of degradation (as evidenced in AF4 and QCM experiments) leads to a non-significant decrease in zeta potential.

The effect of HES molar mass on its biodegradation is not unequivocal as that of MS. Comparing the biodegradation of HES30[0.4], HES70[0.5] and HES60[0.7], which have (to some extent) similar MS but different molar masses, one notices the highest rate of degradation in case of HES70[0.5] followed by HES30[0.4] then HES60[0.7] (see Figure III. 1 and Figure III. 2). The lack of a clear trend in the effect of molar mass could be due to the slight differences in the MS of the investigated polymers. Meanwhile, molar mass has a clear effect on the shielding of the polyplexes, evidenced by a decrease in zeta potential with the increase in molar mass, as was shown previously [23]. This explains why AA had a significant effect on the zeta potential of the HES60[0.7]-coated polyplexes (Figure III. 3), but not on those coated with HES30[0.4], although both are biodegradable as evidenced by AF4

and QCM. As the polyplexes covered with higher molar mass HES were better shielded, that gives room for the effect of enzymatic degradation to show a significant increase in zeta potential.

The observed effects of molar mass and MS have significant influences on the performance of the polyplexes *in vitro*, as evidenced by the transfection experiments using Neuro2A cells in the presence and absence of AA. In the absence of AA, polyplexes coated with high molar mass HES (i.e. HES60[0.7], HES60[1.0], HES60[1.3] and HES70[0.5]) showed a large reduction in luciferase expression compared to the naked polyplexes, and even lower transfection in relation to the polyplexes coated with the low molar mass HES, indicating that indeed the higher molar mass is effective in shielding the charge of the polyplexes as discussed above. Upon addition of AA, a 1-3 orders of magnitude increase in transfection efficiency is observed, most prominently for the biodegradable HES70[0.5] and HES60[0.7], and to a lesser extent with the low molar mass-low MS polymers (HES30[0.4]), and no increase was observed with all the high MS polymers (MS 1.0), and the non-degradable polymers (HES60[1.3] and PEG20). These results can be explained as follows: the high molar mass-low MS HES offers high shielding due to the large polymer chains (evidenced by a high reduction in zeta potential [23], and a high reduction in the transfection efficiency, compared to LPEI in the absence of AA) as well as high biodegradability due to the low MS (as seen in the AF4 and QCM-D results). Addition of AA degrades these highly shielded polyplexes leading to significant increase in the transfection efficiency. Polyplexes coated with low molar mass and low MS HES (HES30[0.4]) show a moderate increase in transfection, despite the fact that they have a highly biodegradable HES (as seen in AF4 and QCM-D) due to their originally low shielding (evidenced by their higher transfection efficiency in the absence of AA), so that the addition of AA does not have room to achieve a significant increase in zeta-potential or transfection. Similarly, the lack of increase in transfection in the HES60[1.0]-coated particles is due to the low degree of degradation as seen in the HES degradation experiments. Finally, the non-degradable polymers (HES60[1.3] and PEG20) as well as naked polyplexes did not show any response to the addition of AA, indicating the specificity of the effect of AA on biodegradable HES.

Finally, the *in vivo* transfection efficiency of the HES shielded polyplexes was tested in tumor bearing mice. In general, the systemic administration of naked LPEI-polyplexes results in an uncontrolled nucleic acid delivery to different organs, with the highest gene expression levels observed in the lung [32], due to the non-specific interaction with blood components and the associated aggregation. Results in Figure III. 5 and Figure III. 6 show that our shielding and

deshielding concept is a promising approach, maintaining particle stability in the bloodstream as well as their transfection efficiency at the tumor site by enzymatic deshielding. For instance, while all shielded polymers show up to 4 orders of magnitude reduction in luciferase expression in the lungs compared to the naked polyplexes, the biodegradable HES70[0.5] maintained the tumor expression similar to or higher than the naked polyplexes, in contrast to the non-degradable polymers HES60[1.3] and PEG20, which nearly abolished the tumor expression (Figure III. 5 and Figure III. 6). The amount of HES70[0.5] in the shell proved to be important too, since increasing this amount reduced the tumor expression significantly to levels similar to the non-degradable PEG20 (Figure III. 6).

5 Conclusions

This study was designed to investigate the effect of HES' molecular characteristics, namely molar mass and molar substitution (MS) on the shielding and deshielding of HES-coated polyplexes, as well as providing evidence for the *in vivo* feasibility of this approach. The AA-catalyzed biodegradation of HES was investigated on different HES homopolymers using AF4-MALS, and on a battery of synthesized HES-PEI conjugates using QCM-D, and finally on HES-decorated polyplexes using zeta potential measurements. Results from these experiments showed higher rates and extents of HES biodegradation in case of low MS, decreasing with the increase in MS, and completely abolished for MS 1.3. Meanwhile, the molar mass and amount of HES played an important role in the shielding of the polyplexes, as evidenced by the decrease in the *in vitro* transfection efficiency in Neuro2A cells with increasing molar mass or amount of HES. Deshielding the polyplexes by addition of AA leads to a 1-3 orders of magnitude increase in the transfection efficiency, particularly for the highly degradable (i.e. low MS) high molar mass polymers, while the non-degradable polymers showed no effect for AA, indicating the specific influence of AA on HES deshielding. Finally, the *in vivo* experiments showed that indeed the concept of HES-mediated shielding can lead to significant reduction in lung expression, while the AA-catalyzed deshielding can maintain or increase tumor transfection levels, as seen with the HES70[0.5]-coated polyplexes. In conclusion, this study shows the importance of the fine balance between molar mass, MS and the amount of HES in controlling the shielding and AA-catalyzed deshielding of HES-coated polyplexes, and proves for the first time, the feasibility of this approach for the *in vivo gene* delivery.

6 Acknowledgements

The authors would like to thank Fresenius Kabi Deutschland GmbH and Serumwerk Bernburg for providing the different HES samples.

7 References

1. **Hacein-Bey-Abina, S., C. von Kalle, M. Schmidt, F. Le Deist, N. Wulffraat, E. McIntyre, I. Radford, J.L. Villeval, C.C. Fraser, and M. Cavazzana-Calvo,** A serious adverse event after successful gene therapy for X-linked severe combined immunodeficiency. *New England Journal of Medicine*, 2003. 348(3): p. 255-256.
2. **Check, E.,** Gene therapy: a tragic setback. *Nature*, 2002. 420(6912): p. 116-118.
3. **Calcedo, R., L.H. Vandenberghe, G. Gao, J. Lin, and J.M. Wilson,** Worldwide epidemiology of neutralizing antibodies to adeno-associated viruses. *Journal of Infectious Diseases*, 2009. 199(3): p. 381-390.
4. **Mingozzi, F. and K. A High,** Immune responses to AAV in clinical trials. *Current gene therapy*, 2011. 11(4): p. 321-330.
5. **McCaffrey, A.P., P. Fawcett, H. Nakai, R.L. McCaffrey, A. Ehrhardt, T.T.T. Pham, K. Pandey, H. Xu, S. Feuss, and T.A. Storm,** The host response to adenovirus, helper-dependent adenovirus, and adeno-associated virus in mouse liver. *Mol. Ther.*, 2008. 16(5): p. 931-941.
6. **Marshall, E.,** Gene therapy death prompts review of adenovirus vector. *Science*, 1999. 286(5448): p. 2244-2245.
7. **Boussif, O., F. Lezoualc'h, M.A. Zanta, M.D. Mergny, D. Scherman, B. Demeneix, and J.-P. Behr,** A Versatile Vector for Gene and Oligonucleotide Transfer into Cells in Culture and in vivo: Polyethylenimine. *Proceedings of the National Academy of Sciences of the United States of America*, 1995. 92(16): p. 7297-7301.
8. **Gosselin, M.A., W. Guo, and R.J. Lee,** Efficient Gene Transfer Using Reversibly Cross-Linked Low Molecular Weight Polyethylenimine. *Bioconjugate Chemistry*, 2001. 12(6): p. 989-994.
9. **Kichler, A., C. Leborgne, E. Coeytaux, and O. Danos,** Polyethylenimine-mediated gene delivery: a mechanistic study. *The Journal of Gene Medicine*, 2001. 3(2): p. 135-144.
10. **Hildebrandt, I., M. Iyer, E. Wagner, and S. Gambhir,** Optical imaging of transferrin targeted PEI/DNA complexes in living subjects. *Gene therapy*, 2003. 10(9): p. 758-764.
11. **Ogris, M., B. S., S. S., K. R., and W. E.,** PEGylated DNA/transferrin-PEI complexes: reduced interaction with blood components, extended circulation in blood and potential for systemic gene delivery. *Gene Therapy*, 1999. 6(4): p. 595-605.
12. **Petersen, H., P.M. Fechner, A.L. Martin, K. Kunath, S. Stolnik, C.J. Roberts, D. Fischer, M.C. Davies, and T. Kissel,** Polyethylenimine-graft-Poly(ethylene glycol) Copolymers: Influence of Copolymer Block Structure on DNA Complexation and Biological Activities as Gene Delivery System. *Bioconjugate Chemistry*, 2002. 13(4): p. 845-854.

13. **Mishra, S., P. Webster, and M.E. Davis**, PEGylation significantly affects cellular uptake and intracellular trafficking of non-viral gene delivery particles. *European Journal of Cell Biology*, 2004. 83(3): p. 97-111.
14. **Hatakeyama, H., H. Akita, and H. Harashima**, A multifunctional envelope type nano device (MEND) for gene delivery to tumours based on the EPR effect: A strategy for overcoming the PEG dilemma. *Advanced Drug Delivery Reviews*, 2011. 63(3): p. 152-160.
15. **Li, W., Z. Huang, J.A. MacKay, S. Grube, and F.C. Szoka**, Low-pH-sensitive poly(ethylene glycol) (PEG)-stabilized plasmid nanolipoparticles: effects of PEG chain length, lipid composition and assembly conditions on gene delivery. *The Journal of Gene Medicine*, 2005. 7(1): p. 67-79.
16. **Mok, H., K.H. Bae, C.H. Ahn, and T.G. Park**, PEGylated and MMP-2 specifically dePEGylated quantum dots: comparative evaluation of cellular uptake. *Langmuir*, 2008. 25(3): p. 1645-1650.
17. **Paoli, E., D. Kruse, J. Seo, H. Zhang, A. Kheirrolomoom, K. Watson, P. Chiu, H. Stahlberg, and K. Ferrara**, An optical and microPET assessment of thermally-sensitive liposome biodistribution in the Met-1 tumor model: Importance of formulation. *Journal of Controlled Release*, 2010. 143(1): p. 13-22.
18. **Nie, Y., M. Günther, Z. Gu, and E. Wagner**, Pyridylhydrazone-based PEGylation for pH-reversible lipopolyplex shielding. *Biomaterials*, 2011. 32(3): p. 858-869.
19. **Walker, G.F., C. Fella, J. Pelisek, J. Fahrmeir, S. Boeckle, M. Ogris, and E. Wagner**, Toward Synthetic Viruses: Endosomal pH-Triggered Deshielding of Targeted Polyplexes Greatly Enhances Gene Transfer in vitro and in vivo. *Mol Ther*, 2005. 11(3): p. 418-425.
20. **Sun, H., B. Guo, R. Cheng, F. Meng, H. Liu, and Z. Zhong**, Biodegradable micelles with sheddable poly (ethylene glycol) shells for triggered intracellular release of doxorubicin. *Biomaterials*, 2009. 30(31): p. 6358-6366.
21. **Hatakeyama, H., H. Akita, K. Kogure, M. Oishi, Y. Nagasaki, Y. Kihira, M. Ueno, H. Kobayashi, H. Kikuchi, and H. Harashima**, Development of a novel systemic gene delivery system for cancer therapy with a tumor-specific cleavable PEG-lipid. *Gene Therapy*, 2006. 14(1): p. 68-77.
22. **Kale, A.A. and V.P. Torchilin**, Enhanced transfection of tumor cells in vivo using "Smart" pH-sensitive TAT-modified pegylated liposomes. *Journal of Drug Targeting*, 2007. 15(7-8): p. 538-545.
23. **Noga, M., D. Edinger, W. Rödl, E. Wagner, G. Winter, and A. Besheer**, Controlled shielding and deshielding of gene delivery polyplexes using hydroxyethyl starch (HES) and alpha-amylase. *Journal of Controlled Release*, 2012. 159(1): p. 92-103.
24. **Schaffert, D., M. Kiss, W. Rödl, A. Shir, A. Levitzki, M. Ogris, and E. Wagner**, Poly(I:C)-Mediated Tumor Growth Suppression in EGF-Receptor Overexpressing Tumors Using EGF-Polyethylene Glycol-Linear Polyethylenimine as Carrier. *Pharmaceutical Research*, 2011. 28(4): p. 731-741.
25. **Plank, C., K. Zatloukal, M. Cotten, K. Mechtler, and E. Wagner**, Gene transfer into hepatocytes using asialoglycoprotein receptor mediated endocytosis of DNA complexed with an artificial tetra-antennary galactose ligand. *Bioconjugate Chemistry*, 1992. 3(6): p. 533-539.
26. **Sauerbrey, G.**, The use of quartz oscillators for weighing thin layers and for microweighing. *zeitschrift fuer physik*, 1959. 155: p. 206-222.
27. **Brethaudiere, J.P., R. Rej, P. Drake, A. Vassault, and M. Bailly**, Suitability of control materials for determination of alpha-amylase activity. *Clinical Chemistry*, 1981. 27(6): p. 806-15.

28. **Greish, K.**, Enhanced permeability and retention of macromolecular drugs in solid tumors: A royal gate for targeted anticancer nanomedicines. *Journal of Drug Targeting*, 2007. 15(7): p. 457 - 464.
29. **Maeda, H., T. Sawa, and T. Konno**, Mechanism of tumor-targeted delivery of macromolecular drugs, including the EPR effect in solid tumor and clinical overview of the prototype polymeric drug SMANCS. *Journal of Controlled Release*, 2001. 74(1-3): p. 47-61.
30. **Neu, M., O. Germershaus, M. Behe, and T. Kissel**, Bioreversibly crosslinked polyplexes of PEI and high molecular weight PEG show extended circulation times in vivo. *Journal of Controlled Release*, 2007. 124(1-2): p. 69-80.
31. **Verbaan, F.J., C. Oussoren, C.J. Snel, D.J.A. Crommelin, W.E. Hennink, and G. Storm**, Steric stabilization of poly(2-(dimethylamino)ethyl methacrylate)-based polyplexes mediates prolonged circulation and tumor targeting in mice. *The Journal of Gene Medicine*, 2004. 6(1): p. 64-75.
32. **Goula, D., C. Benoist, S. Mantero, G. Merlo, G. Levi, and B. Demeneix**, Polyethylenimine-based intravenous delivery of transgenes to mouse lung. *Gene Therapy*, 1998. 5(9): p. 1291.

IV Characterization and biocompatibility of hydroxyethyl starch-polyethylenimine copolymers for DNA delivery

This chapter has been submitted to the *International Journal of Pharmaceutics*:

Noga M*, Edinger D, Wagner E, Winter G, Besheer A**. Characterization and biocompatibility of hydroxyethyl starch-polyethylenimine copolymers for DNA delivery.

* First author

** Corresponding author

Cell culture studies for the analysis of the cytotoxicity of plain HES-PEI conjugates were performed together with Daniel Edinger under his guidance.

Abstract

Hydroxyethyl starch (HES) has been proposed as a biodegradable substitute of PEG for the shielding of DNA polyplexes, where the feasibility of this approach was shown both *in vitro* and *in vivo*. In this study, we report on the physicochemical characterization and biocompatibility of HES-decorated polyplexes. For this purpose, HES with different molar masses and molar substitutions was coupled to a 22 kDa linear polyethylenimine (LPEI22) to produce a library of nine different HES-PEI conjugates. Particle size and morphology of HES-decorated polyplexes were evaluated using DLS, atomic force microscopy (AFM), transmission electron microscopy (TEM) and zeta potential measurement. DLS results showed that, neither the molar mass of HES nor the amount of HES in the polyplexes affected the particle size, as they were all around 70-80 nm in diameter. Additionally, AFM and TEM images showed that both naked and HESylated polyplexes were in the same size range and had a spherical morphology. Meanwhile, the HES-mediated particle-shielding effect, manifested as reduction in the surface charge, strongly correlated with the molar mass of HES, where the charge decreased linearly with the increase in molar mass. Ethidium bromide binding assay showed that HES-PEI did not negatively affect DNA condensation at N/P ratios higher than 4. HES-conjugation also showed a stabilizing effect against salt-induced particle disassembly, and particle aggregation in protein-containing media. Biocompatibility tests included cellular viability with increasing polymer concentration, as well as erythrocyte aggregation and hemolysis assays. HES-PEI conjugates showed lower cytotoxicity, no aggregation and much lower hemolysis compared to unmodified PEI. In conclusion, these results show that the HES-PEI conjugates are promising gene delivery polymers with favorable physicochemical properties and biocompatibility profile.

Keywords

Hydroxyethyl starch (HES), linear polyethylenimine (LPEI), characterization, stability, biocompatibility, gene delivery, shielding

1 Introduction

Polyplexes for non-viral gene and oligonucleotide delivery represent an actively studied field which holds promise for the treatment of acquired or inherited diseases. However, the experience from more than two decades in the field of polymeric gene delivery has shown that still a number of hurdles and limitations must be overcome, most importantly, the development of safe and highly efficient carriers that can overcome intra- and extracellular barriers.

Since these polyplexes are prepared using polycations, most notably polyethylenimine [1, 2], they carry a positive charge, which leads to non-specific interaction with blood components, aggregation and premature elimination by the body's immune system. One way to overcome this problem is using hydrophilic polymers, such as polyethylene glycol, to shield the polyplexes against these interactions. However, PEGylation is known to reduce cell-uptake and endosomal release by steric interference, in what is known as the "PEG-dilemma" [3-5]. Several strategies were introduced for shedding the interfering PEG molecules after reaching their destination by incorporating unstable bonds, which are responsive to diverse stimuli, such as reducing environment or acidic pH [6-9].

We recently proposed the use of hydroxyethyl starch (HES) as a substitute for PEG, with the aim of controlled shielding and enzymatically catalyzed deshielding using amylase [10, 11]. Those core-shell nanoparticles with HES-decoration showed a reduced *in vitro* transfection in the absence of alpha amylase (AA), indicating a successful particle shielding. However, the addition of AA caused up to 3 orders of magnitude increase in gene transfer *in vitro* [11]. An *in vivo* proof-of-concept study showed that HES strongly reduced non-specific aggregation and the associated accumulation in the lungs, and increased gene expression in the tumor, whereas gene-carriers with non-degradable HES or PEG coats showed low gene transfer in both the lung and tumor [10]. These results showed the feasibility of HES-PEI conjugates for effective gene transfer.

For the future use and optimization of such HES-decorated nanoparticles, a thorough investigation of their physicochemical properties and biocompatibility is required. In the current study, we provide a detailed insight into these properties, where the physicochemical characterization focused on the effect of HES molar mass on the particle size and the zeta

potential of the polyplexes, the condensation of DNA by the modified polycation, as well as the stability of the polyplexes in the presence of salt or serum. Additionally, the biocompatibility studies provided information about the cellular toxicity, hemolytic activity and erythrocyte aggregation of different HES-PEI copolymers. The homopolymer LPEI and copolymer PEG-PEI were used as controls in most of the experiments.

2 Experimental section

2.1 Materials

HES 70[0.5] with a weight-average molar mass (M_w , number after HES; nominal value as provided by supplier) of 70 kDa and a molar substitution (MS is the mean number of hydroxyethyl groups per glucose unit; nominal value as provided by supplier; number in square brackets) of 0.5 was kindly provided by Serumwerk Bernburg, Germany. HES20[0.5] was synthesized from HES70[0.5] by acid hydrolysis as reported in [11]. HES10[1.0], HES30[0.4], HES30[1.0], HES60[0.7], HES60[1.0] and HES60[1.3] were kindly provided by Fresenius Kabi (Bad Homburg, Germany). Sodium cyanoborohydride (NaBH_3CN) was purchased from Merck Schuchardt OHG (Hohenbrunn, Germany). Linear polyethylenimine with an average molar mass of 22 kDa (PEI22) and the PEG20-PEI conjugate (PEG20: polyethylene glycol with the average molecular weight of 20 kDa) were synthesized as described in [12]. Plasmid pCMVluc was prepared by PlasmidFactory, Bielefeld, Germany. Ethidium bromide solution and Triton-X 100 were purchased from Sigma-Aldrich (Steinheim, Germany). Cell culture medium, antibiotics and fetal calf serum (FCS) were purchased from Life Technologies (Karlsruhe, Germany). Other solvents and chemicals were reagent grade and were used as received.

2.2 Methods

2.2.1 Synthesis and characterization of HES-PEI co-polymers

Conjugates of different HES molecules with LPEI22 were prepared via Schiff's base formation and reductive amination as described earlier [10, 11]. Additionally, the purified samples were characterized using ^1H -NMR, copper assay, and SEC [11].

2.2.2 Preparation and biophysical characterization of polymer-based transfection particles

Naked LPEI-based polyplexes (nPx) were prepared by the rapid addition and mixing of PEI to the plasmid pCMVluc (pDNA) (at a final DNA concentration of 20 µg/mL in HEPES buffered glucose (HBG); 20 mM HEPES, 5 % glucose (w/v), pH 7.1) at N/P 6.0, then incubated at room temperature for 30 minutes prior to analysis. For instance, PEI/DNA transfection particles at the N/P ratio of 6.0 were composed of 20 µg DNA and 16 µg PEI. HESylated polyplexes were produced in the same fashion as nPx, with the exception that pure PEI was partially replaced by HES-modified PEI, e.g. HES70-PEI/DNA complexes at N/P ratio 6.0 and a ratio of PEI to HES-modified PEI of 90:10 were made of 20 µg DNA, and a mixture of 14.4 µg PEI and 1.6 µg HES70-PEI (based on PEI). HESylated polyplexes were generated with the ratio 90:10 of PEI to HES-PEI conjugates (unless otherwise stated). Polyplexes containing PEG20-PEI were prepared at 90:10 molar rate of free PEI to PEG-PEI conjugates.

2.2.3 Dynamic light scattering (DLS)

The hydrodynamic diameter of LPEI-based polyplexes was studied using the Malvern Zetasizer Nano ZS (Malvern Instruments, Worcestershire, UK). Measurements were performed in disposable 70 µL micro UV-cuvettes (Brand, Wertheim, Germany). Samples were analyzed at 25°C (n ≥ 3).

2.2.4 Transmission Electron Microscopy (TEM)

TEM images were obtained using a TITAN 80-300 S/TEM (FEI Company). Naked polyplexes, HES-modified particles (70Px and 20Px, supplemented with 10% HES-PEI, respectively) were generated following the standard procedure allowing a 30 minutes polyplex formation time. The used grids (Formvar/carbon-filmed 400 mesh copper) were treated with oxidative H₂/O₂ gas chemistry applying the Solarus (Model 950) Advanced Plasma Cleaning System (Gatan GmbH, Germany) for the removal of hydrocarbon contaminations. The DNA-polymer solutions (5 µL) were placed onto the grid for 5 minutes allowing particle immobilization. The grid was dried using filter paper and rinsed twice with highly purified water. After drying, negative staining of the TEM sample was performed by adding a volume of 5 µL of 1% phosphotungstic acid for 5 minutes. Air-dried samples were measured applying a voltage of 80 kV.

2.2.5 Atomic Force Microscopy (AFM)

Measurements were performed on a MFP-3D atomic force microscope (Asylum Research, Santa Barbara, CA), applying the tapping mode in air. Arrow-UHF-10 cantilevers (Nanoworld, Switzerland) were used at a drive frequency of approximately 306 kHz, the scan rate was set to 1 Hz with pixel scan points of 256 x 256 or 512 x 512. AFM images were analyzed using Igor Pro v.5.05A (WaveMetrics, US). LPEI-based polyplexes and HESylated particles (10% shielding domain) were generated following the standard procedure. Polyplexes were placed onto cover glass for 10 min allowing particle-on-surface immobilization. Following rinsing the glass basis cautiously with highly purified water the material was dried in air and analyzed.

2.2.6 Zeta potential measurement

The effect of different HES coatings on the surface charge characteristics of LPEI polyplexes was evaluated by zeta potential measurements using Malvern Zetasizer Nano ZS (Malvern Instruments, Worcestershire, United Kingdom) ($n \geq 3$). Measurements were performed with 750 μ L polyplex solution in folded capillary cells at 25°C.

2.2.7 DNA binding evaluation using ethidium bromide (EtBr) binding assay

HBG pH 7.1 or HBS (HEPES-buffered saline, 20 mM HEPES, 150 mM NaCl, pH 7.1) was pipetted into black 96-well plate (Nunc), six microgram pDNA and the corresponding quantity of polymers were added to give a final DNA concentration of 20 μ g/mL nucleic acid in altogether 300 μ L volume. Polyplexes were allowed to incubate for 30 minutes, before an amount of 20 μ L EtBr solution (concentration 100 μ g/mL in water) was supplemented. The pDNA binding ability of various HES-PEI conjugates was evaluated under the effect of increasing polymer concentrations. The reduction of intercalation of EtBr in DNA was followed using a Cary Eclipse Fluorescence Spectrophotometer (Varian), where λ_{ex} 510 nm and λ_{em} 590 nm was utilized [13]. The relative fluorescence was calculated $F_{\text{polyplex}} / F_{\text{naked DNA}}$, where the fluorescence of naked DNA was 1.0 and the fluorescence of EtBr control solution was 0.

2.2.8 Colloidal stability of HESylated PEI-based DNA complexes

The intercalation behavior of nucleic acid intercalator EtBr was utilized to study the stability of polyplexes against sodium chloride. HBG pH 7.1 was pipetted into black 96-well plate

(Nunc), 6 μ g pDNA and the corresponding quantum polymers were added to give a final DNA concentration of 6 μ g nucleic acid in altogether 300 μ L polyplex solution. DNA-polymer complexes were generated at N/P ratio 6.0. Polyplexes containing HES-PEI were prepared at 90:10, molar ratio of free PEI to HES-PEI conjugates. HES20- and HES70-decorated particles were additionally made at 75:25 and 50:50 ratios to study the impact of the amount of HES on the stability against sodium chloride. Polyplexes were allowed to incubate for 30 min, before 20 μ L EtBr solution (100 μ g/mL) was supplemented. A predefined amount of 5 M NaCl was stepwise added to the polyplex solutions (sodium chloride titration from 0 to 1 M NaCl concentration). Samples were allowed to incubate for 5 min, and the EtBr fluorescence was followed using a Cary Eclipse Fluorescence Spectrophotometer (Varian), where $\lambda_{\text{ex}} = 510$ nm and $\lambda_{\text{em}} = 590$ nm. The relative fluorescence (RF) was calculated as $\text{Fluorescence}_{\text{polyplex}} / \text{Fluorescence}_{\text{naked DNA}}$. A polynomial fit (2nd order) was performed to determine NaCl concentrations at RF 0.5 and 0.75.

2.2.9 Polyplex stability in protein-containing medium

HES20- and HES70-decorated polyplexes (90:10, molar ratio of free PEI to HES-PEI) were prepared according to the standard procedure, following 30 min particle generation time, 100 μ L polyplex solution was mixed with 900 μ L DMEM (1 g/L glucose, 10% FCS). DLS measurements were performed in the high resolution mode (multiple narrow mode), where peak 1 was taken to analyze the large particle aggregates. Naked LPEI- and PEG20-decorated polyplexes served as controls. All measurements are given as mean values of three independent runs performed in triplicates.

2.2.10 Evaluation of the cytotoxicity of plain HES-decorated PEIs

All cultured cells were grown at 37 °C in 5% CO₂ humidified atmosphere. Human hepatoma cells HUH7 (JCRB 0403, Tokyo, Japan) were cultured in DMEM (Dulbecco's Modified Eagle Medium)/HAM's F12 medium (1:1). The medium was supplemented with 10% FCS, 4 mM stable glutamine, 100 U/mL penicillin, and 100 μ g/mL streptomycin. The viability of HUH7 cells after treatment with increasing amounts of HES-modified PEIs was evaluated using the MTT assay. Twenty four hours before polymer treatment, human HUH7 cells were seeded at a density of 1×10^4 cells per well in 100 μ L medium. Directly before addition of HESPEI, the medium was exchanged against fresh medium with/without pancreatic alpha amylase (AA; 100 U/L). Various amounts of co-polymers were added to the cells up to the polymer

concentration 1 mg/mL (based on PEI). 4 h after addition of various amounts of HESPEI, the medium was replaced by fresh medium with/without AA. 24 h after polymer treatment, MTT (3-(4,5-dimethylthiazol-2-yl)-2,5-diphenyltetrazolium bromide) was dissolved in PBS at 5 mg/mL, and 10 μ L aliquots were added to each well reaching a final concentration of 0.5 mg MTT/mL. After an incubation time of 2 h, unreacted dye with medium was removed and the cells were lysed by incubation at -80 °C for 30 minutes. The formazan product was dissolved in 100 μ L/well dimethyl sulfoxide and quantified using a plate reader (Tecan, Groedig, Austria) at 590 nm with background correction at 630 nm. The metabolic activity (%) relative to control wells containing HBG-treated cells was calculated ($A_{\text{test}}/A_{\text{control}} \times 100$).

2.2.11 Erythrocyte aggregation assay

Fresh citrate buffered blood (25mM) from 1-year old female CD-1 nude mice was washed by centrifugation (2500rpm, 700-800g) with a PBS/sodium citrate mixture (9:1, 25mM sodium citrate) until a colorless supernatant was obtained. The erythrocyte pellet was diluted with PBS pH 7.4 at a concentration of 4% (V/V). An amount of 100 μ L red blood cell (RBC) suspension was mixed with 50 μ L of various polymer solutions. LPEI, HES70[0.5]-PEI and PEG20PEI were added at the final concentrations 10, 50 and 100 μ L/mL (based on LPEI), polymer/erythrocyte solutions were incubated in 24-well plates for 30 and 120 minutes at 37°C under constant gentle agitation. For microscopic analysis pictures were taken with a Keyence VHX-500F digital microscope with 1000-fold magnification.

2.2.12 Hemolysis assay

An amount of 75 μ L RBC suspension (for preparation see erythrocyte aggregation assay) was mixed with 75 μ L of various polymer solutions in V-bottom 96 well plates. Polymers were supplemented at the final concentration 10, 50 and 100 μ g/mL based on LPEI and based on total polymer, respectively. Mixtures were incubated for 60 minutes at 37°C under constant gentle shaking. Following centrifugation, the absorbance of the excess was measured at 405 nm. PBS buffer (0% released hemoglobin) and 1% (V/V) Triton-X (100% lysis) were used as controls. Erythrocyte leakage assay data are the means of experiments performed in quadruplicates.

3 Results

3.1 HES-PEI conjugates synthesis and characterization

HES-PEI copolymers were prepared by grafting HES onto the linear polyethylenimine PEI by Schiff's base formation via an unstable aminol intermediate that immediately rearranges to an enamine function. In a second step, the reducing agent sodium cyanoborohydride reduces the enamine to secondary amine groups [10, 11]. A battery of HES-PEI conjugates was synthesized with varying HES molar masses and molar substitution and different ratios of coupled HES to PEI. The synthesized co-polymers were characterized using ^1H NMR, UV spectroscopy (colorimetric copper assay), and SEC, as reported earlier [11]. Both ^1H NMR spectroscopy and photometric copper assay delivered very similar results regarding the extent of coupling of HES to PEI, as illustrated in Table IV. 1. These co-polymers act as the basis for fine-tuning the properties of HES-coated polyplexes, which allow the controlled polyplex shielding and deshielding as previously demonstrated *in vitro* and *in vivo*. In this work, we report on some important physicochemical properties of these polyplexes, as well as the biocompatibility of these conjugates.

Table IV. 1. Mass ratio and molar ratio of HES:PEI for generated HES-PEI copolymers as determined by ^1H -NMR and the copper assay.

	Amount of HES in generated HES-PEI conjugates (^1H NMR)		Amount of HES in generated HES-PEI conjugates (UV)	
	Mass ratio %	Molar ratio HES : PEI	Mass ratio %	Molar ratio HES : PEI
HES10[1.0]-PEI	35.12	1.36 : 1	28.0 ± 2.3	0.98 : 1
HES20[0.5]-PEI	56.70	1.64 : 1	56.7 ± 8.8	1.64 : 1
HES30[0.4]-PEI	74.74	2.47 : 1	72.8 ± 1.0	2.24 : 1
HES30[1.0]-PEI	50.39	0.85 : 1	51.0 ± 3.4	0.87 : 1
HES60[0.7]-PEI	79.97	1.67 : 1	79.6 ± 1.4	1.63 : 1
HES60[1.0]-PEI	75.40	1.28 : 1	76.0 ± 0.7	1.32 : 1
HES60[1.3]-PEI	79.97	1.67 : 1	78.0 ± 4.2	1.49 : 1
HES70[0.5]-PEI	88.20	2.68 : 1	88.3 ± 1.5	2.71 : 1

3.2 Physicochemical characterization of the generated polyplexes

3.2.1 Particle size

The effect of the modification of PEI with HES having different molar masses and degrees of substitution on the formation of polyplexes, their particle size and polydispersity were evaluated using DLS. All HES-decorated polyplexes were generated at N/P ratio of 6.0, where 90% PEI and 10% HES-PEI (based on PEI) were used. For these studies, naked polyplexes (LPEI alone) and PEG20-PEI polyplexes served as controls. DLS results show that all studied polyplexes displayed a very homogenous size distribution, with a polydispersity index of ~ 0.1 , and particle sizes in the range of 70-80 nm, an ideal size range for passive tumor targeting [14], with a slightly higher size for particles shielded with PEG or high molar mass HES (Figure IV. 1A).

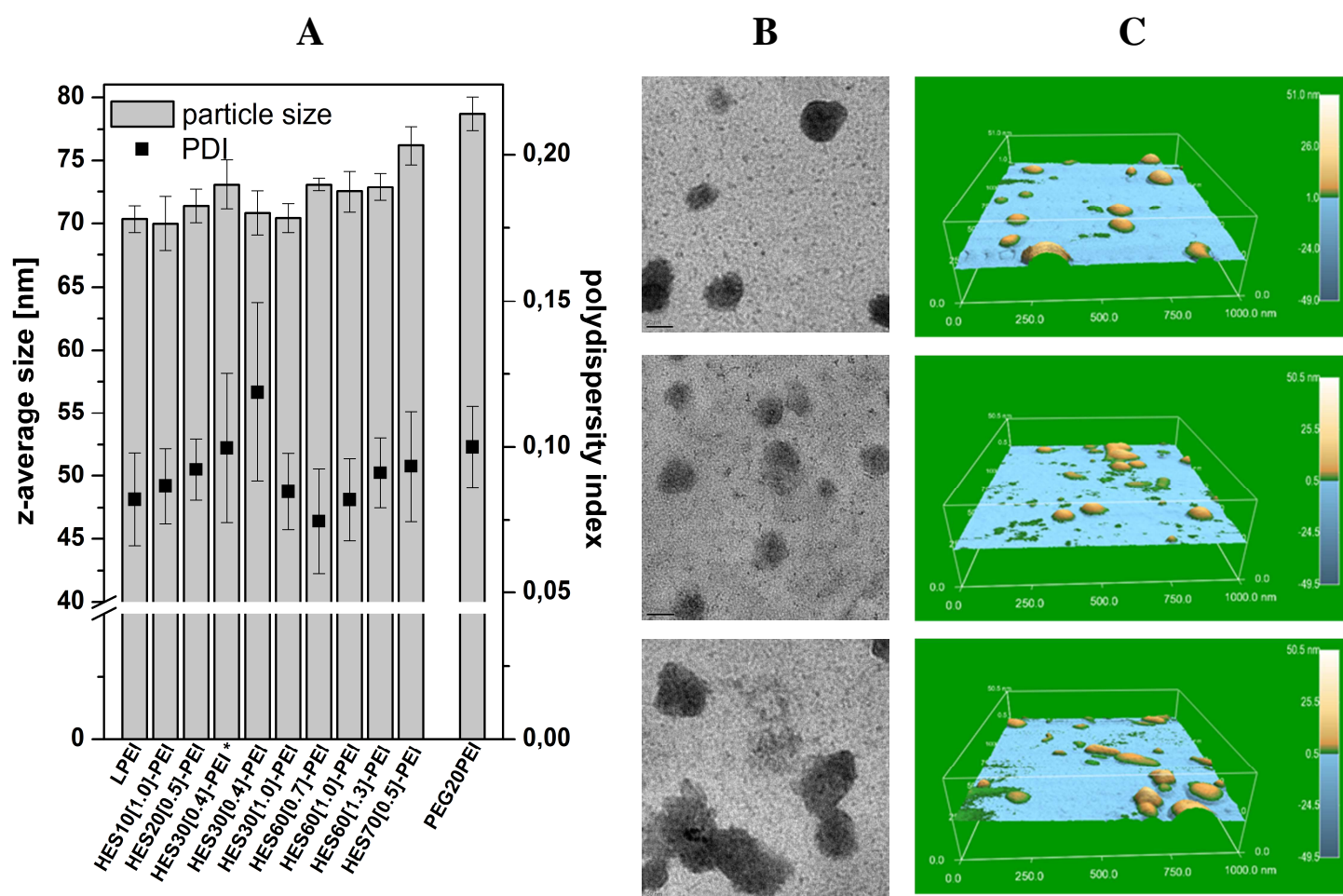


Figure IV. 1. Left panel: Particle size and polydispersity index of various HES-decorated polyplexes. Middle panel: Transmission electron microscopy images

showing the size and morphology of the polyplexes (top: LPEI-Px; middle: HES70[0.5]-Px; bottom: HES20[0.5]-Px). Right panel: Atomic force microscopy images of the polyplexes (top: LPEI-Px; middle: HES70[0.5]-Px; bottom: HES20[0.5]-Px).

Additionally, the morphology and particle size of 2 HES-shielded samples (namely HES70[0.5]-Px and HES20[0.5]-Px) as well as naked polyplexes were studied using TEM and AFM. TEM-samples showed that all 3 particles were spherically shaped, with particle sizes between 50-100 nm, which is in good agreement with the results determined from DLS measurements (see Figure IV. 1 A and B). It is worth noting that no significant difference in shape or size could be observed between the naked or the HES- decorated particles. Similarly, the AFM measurements performed applying the tapping mode in air showed that the LPEI- and HES-PEI complexes were spherical particles with smooth surfaces, with sizes in the same range as DLS and TEM measurements. No free pDNA could be observed in AFM measurements, which is an indication for successful nucleic acid condensation (Figure IV. 1 C).

3.2.2 Surface charge

The effect of incorporation of HES with varying molar masses on the polyplexes' surface charge was evaluated by measuring the zeta potential. As expected, the hydrophilic polymers shielded the nanoparticles and reduced the zeta potential. The effect of molar mass on the reduction of zeta potential showed a strong negative correlation (Figure IV. 2, $R^2 = 0.96$). This shows that the surface charge can be fine-tuned by modifying the molar mass of HES.

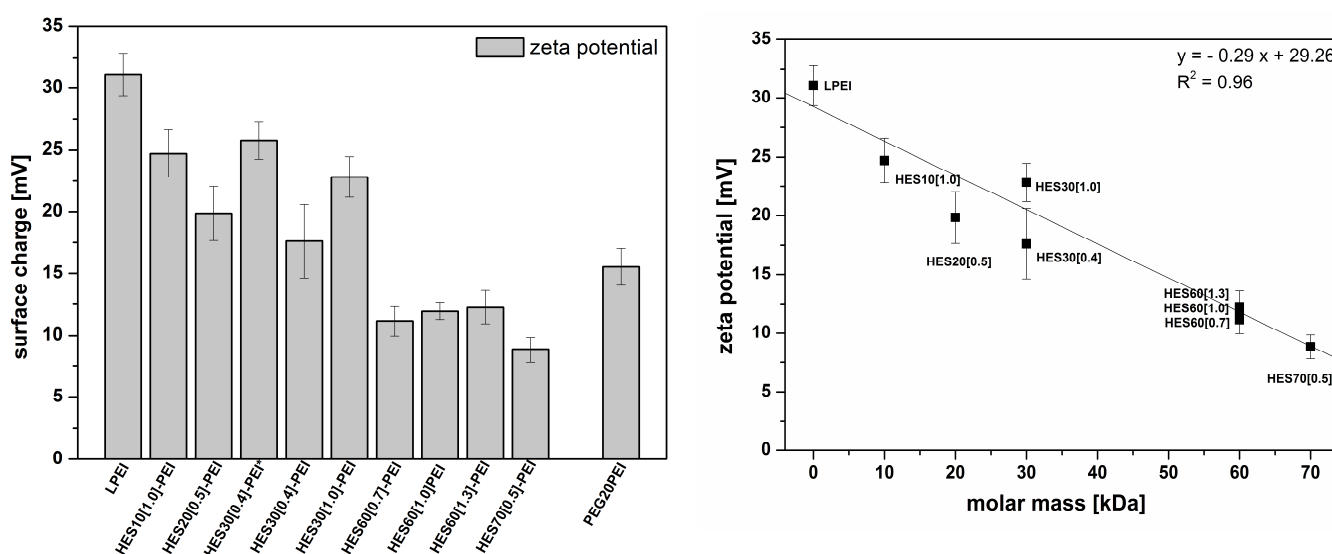


Figure IV. 2. Surface charge HESylated polyplexes at N/P ratio 6.0 with the ratio of free PEI to HES-PEI 90/10 (Left). Zeta potential of HES-decorated particles plotted against the molar mass of HES (Right).

3.3 DNA condensation by HES-PEI

Building stable polyplexes via electrostatic interaction is a prerequisite for efficient delivery of genes.

The effect of HES-PEI copolymers on DNA condensation was further evaluated by an EtBr exclusion assay. This is based on the fact that free EtBr exhibits a very low fluorescence intensity, which increases significantly upon intercalation with DNA. Accordingly, condensation of DNA by cationic polymers decreases fluorescence by inhibiting EtBr intercalation [15]. The DNA binding ability of LPEI and modified PEIs was studied under the effect of increasing N/P ratio. The relative fluorescence (RF) of LPEI-condensed polyplexes decreased with increasing N/P ratio (i.e. with increasing amounts of PEI), leveling-off at around N/P ratio 3, both in HBG and HBS (Figure IV. 3). In comparison to LPEI, the HES-modified PEIs exhibited a lower nucleic acid binding ability at low polymer:DNA ratios up to approximately N/P ratio 4 in both HBG as well as the salt-containing HBS (probably due to steric hindrance), however, no difference in DNA condensation capacity could be observed at N/P ratios higher than 4.0, including N/P ratio 6, which is often used for *in vitro* and *in vivo* experiments [10, 11]. The molar mass of HES did not seem to have a significant influence on DNA binding, since the higher molar mass HES70[0.5]-PEI exhibited similar nucleic acid condensation ability as HES20[0.5]-PEI. Meanwhile, the DNA condensation turned out to be disturbed in the presence of the salt-containing buffer (HBS) in contrast to the sugar-containing one (HBG), with the relative fluorescence leveling-off at approximately 0.2 in the case of salt-free HBG and at 0.4 in HBS, indicating a higher amount of EtBr binding in the latter case, and accordingly a less efficient condensation. This is probably due to ion-shielding of the charged groups and disturbance of the electrostatic interaction between the polycation and DNA.

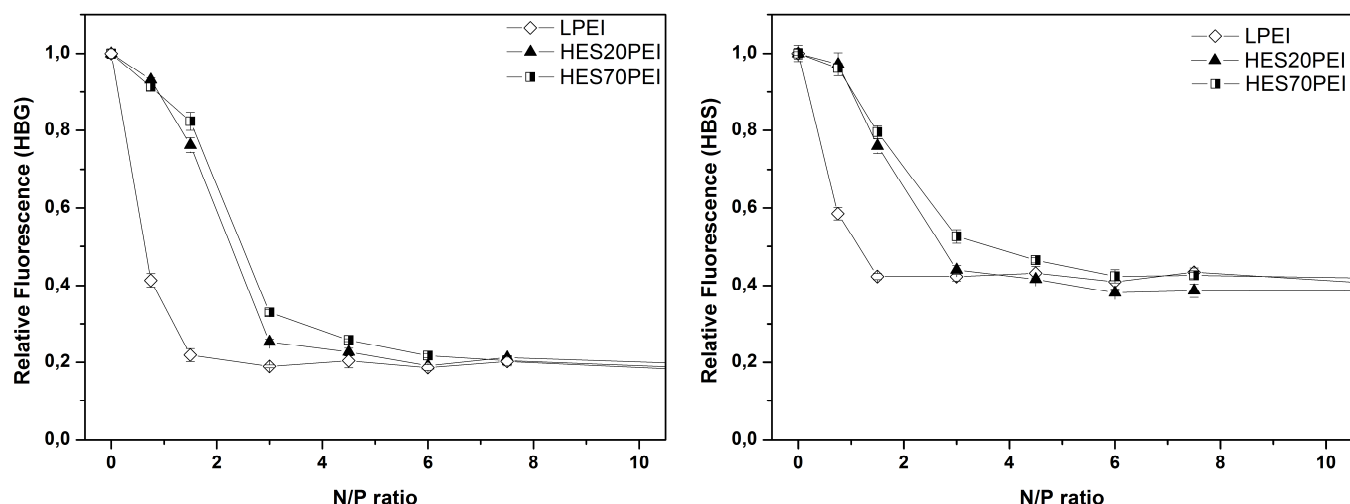


Figure IV. 3. Ethidium bromide (EtBr) exclusion assay - DNA binding ability of HES-modified PEIs. Relative fluorescence of EtBr as a function of N/P ratio for HES20 and HES70- decorated polyplexes in HBG (Left) and HBS (Right).

3.4 Stability of HES-decorated polyplexes

Polyplexes usually suffer from insufficient colloidal stability in physiological environment, leading to their disassembly or aggregation, which represents a major limitation for their *in vivo* application [16, 17]. For this reason, these factors were tested *in vitro*. First, the stability against disassembly due to increasing ionic strength was evaluated. The dissociation behavior of HES-decorated polyplexes was studied by making use of a modified EtBr-based DNA-PEI binding assay at increasing concentrations of sodium chloride. Sodium chloride interfered with the DNA condensation by the polycation leading to partial or complete disassembly of the polyplexes, allowing the intercalation of DNA and EtBr. Accordingly, at higher salt concentrations, the DNA was not bound sufficiently and the RF took the value 1 similar to uncondensed pDNA. Results show that the naked polyplexes were more sensitive towards NaCl, while the presence of HES seemed to reduce the disassembly of the polyplexes (Figure IV. 4 and Table IV. 2). The effect of the molar mass and the total amount of HES on the polyplex stability against NaCl-induced disassembly was investigated with the HES20- and HES70-PEI conjugates. HES20 increased the resistance of the particles to disassembly with increasing amount of HES (Figure IV. 4 A and Table IV. 2), while increasing amounts of HES70 led to reduction in terms of colloidal stability (Figure IV. 4 B and Table IV. 2).

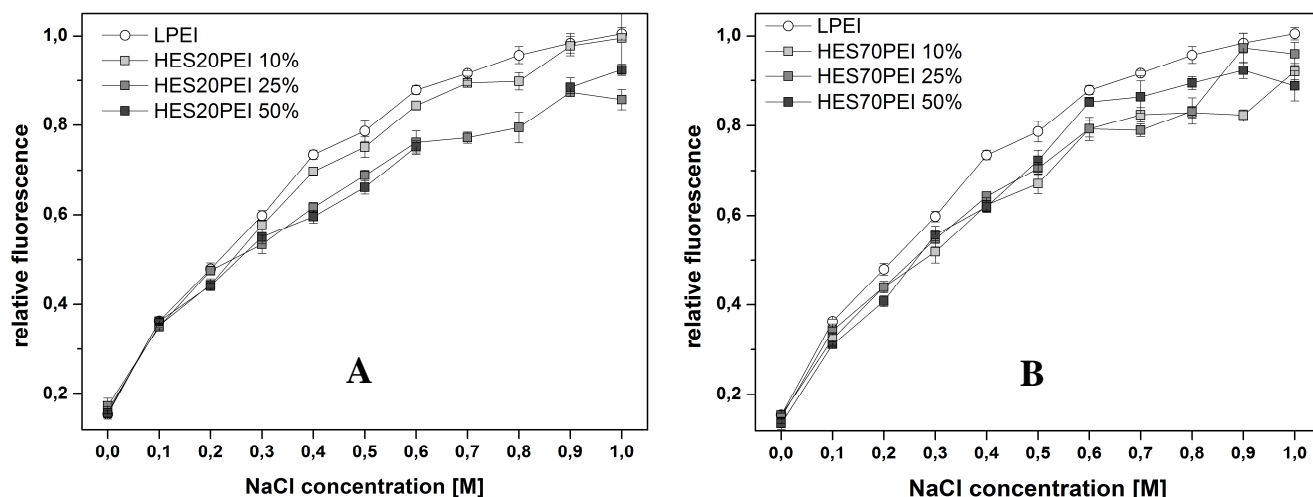


Figure IV. 4. Colloidal stability of HES-modified polyplexes. Relative fluorescence of EtBr in a polyplex solution as a function of increasing NaCl concentration for different HES-PEI:PEI ratios of HES20-decorated (A) and HES70-decorated (B) polyplexes.

Table IV. 2. Colloidal stability of HES-modified polyplexes. The relative fluorescence (RF) of 1.0 represents naked pDNA, RF ~ 0.15 is the initial RF for compactly bound pDNA in the polymeric matrix.

	Conc. of NaCl [M] leading to RF 0.50	Conc. of NaCl [M] leading to RF 0.75
LPEI	0.210	0.435
10%	0.222	0.466
HES20PEI 25%	0.254	0.591
50%	0.263	0.591
10%	0.269	0.573
HES70PEI 25%	0.254	0.553
50%	0.249	0.500

Another experiment evaluated the aggregation behavior of the nanoparticles in the presence of serum proteins. For this purpose, the particle size of the polyplexes was followed in DMEM cell culture medium supplemented with 10% fetal calf serum (FCS) using DLS. Once in contact with the cell culture medium, naked polyplexes showed a significant increase in size,

probably because the negatively charged proteins seemed to physically cross-link the positively charged particles. Meanwhile, particle shielding using HES and PEG diminished the tendency to form large protein aggregates with the effect $\text{HES20} < \text{PEG20} = \text{HES70}$ (Figure IV. 5).

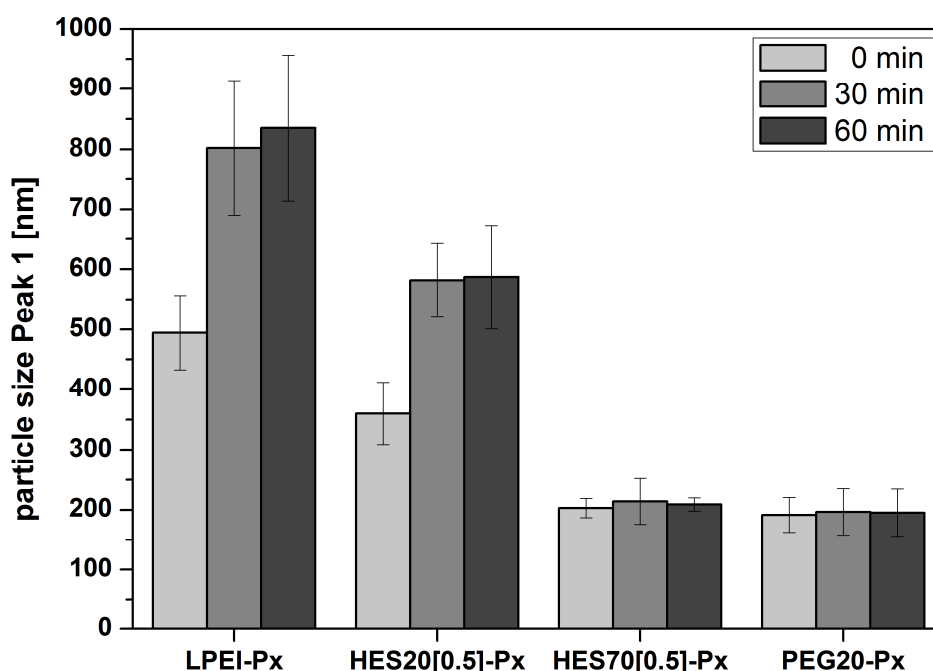


Figure IV. 5. Polyplex stability in protein-containing medium. DLS measurements of particle size for naked polyplexes, as well as polyplexes decorated with HES20, HES70 and PEG20 at time points 0, 30 and 60 min after mixing the polyplexes with DMEM supplemented with 10% FCS.

3.5 Biocompatibility of HES-PEI conjugates

3.5.1 Cytotoxicity of HES-PEI to HUH7 cells

The cytotoxicity of HES-PEI copolymers was tested on HUH7 cells using the MTT assay. Results show that the cellular metabolic activity of the HUH7 cells decreased with increasing polymer concentrations, where LPEI homopolymer induced significant cell death at concentrations $> 10 \mu\text{g/mL}$. Meanwhile, all HES-PEI copolymers exhibited reduced cell toxicity, manifested as higher metabolic activity compared to LPEI at the same concentrations (Figure IV. 6). While HES70[0.5]-PEI showed the lowest cytotoxicity, probably due to the fact that it has the highest molar mass, and accordingly the best steric hindrance, the effect of

HES' molar mass is not unequivocal, since lower molar masses showed mixed cytotoxicities (Figure IV. 6).

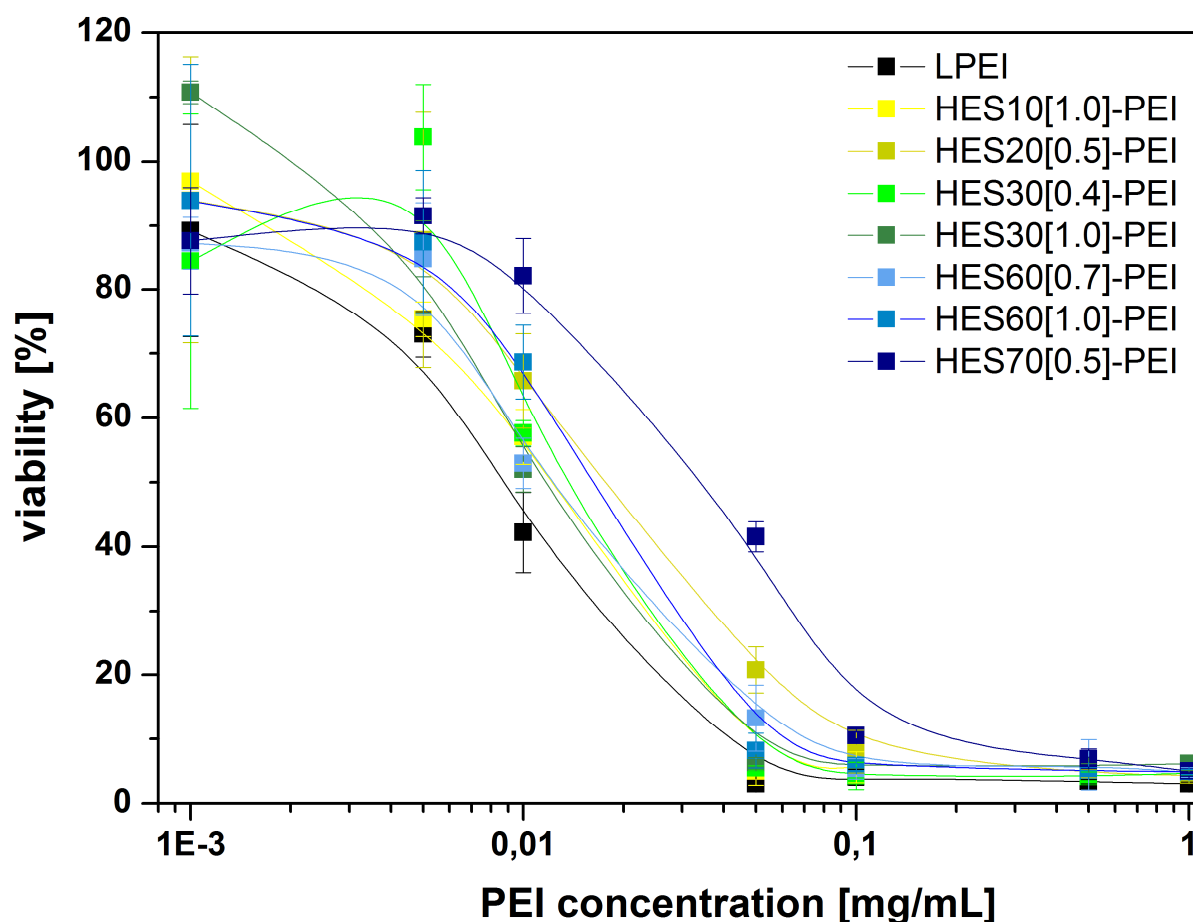
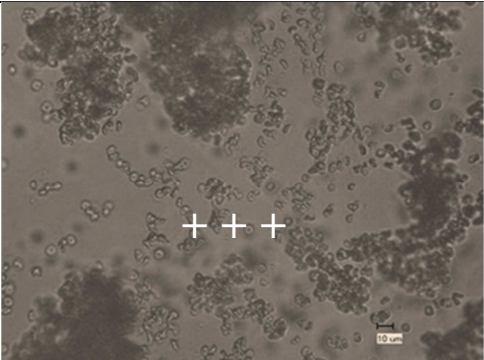
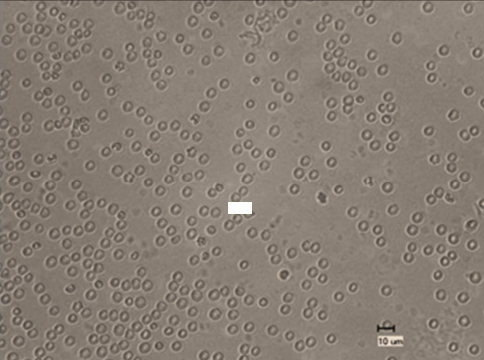
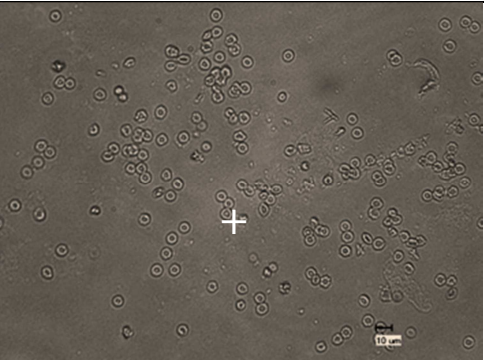


Figure IV. 6. The viability of HUH7 cells under the effect of increasing concentrations of PEI or HES- PEI conjugates as determined by the MTT assay.

3.5.2 Hemocompatibility of modified LPEIs

The erythrocyte aggregation assay was performed to study the interaction of modified PEIs with RBCs. For this purpose, erythrocytes were incubated with different concentrations of LPEI and modified LPEIs ranging from 10 $\mu\text{g/mL}$ to 100 $\mu\text{g/mL}$. Homopolymer LPEI formed large aggregates via electrostatic interaction between the cationic polyamine and anionic cell membranes. PEG20-modified PEI showed a tendency to form small erythrocyte aggregates at high concentration after 2 h incubation. Modification of LPEI with HES70[0.5] could prevent polymer-induced RBC aggregation by the effect of charge shielding at 10, 50 and 100 $\mu\text{g/mL}$ PEI concentration after 30 and 120 minutes incubation time (see Table IV. 3 and SI).

Table IV. 3. Erythrocyte aggregation assay. LPEI, PEG-PEI and HES70[0.5]-PEI in concentrations of 10, 50 and 100 µg/mL were incubated with RBCs for 30 or 120 min, and the aggregation was observed using an optical microscope. Classification: - no aggregation, + weak aggregation, ++ medium aggregation, +++ strong aggregation

	Conc. [µg/mL] based on LPEI	Incubation time [min]		Visual characterization (100 µg/mL, 120min)
		30	120	
LPEI	10	+	+++	
	50	++	+++	
	100	+++	+++	
				+++
HES70[0.5]- PEI	10	-	-	
	50	-	-	
	100	-	-	
PEG20-PEI	10	-	-	
	50	-	-	
	100	+	+	
				+

Additionally, hemolytic activity of HES70[0.5]-PEI was compared to LPEI and PEG-PEI. It was calculated after 60 minutes of incubation using the following correlation:

$$\text{Hemolysis} = \frac{(OD_{\text{Polymer}} - OD_{\text{buffer}})}{(OD_{\text{Triton-X}} - OD_{\text{buffer}})} \times 100\%$$

where OD is the optical density measured at 405 nm.

The hemolytic activity of LPEI, HES70[0.5]-PEI and PEG20-PEI showed a strong concentration-dependence, increasing with increasing concentration. HESylation of PEI drastically reduced the PEI-induced hemolysis, whereas PEG20-PEI resulted in a marginally reduced hemolytic activity in comparison to LPEI (Figure IV. 7). For instance, erythrocyte treatment with 100 $\mu\text{g/mL}$ of HES70[0.5]-PEI (based on LPEI) induced significantly lower hemolysis compared to 10 $\mu\text{g/mL}$ LPEI and is considered to be not hemolytically active according to Richardson *et al.* [18].

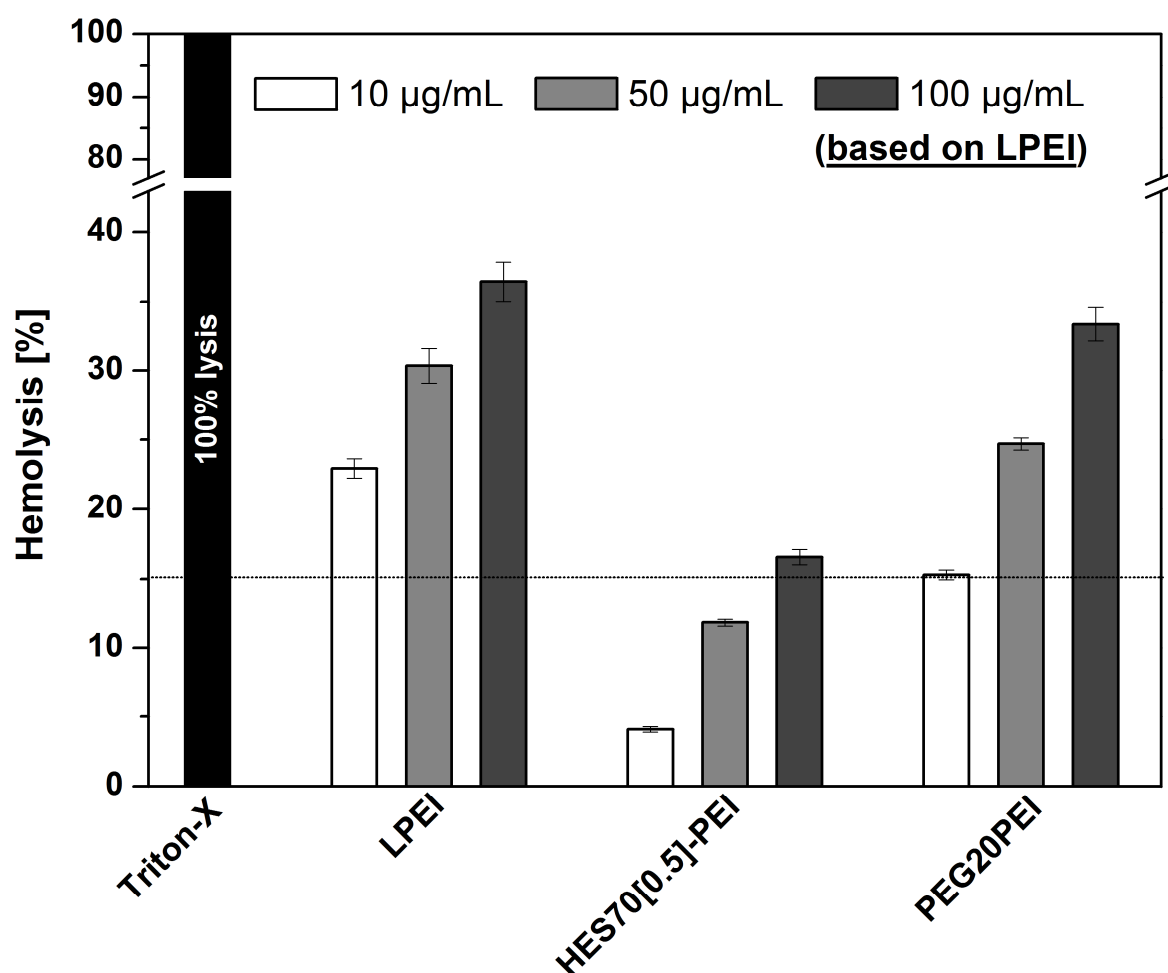


Figure IV. 7. Hemolytic activity of shielded and naked LPEI polymers. Erythrocytes were treated with different amounts of LPEI and modified PEIs. The hemolysis was determined by measuring the optical density relative to Triton X (100% lysis) and buffer (0% lysis) after 60 min incubation at 405 nm.

4 Discussion

The design and development of stable and biocompatible non-viral DNA carriers is an inevitable prerequisite for safe and efficient *in vivo* applications. We reported earlier on the use of HES-PEI for the controlled delivery of pDNA *in vitro* and *in vivo* [10, 11]. *In vitro* results showed that HES-coated polyplexes have a reduced transfection in comparison to naked polyplexes in the absence of alpha amylase (AA). Addition of AA increased the transfection efficiency by 2-3 orders of magnitude, indicating the effective deshielding of the particles using AA [11]. *In vivo* results showed that HES coating reduced the transfection in the lung approximately 3 orders of magnitude, indicating effective shielding of the particles and prevention of aggregation in the blood stream. At the same time, the transfection efficiency in the tumor was nearly doubled compared to PEGylated polyplexes, pointing to the deshielding action of serum alpha amylase *in vivo* [10].

For the sake of a better understanding of these novel polyplexes, and their optimum use for nucleotide delivery, we further studied their physicochemical properties and biocompatibility. Accordingly, a battery of HES-PEI copolymers was synthesized by reductive amination, with different HES molar masses and degrees of hydroxyethylation. The polymers were characterized using ^1H NMR and UV-spectroscopy, and the results were reported earlier (see Reference [10] and Table IV. 1).

Regarding the physicochemical characterization of the HES-decorated polyplexes, we found that surface modification with HES did not affect the particle size, polydispersity index or the morphology of the polyplexes. Regardless of the coating polymer, all polyplexes showed hydrodynamic diameters of ~70-80 nm, as well as a spherical morphology with smooth surface as determined by TEM and AFM (see Figure IV. 1). This size range is ideal for passive tumor targeting, since particles with approximately 100 nm size can passively accumulate into leaky tumor tissue by the help of the EPR effect [19]. Meanwhile, the incorporation of the hydrophilic polymer HES reduced the zeta potential of LPEI-based transfection complexes from more than +30 mV in the case of naked polyplexes down to less than +10 mV for HES70-decorated particles. The effect of shielding strongly correlated with the molar mass of HES (see Figure IV. 2). The effective reduction in zeta potential is important in preventing non-specific electrostatic interaction with blood components, thus hindering the formation of aggregates and lung accumulation [20]. These results show that it

is possible to fine tune the charge of the particles by controlling the molar mass of the utilized HES.

Another important issue in polyplex formation is the effect of the conjugated HES on the DNA condensation by LPEI. As described by other groups [21-23], polycation modification using hydrophilic polymers often leads to hindered nucleic acid compaction capacity of the homo-polymer. This conforms to the observed ethidium bromide binding experiments showing a reduction in the DNA binding ability of HES-PEI copolymers at low N/P ratios compared to LPEI. However, no differences in DNA compaction could be observed at N/P ratios higher than 4 (Figure IV. 3). This means that at the N/P ratio of 6, the commonly used ratio for polyplex formation and use, DNA condensation should not be a concern for HES-modified PEIs.

The stability of the polyplexes towards disassembly by increasing ionic strength or aggregation upon addition to protein-containing medium is essential for evaluating polyplex efficiency and performance. Accordingly, the polyplex stability against sodium chloride-induced disassembly was evaluated using a modified EtBr exclusion assay. Small amounts of NaCl solution were added to pre-generated particles and the fluorescence was followed under the effect of increasing salt concentrations. Incorporation of HES-PEI into LPEI/pDNA polyplexes increased their colloidal stability towards disassembly, presumably due to steric hindrance. The disassembly between the 2 polyelectrolytes requires coordinated movement between their many building units, and this movement seems to be hindered by the presence of the bulky HES molecules leading to higher resistance to disassembly. While this theory is supported by the fact that using higher amounts of HES20[0.5]-PEI results in better stability, HES70[0.5]-PEI showed a lower stability with increasing ratio in the polyplexes (Figure IV. 4 and Table IV. 2). This is probably due to the interference of the higher amounts of the larger HES with polyplex condensation, so that it becomes easier to disassemble the particles. As for the stability against aggregation in protein-containing medium, monitoring the particle size of HES-coated polyplexes by DLS showed that HES-decoration reduced LPEIs tendency for building large aggregates by the effect of steric hindrance (Figure IV. 5). The larger HES70[0.5] molecule shielded and stabilized the particles more effectively than the smaller HES20[0.5]. However, incorporation of hydrophilic stealth polymers HES or PEG onto the nanoparticle surface could not completely prevent protein adsorption, leading to a slight increase in particle size to approximately 200 nm.

For assessing the biocompatibility of HES-PEI conjugates, we tested their cytotoxicity in HUH7 cells, as well as their interaction with RBCs. As for cytotoxicity, the high density of amino groups of LPEI was described to be the trigger for toxicity [24-26], where the cellular membrane integrity is disturbed by the electrostatic interaction between the cationic polymer and the anionic cell structures [27]. Coupling PEG onto the polyamine was found to decrease the polymer toxicity by the effect of steric hindrance and decreased zeta potential [23, 24]. The homopolymer LPEI induced complete cell death at a concentration of 50 $\mu\text{g/mL}$, while all HES-modified conjugates exhibited improved cell viability. Similar to PEGylation [23], polyamine modification using HES shielded the amino groups and reduced the cytotoxicity, where HES with the highest molecular weight showed the best cellular viability (approximately 50% viability at 50 $\mu\text{g/mL}$ based on PEI concentration, Figure IV. 6). Testing the hemolytic activity, LPEI and PEG20-PEI exhibited hemolysis $> 15\%$ for all the tested concentrations. Meanwhile, conjugation of HES70[0.5] to LPEI significantly reduced the hemolytic activity of $< 15\%$ for concentrations up to 50 $\mu\text{g/mL}$ (see Figure IV. 7). This is considered negligible, as polymers are regarded as not hemolytically active in case of $< 15\%$ hemolysis [18]. As for the PEI-induced erythrocyte aggregation, it could be efficiently prevented using HES- and PEG-decoration (Table IV. 3). Such prevention of polymer-induced red blood cell aggregation and hemolysis are few of many prerequisites for *in vivo* applications of polyplexes.

5 Conclusion

In this work we performed detailed studies on the physicochemical properties and biocompatibility of HES-PEI conjugates and HES-coated pDNA polyplexes. Physicochemical characterization involved particle size and morphology determination using DLS, TEM and AFM. DLS measurements showed that all the particles had hydrodynamic diameters of approximately 70-80 nm, with no significant effect for HES-decoration on size. These findings could be confirmed by particle visualization using AFM and TEM analysis, where the latter 2 methods additionally demonstrated the spherical morphology of the naked and HES-decorated particles. Zeta potential measurements revealed the effective shielding of LPEI polyplexes using HES, with a clear molar mass dependence, allowing fine tuning of the nanoparticle charge. The ethidium bromide exclusion assay showed the effective DNA condensation by the HES-PEI at N/P ratios above 4.0, which is relevant to *in vitro* and *in vivo*

transfection experiments. The biocompatibility of HES-decorated polyplexes was also evaluated, showing a lower cytotoxicity, no erythrocyte aggregation and much lower hemolysis compared to unmodified LPEI. Together with the previous *in vitro* and *in vivo* experiments, these results show the promise of HES-PEI conjugates as comparatively safe and effective polymers for gene delivery.

6 Acknowledgements

Michael Budde (group Prof. Dr. Jens Michaelis, LMU Munich) and Dr. Markus Döblinger (group Prof. Dr. Bein, LMU Munich) are kindly acknowledged for AFM and TEM measurements. Olga Mykhaylyk is kindly acknowledged for providing negative staining material for TEM analysis. The authors thank Coriolis Pharma, Martinsried for the possibility to use the DynaPro Titan DLS plate reader.

7 References

1. **Gosselin, M.A., W. Guo, and R.J. Lee**, Efficient Gene Transfer Using Reversibly Cross-Linked Low Molecular Weight Polyethylenimine. *Bioconjugate Chemistry*, 2001. 12(6): p. 989-994.
2. **Sonawane, N.D., F.C. Szoka, and A.S. Verkman**, Chloride Accumulation and Swelling in Endosomes Enhances DNA Transfer by Polyamine-DNA Polyplexes *J. Biol. Chem.* 2003 2003. 278(45): p. 44826-44831.
3. **Hatakeyama, H., H. Akita, and H. Harashima**, A multifunctional envelope type nano device (MEND) for gene delivery to tumours based on the EPR effect: A strategy for overcoming the PEG dilemma. *Advanced Drug Delivery Reviews*, 2011. 63(3): p. 152-160.
4. **Mishra, S., P. Webster, and M.E. Davis**, PEGylation significantly affects cellular uptake and intracellular trafficking of non-viral gene delivery particles. *European Journal of Cell Biology*, 2004. 83(3): p. 97-111.
5. **Romberg, B., W. Hennink, and G. Storm**, Sheddable Coatings for Long-Circulating Nanoparticles. *Pharmaceutical Research*, 2008. 25(1): p. 55-71.
6. **Li, W., Z. Huang, J.A. MacKay, S. Grube, and F.C. Szoka**, Low-pH-sensitive poly(ethylene glycol) (PEG)-stabilized plasmid nanolipoparticles: effects of PEG chain length, lipid composition and assembly conditions on gene delivery. *The Journal of Gene Medicine*, 2005. 7(1): p. 67-79.
7. **Nie, Y., M. Günther, Z. Gu, and E. Wagner**, Pyridylhydrazone-based PEGylation for pH-reversible lipopolyplex shielding. *Biomaterials*, 2011. 32(3): p. 858-869.
8. **Takae, S., K. Miyata, M. Oba, T. Ishii, N. Nishiyama, K. Itaka, Y. Yamasaki, H. Koyama, and K. Kataoka**, PEG-detachable polyplex micelles based on disulfide-linked block cationomers as bioresponsive nonviral gene vectors. *Journal of the American Chemical Society*, 2008. 130(18): p. 6001-6009.

9. **Matsumoto, S., R.J. Christie, N. Nishiyama, K. Miyata, A. Ishii, M. Oba, H. Koyama, Y. Yamasaki, and K. Kataoka**, Environment-responsive block copolymer micelles with a disulfide cross-linked core for enhanced siRNA delivery. *Biomacromolecules*, 2008. 10(1): p. 119-127.
10. **Noga, M., D. Edinger, R. Klager, S.V. Wegner, J.P. Spatz, E. Wagner, G. Winter, and A. Besheer**, The effect of molar mass and degree of hydroxyethylation on the controlled shielding and deshielding of hydroxyethyl starch-coated polyplexes. *Biomaterials*. 34(10): p. 2530-8.
11. **Noga, M., D. Edinger, W. Rödl, E. Wagner, G. Winter, and A. Besheer**, Controlled shielding and deshielding of gene delivery polyplexes using hydroxyethyl starch (HES) and alpha-amylase. *Journal of Controlled Release*, 2012. 159(1): p. 92-103.
12. **Schaffert, D., M. Kiss, W. Rödl, A. Shir, A. Levitzki, M. Ogris, and E. Wagner**, Poly(I:C)-Mediated Tumor Growth Suppression in EGF-Receptor Overexpressing Tumors Using EGF-Polyethylene Glycol-Linear Polyethylenimine as Carrier. *Pharmaceutical Research*, 2011. 28(4): p. 731-741.
13. **Parker, A.L., D. Oupicky, P.R. Dash, and L.W. Seymour**, Methodologies for Monitoring Nanoparticle Formation by Self-Assembly of DNA with Poly(l-lysine). *Analytical Biochemistry*, 2002. 302(1): p. 75-80.
14. **Davis, M.E.**, Nanoparticle therapeutics: an emerging treatment modality for cancer. *Nature Reviews Drug Discovery*, 2008. 7(9): p. 771-782.
15. **Kunath, K., T. Merdan, O. Hegener, H. Haberlein, and T. Kissel**, Integrin targeting using RGD-PEI conjugates for in vitro gene transfer. *J.Gene Med.*, 2003. 5(7): p. 588-599.
16. **Oupicky, D., M. Ogris, K.A. Howard, P.R. Dash, K. Ulbrich, and L.W. Seymour**, Importance of lateral and steric stabilization of polyelectrolyte gene delivery vectors for extended systemic circulation. *Mol. Ther.*, 2002. 5(4): p. 463-472.
17. **Verbaan, F.J., C. Oussoren, C.J. Snel, D.J.A. Crommelin, W.E. Hennink, and G. Storm**, Steric stabilization of poly(2-(dimethylamino)ethyl methacrylate)-based polyplexes mediates prolonged circulation and tumor targeting in mice. *The Journal of Gene Medicine*, 2004. 6(1): p. 64-75.
18. **Richardson, S.C.W., H.V.J. Kolbe, and R. Duncan**, Potential of low molecular mass chitosan as a DNA delivery system: biocompatibility, body distribution and ability to complex and protect DNA. *International Journal of Pharmaceutics*, 1999. 178(2): p. 231-243.
19. **Duncan, R. and T.A. Connors**, Drug targeting in cancer therapy: the magic bullet, what next? *Journal of Drug Targeting*, 1996. 3(5): p. 317-319.
20. **Ogris, M., B. S., S. S., K. R., and W. E.**, PEGylated DNA/transferrin-PEI complexes: reduced interaction with blood components, extended circulation in blood and potential for systemic gene delivery. *Gene Therapy*, 1999. 6(4): p. 595-605.
21. **Ogris, M., G. Walker, T. Blessing, R. Kircheis, M. Wolschek, and E. Wagner**, Tumor-targeted gene therapy: strategies for the preparation of ligand-polyethylene glycol-polyethylenimine/DNA complexes. *Journal of Controlled Release*, 2003. 91(1-2): p. 173-181.
22. **Lungwitz, U., M. Breunig, R. Liebl, T. Blunk, and A. Göpferich**, Methoxy poly (ethylene glycol)-Low molecular weight linear polyethylenimine-derived copolymers enable polyplex shielding. *European Journal of Pharmaceutics and Biopharmaceutics*, 2008. 69(1): p. 134-148.
23. **Petersen, H., P.M. Fechner, A.L. Martin, K. Kunath, S. Stolnik, C.J. Roberts, D. Fischer, M.C. Davies, and T. Kissel**, Polyethylenimine-graft-Poly(ethylene glycol) Copolymers: Influence of Copolymer Block Structure on DNA Complexation and

- Biological Activities as Gene Delivery System. *Bioconjugate Chemistry*, 2002. 13(4): p. 845-854.
24. **Luo, X., M. Feng, S. Pan, Y. Wen, W. Zhang, and C. Wu**, Charge shielding effects on gene delivery of polyethylenimine/DNA complexes: PEGylation and phospholipid coating. *Journal of Materials Science: Materials in Medicine*, 2012: p. 1-11.
 25. **Fischer, D., T. Bieber, Y. Li, H.-P. Elsässer, and T. Kissel**, A Novel Non-Viral Vector for DNA Delivery Based on Low Molecular Weight, Branched Polyethylenimine: Effect of Molecular Weight on Transfection Efficiency and Cytotoxicity. *Pharmaceutical Research*, 1999. 16(8): p. 1273-1279.
 26. **Fischer, D., Y. Li, B. Ahlemeyer, J. Krieglstein, and T. Kissel**, In vitro cytotoxicity testing of polycations: influence of polymer structure on cell viability and hemolysis. *Biomaterials*, 2003. 24(7): p. 1121-1131.
 27. **Moghimi, S.M., P. Symonds, J.C. Murray, A.C. Hunter, G. Debska, and A. Szewczyk**, A two-stage poly (ethylenimine)-mediated cytotoxicity: implications for gene transfer/therapy. *Molecular Therapy*, 2005. 11(6): p. 990-995.

V Effect of HES-decoration on storage stability of pDNA polyplexes – A benchmark study against PEGylation

This chapter is prepared for submission to the *European Journal of Pharmaceutics and Biopharmaceutics*:

Noga M, Edinger D, Wagner E, Winter G, Besheer A. Lyophilized HESylated pDNA polyplexes for increased nanoparticle stability and maintained gene transfer efficiency – A benchmark study against PEG

* First author

** Corresponding author

All cell culture experiments, namely studies of the luciferase reporter gene expression and the metabolic activity of transfected cells were performed together with Daniel Edinger under his guidance.

Abstract

Despite their great potential, gene delivery polyplexes have a number of limitations, including their tendency for aggregation *in vivo* due to interaction with blood components, as well as upon storage due to their propensity to reduce the interfacial energy. In previous studies, we could show that hydroxyethyl starch (HES)-decoration of polyplexes reduces aggregation *in vitro* and *in vivo*, in a manner comparable to, or better than polyethylene glycol (PEG), the standard polymer for nanoparticle stabilization. Since HES is a well-known cryo- and lyopreservative, this study investigates the ability of HES-decoration in improving the storage stability of polyplexes after frozen storage or lyophilisation. For this purpose, freeze thaw (FT) studies were conducted to assess the action of HES- and PEG-coats in the presence of standard excipients (glucose, sucrose or trehalose) on the particle size of LPEI-based pDNA polyplexes. While HES-decoration showed a better stabilization compared to PEGylated and naked polyplexes in solutions containing glucose as an amorphous excipient, both polymers were effective in inhibiting particle aggregation in the presence of trehalose or sucrose. The protection from polyplex aggregation changed after lyophilisation, where freshly lyophilized samples showed that the HES shield acted both cryo- and lyoprotective, while PEGylation enhanced polyplex aggregation after freeze-drying. Storage stability studies were conducted for 10 weeks at 2-8, 25 and 40°C, and the results show that the particle size of naked, HES- and PEG-decorated polymeric complexes was not affected by storage compared to freshly lyophilized particles. Evaluating the gene transfer efficiency of the stored lyophilized particles showed that efficiency of the naked polyplexes decreased by a factor of 10 compared to freshly prepared polyplexes, while the polymer-coated polyplexes were not negatively affected by the storage for 10 weeks. In general, the results show that while both the HES and PEG coats could prevent aggregation of polyplexes under frozen storage, the HES-coat resulted in distinctly superior protective effect in the case of lyophilization, with possible consequences for the *in vivo* application, where aggregated particles cannot be used. In summary, our developed HES-coats provided effective cryo- and lyoprotection to LPEI-based polyplexes.

Keywords

Hydroxyethyl starch (HES), polymeric gene delivery, lyophilization, storage stability

1 Introduction

Non-viral gene delivery systems based on cationic polymers like polyethylenimine (PEI) show great potential for the treatment of severe diseases, such as metastatic cancer. However, they tend to aggregate in the blood stream due to interaction with different blood components, leading to rapid elimination and lack of tissue specificity. In order to enhance their stability in the bloodstream, prolong their circulation time, and allow time for passive tumor targeting by the enhanced permeability and retention effect (EPR effect [1-3]), such cationic nanosystems are mostly equipped with a stealth polyethylene glycol (PEG) coat [4-6]. These non-degradable coats, however, reduce transfection efficiency *in vitro* and *in vivo* by steric hindrance of the cellular uptake and endosomal release [7, 8]. Methods to overcome this problem include the use of stimuli-sensitive linkers, which respond to local triggers, such as pH changes, reducing milieu or tumor-specific enzymes, shedding the PEG coat at the site of action [9-12]. Recently, we proposed the use of hydroxyethyl starch (HES) as a biodegradable substitute for PEG, and showed that it can be degraded by the action of alpha amylase, leading to stabilization in the bloodstream and slow degradation at the tumor site of action [13, 14].

Still one of the major limitations for developing pharmaceutically acceptable products concerns from polymeric gene delivery systems is their poor stability in aqueous solutions, necessitating tedious fresh preparation before use. This is because of their thermodynamically-driven tendency for reducing the interfacial surface area over time, leading to particle aggregation. Since size integrity is crucial for efficient and safe gene transfer [15, 16], frozen storage or dehydration by lyophilization could be viable options to maintain long-term stability and reducing the risk of batch-to-batch variations by fresh preparation prior to each application. Contrary to protein formulations, immobilization of nanoparticles by the formation of a rigid glassy matrix using protective additives is a helpful mechanism for preventing particle aggregation, however not necessarily required [17, 18]. Separating individual colloidal particles during freezing and dehydration is the key to hinder particle aggregation regardless of whether a glass matrix is formed, as assumed in the particle isolation hypothesis [18]. Among the excipients used for preservation of frozen or lyophilized samples, HES has been extensively studied with many successful outcomes. Several approaches report on the successful use of hydroxyethyl starch as cryo- and lyoprotector, for instance for the cryopreservation of red blood cells [19], keratinocytes [20] and stem cells [21]. Based on these observations, we wanted to test if our previously-reported use of HES for

nanoparticle decoration would impart positive effects on storage stability in frozen and lyophilized states. For this purpose, HES-decorated polyplexes were compared to PEG-decorated ones, as well as to naked polyplexes. We studied the effect freeze-thawing and freeze-drying as well as storage at different temperatures for 10 weeks on particle size (by DLS measurements) as well as the *in vitro* transfection efficiency of luciferase reporter gene and toxicity in Neuro2A cells.

2 Experimental Section

2.1 Materials

HES 70[0.5] with an average molar mass (M_w , number after HES; nominal value as provided by supplier) of 70 kDa and a molar substitution (MS is the mean number of hydroxyethyl groups per glucose unit; nominal value as provided by supplier; number in square brackets) of 0.5 was kindly provided by Serumwerk Bernburg, Germany. Sodium cyanoborohydride (NaBH_3CN) was purchased from Merck Schuchardt OHG (Hohenbrunn, Germany). Linear polyethylenimine with an average molar mass of 22 kDa (PEI22) and the PEI22 – PEG20 conjugate (PEG20: polyethylene glycol with the average molecular weight of 20 kDa) were synthesized as described in [22]. The excipients sucrose (AppliChem GmbH, Darmstadt, Germany) and trehalose (VWR International BVBA, Leuven, Belgium) were used without further purification. Alpha-amylase (AA) from porcine pancreas was bought from Sigma-Aldrich (Steinheim, Germany, catalogue number A3176). Phadebas[®] Amylase Test was from Magle AB, Lund, Sweden. Plasmid pCMVluc was prepared by PlasmidFactory, Bielefeld, Germany. Cell culture medium, antibiotics and fetal calf serum (FCS) were purchased from Life Technologies (Karlsruhe, Germany). Other solvents and chemicals were reagent grade and were used as received.

2.2 Methods

2.2.1 Synthesis and characterization of HESPEI co-polymers using ¹H-NMR, copper assay, and SEC.

The synthesis and characterization of HES-PEI conjugates was performed as described previously [13]. In short, conjugates of transfection agent LPEI22 and different HES types

with a wide range of molar masses (from 10-70kDa) and degrees of hydroxyethylation (from 0.4-1.3) was prepared in the molar ratio of 1:25 LPEI to HES via Schiff's base formation and reductive amination using sodium cyanoborohydride, the product was purified by ion exchange chromatography and characterized using $^1\text{H-NMR}$, UV-photometric copper assay and size exclusion chromatography.

2.2.2 Preparation of LPEI-based pDNA polyplexes.

Naked LPEI-based polyplexes (nPx) were manufactured by the rapid addition and mixing of PEI to the plasmid pCMVluc (pDNA) at N/P ratio 6.0 and a final pDNA concentration of 20 $\mu\text{g/mL}$ in HBG pH 7.1 (HEPES buffered glucose; 20 mM HEPES, 5 % glucose (w/v)). Polyplexes were allowed to incubate at RT for 30 minutes prior to analysis. For instance, a volume of 1 mL of naked PEI/DNA transfection particles at N/P ratio of 6.0 was composed of 20 μg pDNA and 16 μg LPEI. HESylated and PEGylated polyplexes were prepared in the same fashion as nPx, with the exception that pure PEI was partially replaced by modified PEI, e.g. HES70[0.5]-PEI/DNA complexes at N/P ratio 6.0 and a ratio of PEI to HES-modified PEI of 75:25 were made of 20 μg DNA, and a mixture of 12.0 μg PEI and 4.0 μg HES70[0.5]-PEI22 per 1 mL (based on PEI). HES- and PEG-decorated polyplexes were generated with the ratio 90:10, 75:25, 70:30 and 50:50 of PEI to HES-PEI or PEG-PEI conjugates.

2.2.3 Polyplex stability against shelf-freezing (SF) and liquid nitrogen (LN_2) immersion stress.

For freeze-thaw (FT) studies, naked, HES-decorated and PEGylated polymeric pDNA complexes were prepared following the afore-mentioned standard preparation (20 $\mu\text{g/mL}$ final pDNA concentration, N/P ratio 6.0, HBG pH 7.4). Controlled SF cycles were conducted once or three times in 2R vials using a Lyostar II freeze drier (SP Scientific, Stone Ridge, US). Polyplex solutions were treated following the scheme: freezing at -1°C/min from 10°C to -50°C with a 30 minutes hold at -50°C , thawing at 1°C/min to 10°C with 30 minutes hold. For fast freezing, polyplexes were frozen by 5 minutes LN_2 immersion. To control the thawing step, SF- and LN_2 -treated samples were tempered at 25°C (water-bath) prior to analysis.

2.2.4 Excipient screening.

For glucose replacement, polymeric complexes were prepared in isotonic (9.25 m/V %), glucose-free 20mM HEPES buffer (pH 7.4) in presence/absence of the following cryo- and lyoprotectors: trehalose (Tre; HEPES buffer trehalose, “HBTre”), sucrose (Suc, HEPES buffered sucrose, “HBSuc). Unmodified LPEI particles and modified polyplex nanosystems were treated once and three times by SF as described above.

2.2.5 Lyophilization studies of HES-decorated polyplexes.

Polyplex samples (20µg/mL DNA concentration, N/P ratio 6.0) for freeze-drying (FD) were formulated in HBTre buffer pH 7.4 (Tre, 9.25%, m/V) and HBSuc buffer pH 7.4 (Suc, 9.25%, m/V) and aseptically produced. Freeze-drying was performed using a Christ EPSILON 2-6D freeze-dryer (Martin Christ Freeze Dryers GmbH, Osterode am Harz, Germany). An amount of 150 µL polyplex solution per 2R vial was lyophilized following the scheme: freezing at -1°C/min from 10°C to -50°C, hold time 120 minutes; primary drying at 0.5°C/min from -50°C to -20°C, hold time 24 hours; secondary drying at 0.1°C/min from -20°C to 30°C, hold time 10 hours. Afterwards the system was vented with nitrogen and the polyplex samples were stoppered at approximately 800mbar. Lyophilized as well as frozen polyplex samples were stored at 2-8°C, 25°C and 40°C for 10 weeks. Transfection particles were characterized in terms of particle size, surface charge, residual moisture, thermic stability, *in vitro* reporter gene transfer and metabolic activity before and after 10 week mid-term storage.

2.2.6 Biophysical characterization of pDNA polyplexes.

The particle size and zeta potential of naked LPEI, HES-decorated and PEGylated polyplexes with/without FT stress was studied using the Zetasizer Nano ZS (Malvern Instruments, Worcestershire, United Kingdom) in semi-micro PMMA cuvettes and in folded capillary cells. The viscosity of polyplex samples in HBG was set to 1.0366 mPas at 25°C. Malvern software (version 6.32) was used for data analysis and acquisition. Measurements of the hydrodynamic diameter of frozen/freeze-dried samples were performed at room temperature on a DynaPro Titan platereader (Wyatt Technology Europe, Dernbach, Germany). 30 minutes prior to DLS analysis the lyophilized product was reconstituted with 150 µL highly purified water. DLS studies were performed at an acquisition time of 5 seconds and the number of 5 acquisitions in 96 well-plates (Costar, Corning, USA). The viscosity was set to 1.3045 cP at 20°C. Dynamics V6.12.03 was used DLS data analysis and data acquisition.

2.2.7 Thermoanalytical analysis.

Dynamic scanning calorimetry (DSC) measurements (n=3) were carried out using a Mettler Toledo DSC821 (Mettler Toledo GmbH, Giessen, Germany) to study the glass transition temperature of the maximally frozen concentrate (T_g'), as well as the glass transition temperature of the lyophilized product (T_g) directly after FD and after 10 week storage at 2-8°C, 25°C and 40°C. For T_g determination, an amount of 25 μ L polyplex solution in HBTre or HBSuc was analyzed in 40 μ l aluminum crucibles. The samples were frozen at -1°C/min from 20°C to -50°C, with 60 minutes hold, and reheated at 5°C/min from -50°C to 20°C. An amount of around 15 mg lyophilized product in 40 μ l aluminum crucibles was cooled (-10°C/min) from RT to -10°C, heated up to 110°C (10°C/min). This procedure was repeated once. The T_g value of various lyophilized polyplexes was determined in the second heating step to eliminate relaxation phenomena.

2.2.8 Karl-Fischer titration.

Residual moisture content of lyophilized polyplex samples was determined directly after freeze-drying process and after 10 week mid-term storage (n=3). Coulometric Karl-Fischer titrations of approximately 15 mg lyophilisate were conducted using an Aqua 40.00 titrator (Analytik Jena AG, Jena, Germany) with headspace module without special or a 737 KF Coulometer (Metrohm, Filderstadt, Germany). Using 737 KF Coulometer polyplex lyophilisates were dissolved in dry Methanol, the methanol solutions were injected into the titration solution (HydranalTM-Coulomat AG, Riedel-de Haen, Seelze, Germany), and the water content was determined. Empty vials served as blanks.

2.2.9 Cell culture experiments.

Cultured cells were grown at 37 °C in 5% CO₂ humidified atmosphere. Murine neuroblastoma, Neuro2A (ATCC CCL-131, purchased from DSMZ, Braunschweig, Germany) were cultured in Dulbecco's Modified Eagle Medium (DMEM). DMEM medium was supplemented with 10% FCS, 4 mM stable glutamine, 100 U/mL penicillin, and 100 μ g/mL streptomycin.

2.2.10 Luciferase reporter gene expression studies.

For assessing the transfection activity of HES-decorated polyplexes after lyophilisation, freeze-thawing and 10 week mid-term storage at 2-8°C, 25°C and 40°C, *in vitro* pDNA transfection efficiency study was carried out in murine Neuro2A cell lines. The gene transfer performance of HES-decorated polyplexes after FT-, FD- and storage stress was benchmarked against the transfection efficiency of identically treated naked LPEI- and PEGylated particles. Experiments were performed in 96 well plates by seeding 1×10^4 cells per well in 100 μ L medium 24 h prior to transfection. A cell confluency of around 60-80% was reached at the point of transfection. Directly before transfection, the medium was exchanged against fresh medium. Polyplex lyophilisates were reconstituted 30 minutes prior to transfection with an amount of 150 μ L highly purified water to give a final pDNA concentration of 20 μ g/mL. N2A cells were treated with freshly prepared transfection particles, 10 week stored freeze-dried polyplexes, as well as nanocomplexes after 10 week frozen storage at -80°C. HBTre and HBSuc (20 mM HEPES, 9.25% m/V Tre or Suc, pH 7.4, respectively) served as negative controls. An amount of 10 μ L polyplex solution (N/P 6.0, 20 μ g/mL DNA concentration) was added to the cells to give a total volume of 100 μ l per well. The medium was replaced 4 hours after point of transfection by 100 μ L fresh medium. Luciferase transfection efficiency was evaluated 24 h after pDNA transfection. Cells were treated with 100 μ L cell lysis buffer (25 mM Tris pH 7.8, 2 mM EDTA, 2 mM DTT, 10% glycerol, 1% Triton X-100) for 30 minutes and the luciferase activity in 35 μ l cell lysate was measured in white 96 well plates using a luciferase assay kit (100 μ L Luciferase Assay buffer, Promega, Mannheim, Germany) on a luminometer for 10 s (Centro LB 960 instrument, Berthold, Bad Wildbad, Germany). Values are given as relative light units (RLU) per well (mean \pm standard deviation of quadruplicates).

2.2.11 Metabolic activity of transfected cells.

The viability of Neuro2A cells after LPEI-based pDNA transfection was evaluated using MTT assay. For determination of the metabolic activity of transfected cells, N2A cells were seeded and transfected as explained above. 24 h after transfection, MTT (3-(4,5-dimethylthiazol-2-yl)-2,5-diphenyltetrazolium bromide) (Sigma-Aldrich, Germany) was dissolved in phosphate buffered saline at 5 mg/mL, and an amount of 10 μ L of a 5 mg/mL solution of MTT was added to each well reaching a final concentration of 0.5 mg MTT/mL. Cells were incubated for 2 h, the unreacted dye with medium was removed and the cells were lysed by incubation at -80 °C for at least 30 min. The formazan product was dissolved in 100

μL /well dimethyl sulfoxide, incubated at 37°C for 30 minutes under constant agitation and quantified by optical absorbance using a plate reader (Tecan, Groedig, Austria) at 590 nm with background correction at 630 nm. The metabolic activity [%] relative to control wells containing HBG treated cells (set to 100%) was calculated as follows (Metabolic activity = $A_{\text{test}}/A_{\text{control}} \times 100$).

3 Results

In the present work, we report on the effect of HES-decoration on the stability of frozen and lyophilized pDNA polyplexes. In all the experiments, naked polyplexes as well as PEG-coated polyplexes were used for comparison.

Before studying the biophysical behaviour of LPEI/DNA complexes with HES-decoration after freeze-drying process, the effect of freeze-thaw (FT) stress on the particle stability was investigated. Since HBG (HEPES buffered glucose; 20 mM HEPES, 5 % w/v glucose, pH 7.4) is a widely used formulation buffer for the preparation and application of polymeric polyplexes, it was used for the preliminary FT experiments. The latter were performed by applying either controlled shelf-freezing (SF) or fast liquid nitrogen immersion (LN_2), and the particle size of unmodified-, HES-decorated and PEGylated polyplexes was measured. Figure V. 1 shows that SF leads to a stronger aggregate formation for all polyplexes compared to LN_2 . For instance, the particle size of naked polyplexes increased $> 1 \mu\text{m}$ after 1 FT cycle of SF, and $> 3 \mu\text{m}$ following 3 FT, compared to only 150 and 400 nm for 1 and 3 FT cycles of LN_2 , respectively. The use of PEG coat did not prevent aggregation under both FT techniques, while the HES coat significantly reduced the aggregation tendency, particularly with the more stressful SF procedure. It is worth noting that the ratio of HES-PEI:PEI did not show a difference in the stabilizing effect, while increasing the ratio of PEG-PEI:PEI seemed to have a negative effect on nanoparticle aggregation.

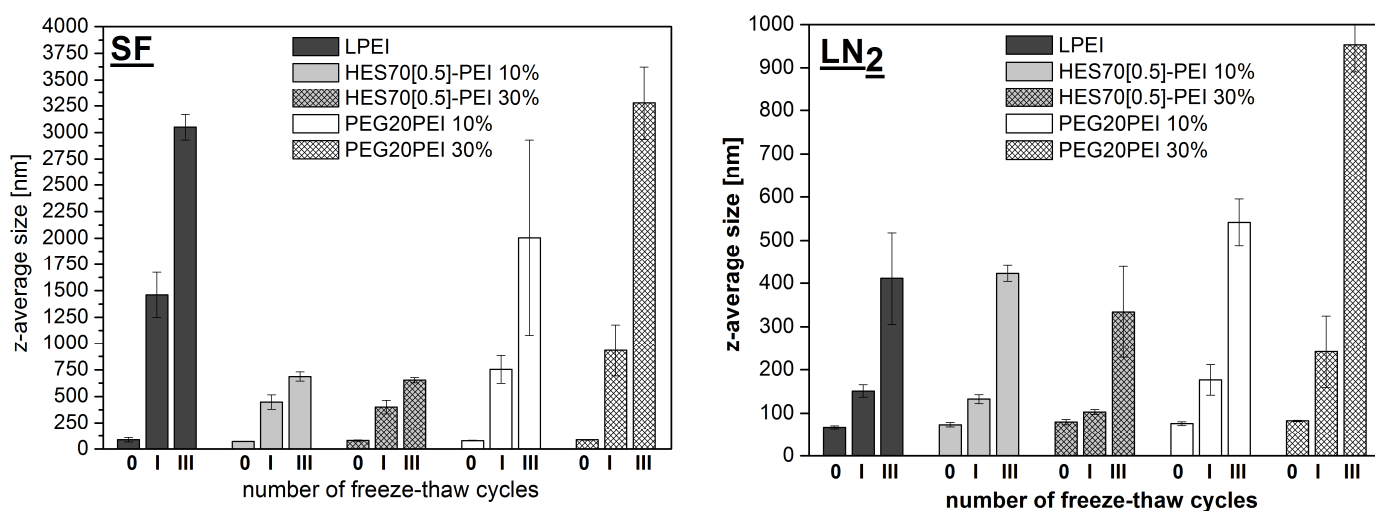


Figure V. 1. Freeze-thaw stress studies (SF: shelf-freezing; LN₂: liquid nitrogen immersion). Incorporation of hydrophilic polymers provided steric stabilization of polyplexes against controlled SF with the effect of HES > PEG > no hydrophilic component. Fast freezing reduced the tendency of aggregation.

Since glucose is known to have a very low T_g, besides its tendency to react with amino groups through Maillard's reaction, sucrose (Suc) and trehalose (Tre) were evaluated as better alternatives and well-established cryo- and lyoprotectors. The particle size of naked LPEI-, HES70- and PEG20-decorated polyplexes was studied under the effect of controlled (SF) FT treatment in isotonic formulations of Tre or Suc. The minimal freezing temperature for FT and subsequent FD processes was kept below the T_g' of various formulations at -50°C (Table V. 1). Results in Figure V. 2 show that in the absence of any cryoprotective excipient – the so-called “HEPES” formulation – all generated polymeric complexes formed large aggregates in the micron-range under the effect of freezing and thawing. The tendency towards particle clustering was markedly reduced by the addition of cryoprotective excipients. Even in the presence of Tre and Suc, naked LPEI polyplexes showed the strongest proneness towards the formation of aggregates. Meanwhile, incorporation of both hydrophilic polymers PEG and HES onto the polyplex surface markedly reduced the aggregation. Surface masking using 10% HES-PEI:PEI or PEG-PEI:PEI significantly improved the resistance of LPEI-based polyplexes against FT stress. Higher amounts of HES-PEI or PEG-PEI completely stabilized the polyplexes and maintained the initial particle size of freshly prepared particles (~ 80 nm). These results demonstrate the stabilizing and cryoprotective action of both the HES and PEG coats for polyplexes, and show the beneficial effect of Tre and Suc as stabilizing excipients. Accordingly, they were further tested in freeze-drying (FD) experiments.

Table V. 1. Glass transition temperatures of the maximally frozen concentrates (T_g'). All FT and FD studies were kept far below the T_g' of the formulation buffers to ensure entire sample freezing.

Tre 9.25% m/V	-29.72 ± 0.18
Suc 9.25% m/V	-32.12 ± 0.16

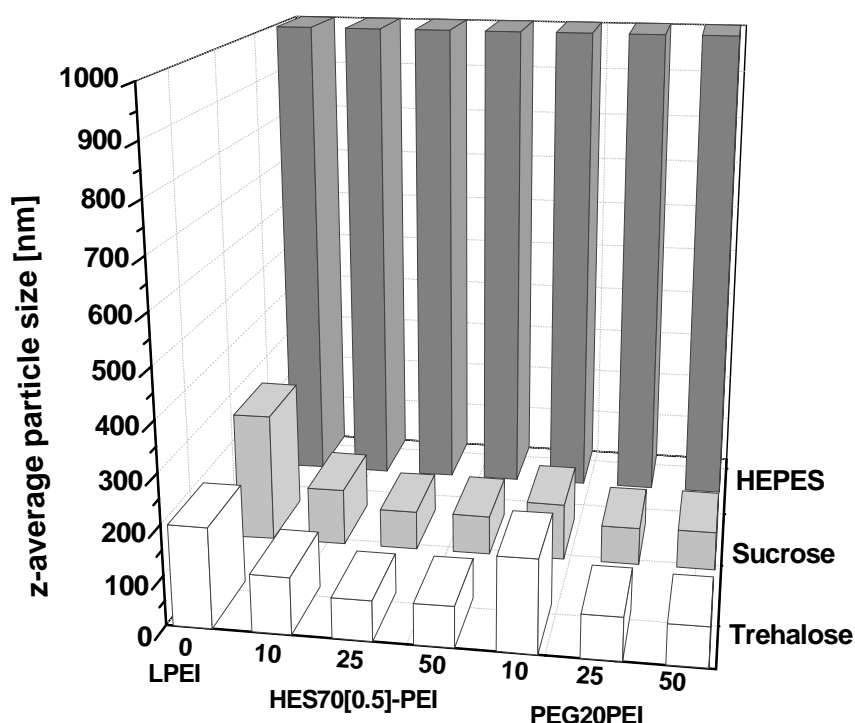


Figure V. 2. Excipient screening studies. 20mM HEPES pH 7.4 supplemented with 9.25 m/V % Tre or Suc provided high resistance against FT stress. In addition, HES and PEG acted cryoprotective by steric stabilization.

In freeze drying experiments, naked polyplexes as well as HES70- and PEG20- coated polyplexes with 10, 25 and 50% shielding agent in 20 mM HEPES and 9.25 % (w/v) Tre or Suc were lyophilized and analyzed directly after lyophilization. All lyophilized polyplexes showed good lyo-cake appearance after FD process with short reconstitution times in water (<

3s). Naked LPEI polyplexes in Tre or Suc showed acceptable stability, manifested as a small increase in hydrodynamic diameter to approximately 130 nm following the FD process. Highest resistance and lowest tendency to the formation of aggregates under the effect of freeze drying was observed for HESylated polyplexes (size ~ 110-120 nm). The total amount of incorporated HES-PEI played a minor role in the steric stabilization of polymeric polyplexes during FD process, since already the amount of 10% HES-PEI provided high lyo-resistance. Increasing the amount of HESPEI to 25 % and 50 % did not show any additional stabilizing effect. Meanwhile, PEG-decoration led to the formation of large particle clusters of around 250-350 nm after lyophilization (see Figure V. 3). These results show that, in contrast to FT experiments, where the PEG-coat showed good cryoprotective effect, it did not act as a good lyoprotectant, but was even worse than the naked polyplexes, promoting particle aggregation.

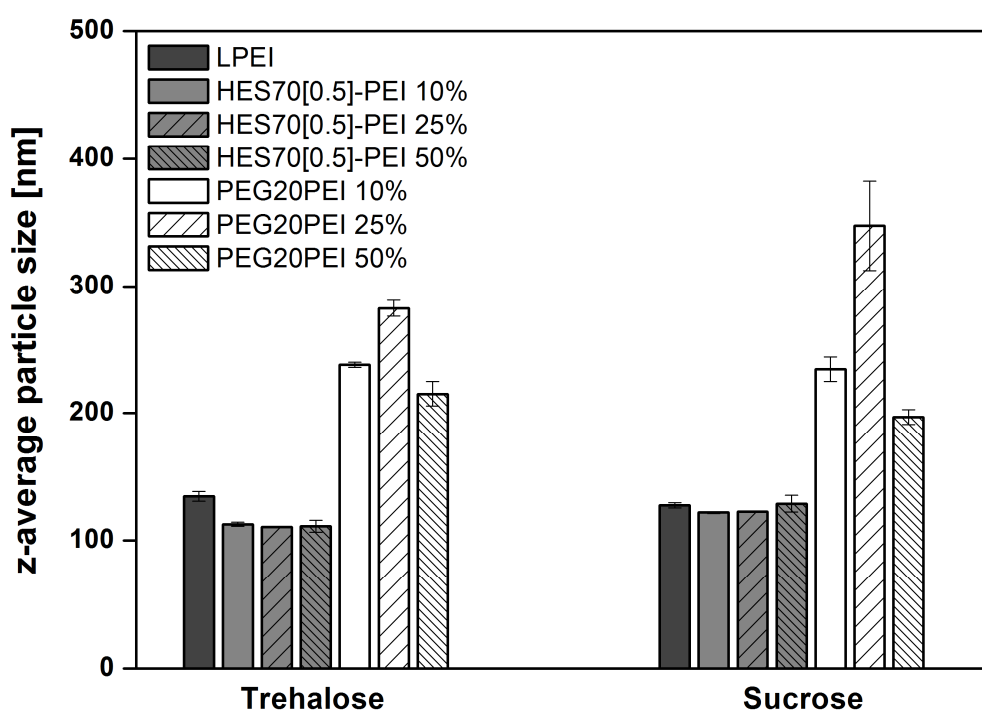
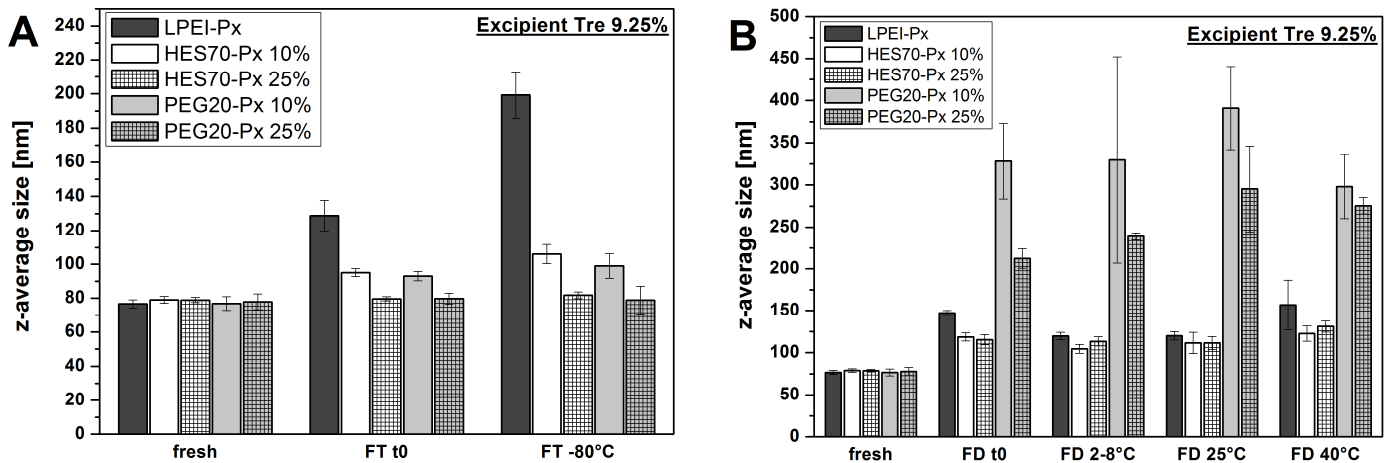


Figure V. 3. *Excipient screening and FD pre-experiments. HBTre and HBSuc formulations showed the best protection against lyo-induced particle aggregation. Incorporation of HES onto the polyplex surface increased the particle stability against FD stress by steric stabilization compared to unmodified LPEI polyplexes, PEG decoration resulted in poor stabilizing effect.*

Finally the effect of 10 weeks mid-term storage of frozen (at -80°C) and lyophilized polyplexes, stored at 2-8 °C, 25 °C and 40 °C, on the physicochemical properties of the

lyophilisate (particle size, glass transition temperature and residual moisture) was investigated. Additionally, the *in vitro* reporter gene expression and metabolic activity of the polyplexes were assessed. For this purpose, naked, HES- and PEG-decorated nanoparticles were used, and the results were compared to freshly prepared particles. Results of DLS for the particle size of the 10 weeks frozen storage are similar to the 1 freeze thaw cycle, where the HES- and PEG-coated polyplexes maintain their original particle size, while the naked polyplexes markedly increase in size to approximately 130 nm after 1 FT cycle, and to ~200 nm after 10 weeks storage, irrespective of the stabilizing excipient. Similarly, results of the 10 weeks storage of the freeze dried samples are similar to the sample analyzed directly after lyophilization, with no significant difference between the different temperatures or the stabilizing excipient used (Tre vs. Suc), where the HES-coat showed the lowest increase in particle size (~120 nm particle size), followed by a slightly larger size for the naked polyplexes (~140 nm), and a dramatic increase for the PEGylated ones (~200-350 nm). In general, the results show that HES-decoration is good both as cryo- and lyoprotectant, with the particles maintaining the size for 10 weeks storage at different temperatures, while PEGylation was only effective as a cryoprotectant but not as a lyoprotectant.



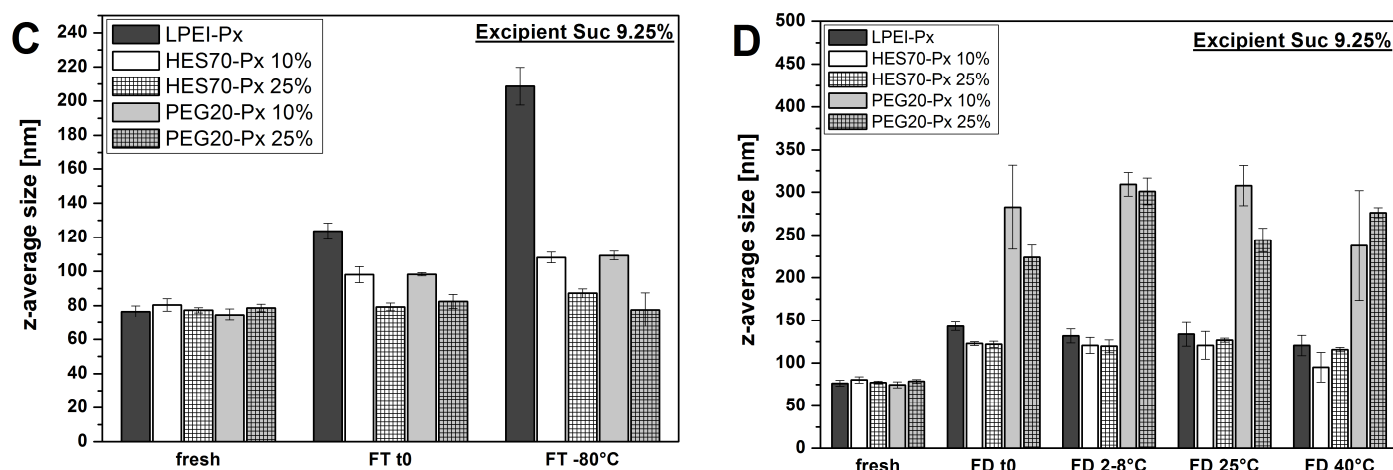


Figure V. 4. Z-average particle size of freshly prepared polyplexes, freeze-thawed (FT) and freeze-dried (FD) nanoparticles. A+B: HBTre formulation, C+D: HBSuc formulation. The particle size was studied directly after FT and FD (FT t0 and FD t0) and after storage of 10 weeks at different storage conditions (-80 °C, 2-8 °C, 25 °C and 40 °C).

Analysis of the glass transition temperature of the lyophilisates (T_g) and the residual moisture are shown in Table V. 2. Results show an increase in residual moisture with time and temperature, associated with decrease in T_g for both stabilizing excipients Tre and Suc. For instance, the T_g of Tre-containing formulations moved from around 90 °C directly after lyophilization to approximately 70 °C after 10 weeks storage at 2-8 °C and to 54 °C for storage at 40 °C. Simultaneously, the residual moisture increased from ~ 0.4 % (w/w), to ~ 0.9 % (w/w) and to 1.7 % (w/w), respectively. Modifying the surface of LPEI polyplexes using hydrophilic polymers HES and PEG did not affect the T_g and RM of lyophilized samples, since the excipient to nanoparticle mass ratio exceeded 2000 : 1, stabilizer to polyplex. The reduction of T_g of Suc formulations stored at 40°C to 38°C lead to a macroscopic collapse of the cakes, while all the other samples maintained their cake appearance. It is worth noting that changes in residual moisture and T_g did not have a strong impact on the particle size of the stored particles as shown above.

Table V. 2. Physical characterization of polymeric nanocomplexes using DSC and KF titrations. FT and FD studies were run below the T_g' of HBTre and HBSuc at -50°C to ensure entire glass formation. T_g and RM of lyophilized samples were studied directly after FD and after 10 weeks of storage at 2-8 °C, 25 °C and 40 °C (n=3).

			After FD	Storage @ 2-8°C	Storage @ 25°C	Storage @ 40°C
Tre 9.25%	Tg [°C]	LPEIPx	89.00±6.63	67.15±9.16	56.87±2.59	54.78±2.79
		HES70Px 10%	91.29±2.71	69.81±4.25	59.08±3.23	54.97±2.83
		HES70Px 25%	91.12±3.00	71.23±2.46	57.56±2.17	53.76±3.21
		PEG20Px 10%	91.52±2.33	70.81±2.82	57.23±2.30	52.49±4.43
		PEG20Px 25%	89.80±5.26	70.39±3.34	58.19±2.32	53.96±3.05
	RM [%w/w]	LPEIPx	0.40±0.07	0.87±0.30	1.31±0.37	1.70±0.48
		HES70Px 10%	0.39±0.06	0.93±0.24	1.42±0.21	1.60±0.24
		HES70Px 25%	0.38±0.04	0.83±0.21	1.46±0.41	1.73±0.51
		PEG20Px 10%	0.37±0.02	1.00±0.41	1.36±0.17	1.57±0.53
		PEG20Px 25%	0.38±0.04	0.90±0.28	1.38±0.29	1.87±0.14
Suc 9.25%	Tg [°C]	LPEIPx	61.73±2.54	51.13±2.36	44.67±0.73	38.26±0.89
		HES70Px 10%	62.68±1.22	51.62±2.11	44.56±0.55	37.24±1.93
		HES70Px 25%	63.23±1.06	51.83±2.10	44.34±0.33	37.91±1.05
		PEG20Px 10%	61.67±2.64	51.97±2.14	44.23±0.41	37.57±1.45
		PEG20Px 25%	61.08±3.59	50.84±2.63	44.73±0.83	38.10±0.92
	RM [%w/w]	LPEIPx	0.43±0.04	0.95±0.33	1.32±0.41	1.54±0.29
		HES70Px 10%	0.44±0.04	0.88±0.27	1.26±0.34	1.68±0.37
		HES70Px 25%	0.42±0.05	1.00±0.18	1.22±0.24	1.44±0.48
		PEG20Px 10%	0.44±0.04	1.05±0.25	1.16±0.51	1.63±0.23
PEG20Px 25%		0.48±0.10	0.97±0.28	1.34±0.27	1.54±0.45	

We also investigated the effect of frozen and lyophilized storage of the polyplexes with HES and PEG corona on the *in vitro* transfection efficiency using a luciferase reporter gene expression in murine Neuro2A cells as well as metabolic activity of those cells (as a surrogate for toxicity). Results of the transfection efficiency show that freeze drying and mid-term storage of lyophilized LPEI polyplexes reduced their initial transfection efficiency up to 1 order of magnitude, independent of the storage condition. The 10% HES-decorated polyplexes seemed to maintain their transfection efficiency upon storage at 2-8 and 25°C, but the transfection efficiency seemed to reduce by an order of magnitude upon storage at 40°C for 10 weeks. On the other hand, the transfection efficiency of the higher level of HES-decoration (25%) increases slightly upon storage for 10 weeks, irrespective of the storage temperature. As for the PEGylated polyplexes, transfection efficiency remains relatively constant at both concentration levels and irrespective of the storage temperature. Meanwhile, results of the viability test show that the Neuro2A cells were not negatively affected upon exposure to freshly-prepared, or stored frozen and lyophilized polyplexes (Figure V. 65). This is a clear indication for safety of the polyplexes at the applied dose.

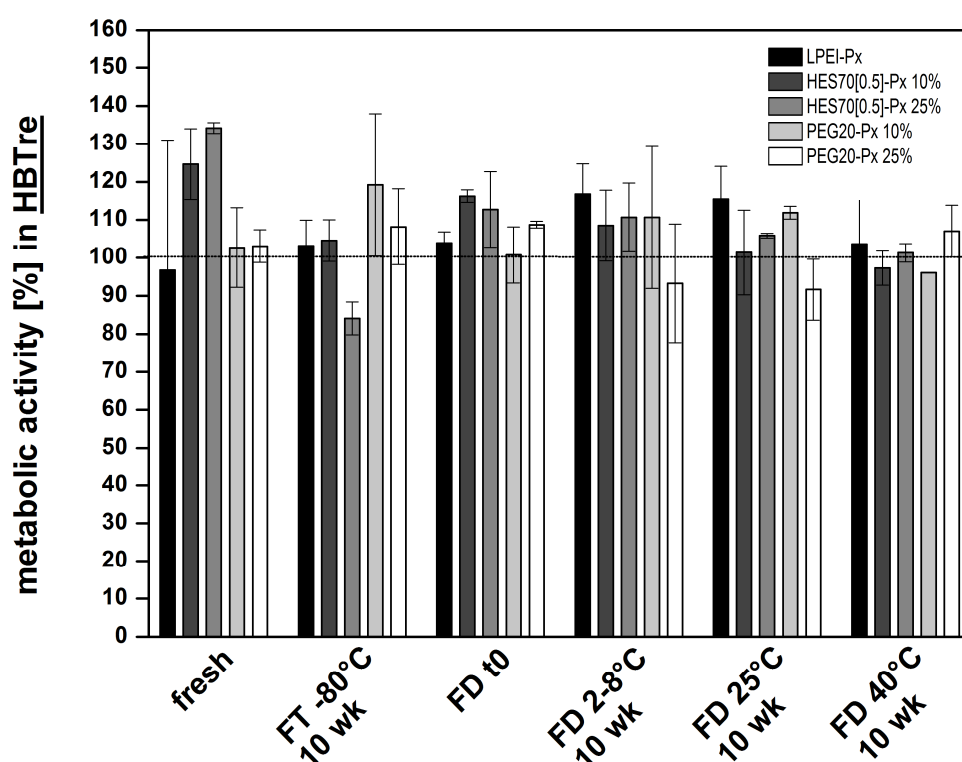


Figure V. 5. The metabolic activity of N2A 24h after polyplex treatment. N2A cell incubation with differently treated nanoparticles (fresh, FT and FD) did not affect the cellular viability.

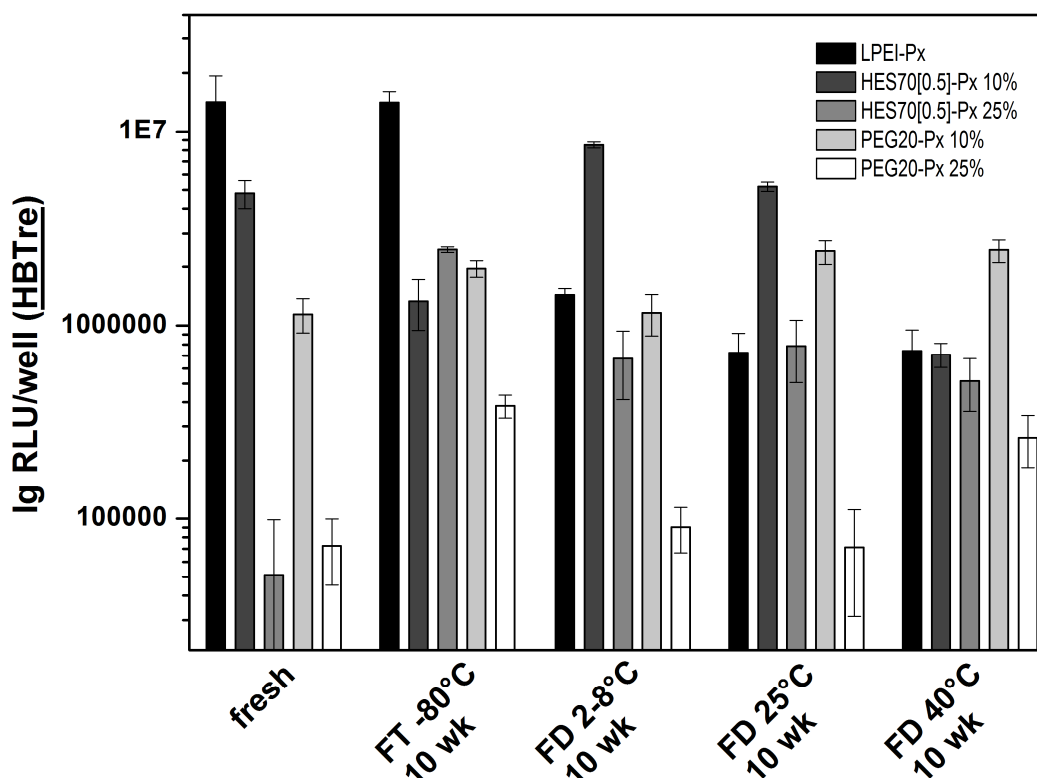


Figure V. 6. Luciferase reporter gene expression studies in N2A cells. Cell culture experiments were performed with naked, HES70[0.5]- and PEG20-decorated polyplexes after 10 weeks of lyophilized storage at different storage conditions. Freshly prepared particles formulated in HBTre served as controls.

4 Discussion

Non-viral gene vectors face many hurdles that hamper their development to pharmaceutically-acceptable products. These include their tendency to aggregate in the blood stream and their rapid elimination by phagocytosis. Even PEGylation, the state-of-the-art solution to these problems, can reduce transfection efficiency, because PEG interferes with cellular-uptake and DNA release (so-called “PEG-dilemma” [8, 23-26]). An optimum coat would thus show effective shielding to increase stability in blood stream and reduce in vivo elimination, as well as a controlled deshielding to enhance cellular uptake and release. In previous studies, we reported on the successful use of biodegradable HES coats for polyplex shielding and enzymatically-catalyzed deshielding under the effect of alpha-amylase, both *in vitro* and *in*

vivo [13, 14]. In this study we evaluate if the proposed use of HES coats would also offer an advantage for long term storage stability of polymeric gene delivery systems. The latter are known to have poor stability and short shelf-life as they aggregate in solution or after freeze-drying [27, 28], thus requiring fresh preparation of the nanoparticles before application. Due to the documented advantages of HES as a cryo- and lyopreservative [19-21], its use as a nanoparticle shielding agent might have additional advantages towards frozen or freeze-dried stability compared to the more commonly used PEG coat. This is because the latter is known to crystallize upon freezing, leading to possible stability problems [29-31].

Initially, the effect of freeze-thaw stress on the particle size of polyplexes was studied in the standard formulation buffer HBG pH 7.4. Differently composed polymeric complexes were frozen by controlled shelf-freezing (SF, freezing rate $-1^{\circ}\text{C}/\text{min}$), as well as faster uncontrolled freezing using liquid nitrogen immersion (LN_2). DLS results after 1 and 3 FT cycles showed that all LPEI-based pDNA particles were prone to aggregation following freezing and thawing, however the extent of aggregation significantly differed between naked LPEI polyplexes, HES-decorated and PEGylated nanoparticles. Incorporation of hydrophilic polymer HES delivered the best results in terms of particle size maintenance under controlled FT treatment by the effect of steric stabilization, while PEGylated and also naked LPEI polyplexes formed larger particle clusters compared to HES-shielded polyplexes (Figure V. 1). Glucose is known to have a very low T_g (-45°C according to [32]), and together with the low T_g of PEG (-67°C as reported by [33]) compared to HES (-15°C according to [34]), this might be one reason for the aggregation of PEG coated particles under the slow shelf freezing, where the nanoparticles remained in a viscous environment long enough to aggregate, while the higher T_g of HES might have prevented such aggregation. Nevertheless, and due to the potential interaction of glucose with amines through Maillard's reaction, we further tested Tre and Suc (in isotonic concentration, 9.25 % m/V) as better and well-established stabilizers. While those disaccharides could not prevent the aggregation of naked polyplexes after FT treatment, both HES- and PEG-decoration could stabilize the polyplexes against aggregation in those formulations (Figure V. 2). Accordingly, they were further investigated under freeze drying conditions.

Upon DLS measurement of particle size of the nanoparticles directly after lyophilisation, one notices that, while both HES- and PEG-coats had a cryostabilizing effect on the polyplexes under FT conditions, only HES possessed lyostabilizing effect, while the PEG-decoration

seemed to destabilize the particles in comparison to the naked polyplexes (see Figure V. 3). Incorporation of HES onto the surface of the nanocomplexes provided very good resistance against freeze-drying stress, with nearly maintained initial particle sizes of freshly prepared particles. Surface charge shielding using PEG induced strong particle aggregation after lyophilisation compared to the naked polyplexes (presumably due to PEG crystallization), irrespective of the stabilizing excipient.

We further studied the effect of 10 weeks storage of naked, HES- and PEG-coated polyplexes in the frozen as well as the freeze-dried states. The z-average particle size measured by DLS showed that 10 weeks of frozen storage at -80°C leads to an increase in the particle size of naked polyplexes (to > 200 nm). Meanwhile, the particle size of HES- and PEG-coated particles remains constant, indicating the effectiveness of these coats in protecting the particles for such a relatively long period of time. It is worth noting that the effect on particle size is similar to that after 1 FT cycle (see Figure V. 4), indicating that storage at -80°C was at low enough temperature to inhibit any dynamic processes in the frozen liquid, and that the destabilization of the naked particles occurred during the freezing and/or thawing procedure similar to what happened after 1 FT cycle. Meanwhile, the freeze-dried particles showed a different picture, where the HES-coated particles showed the lowest increase in particle size (from 80 to 120 nm), followed by the naked particles, while the PEG –coat seemed to destabilize the lyophilized particles, increasing the particle size up to 300 nm. The aggregation of PEGylated nanoparticles after lyophilisation due to PEG crystallization is mentioned several times in literature. For instance, lyophilisation of PEO-grafted PLA nanoparticles induced aggregation. The addition of lyoprotectors improved the particle resistance against freeze-drying, however the size integrity of PLA particles decorated with high surface density of low molecular weight PEO was impaired by FD in the presence of lyoprotectors due to crystallization of PEO [35]. Also in the case of PEGylated cross-linked polyplex micelles [10] and drug-loaded PLGA-mPEG nanoparticles [30] PEG crystallization during lyophilisation induced particle aggregation. In addition, Hinrichs and co-workers reported on the importance of the optimal choice of the protective additives [36, 37]. PEGylated lipoplexes in inulin were stable after FD, while the dextran formulation resulted in particle clustering due to the incompatibility of PEG and dextran leading to phase separation. [18]. It is worth noting that the particle size of the naked, HES- and PEG-decorated polyplexes after 10 weeks of storage seemed to be independent of storage temperature, and

similar to the results obtained with freshly lyophilized samples, indicating that the main effect was due to the water removal process and not much affected by the storage time.

In general, the particle size of polymeric complexes is not only an important quality feature, but represents also a crucial factor affecting the levels of gene transfer. The size of nanoparticles can influence the *in vitro* transfection efficiency as well as the *in vivo* performance of gene delivery polyplexes, such as biodistribution, cellular uptake, endosomal release, cytoplasmic and nuclear trafficking [8, 38, 39]. As a surrogate for these effects, we measured the gene expression rate of LPEI polyplexes *in vitro* on Neuro2A cells using luciferase as a reporter gene. The transfection efficiency of naked polyplexes decreased upon lyophilisation and storage approximately by the factor 10, while the transfection efficiency of particles with HES- and PEG-coats was not diminished (Figure V. 6). Finally, results in Figure V. 5 showed that the metabolic activity of Neuro2A cells was not affected by treatment with freshly prepared, as well as frozen-stored and freeze-dried naked and modified (HES- and PEG-decorated) LPEI polyplexes, indicating fairly low cell toxicity. The residual moisture as well as the glass transition temperature of the lyophilized polyplex samples (Table V. 2) had no significant impact on the particle size or the gene transfection efficiency, despite the slight increase in RM and decreasing Tg of the lyophilisates during the storage for 10 weeks.

Evaluation of the different results of this study shows that frozen storage of both HESylated and PEGylated could be used to maintain the stability of the polyplexes, with no influence on the particle size or transfection efficiency. Meanwhile, lyophilisation results show that although both polymers showed acceptable results in the *in vitro* transfection efficiency experiments, HES offers significant advantages over PEG in stabilising the particles against aggregation. The latter is important for *in vivo* application, since aggregated particles could lead to changes in biodistribution, and most importantly accumulation in the lung and premature elimination from the circulation. The apparent particle stability shown in this study could avoid such problems.

5 Conclusions

The present work was designed for studying if using HES for coating polyplexes would offer advantages for their frozen storage and lyophilisation. FT studies in the standard formulation buffer HBG were conducted to assess the action of HES- and PEG-coats in the presence of glucose on the particle size of LPEI-based pDNA complexes. HES coats significantly reduced the tendency to formation of aggregates upon FT treatment, though not optimally due to the poor stabilizing ability provided by glucose. Subsequently Tre and Suc in isotonic concentrations were tested with good results for polymer-decorated particles in freeze-thaw cycles. The protection from polyplex aggregation changed after lyophilisation, where HES shields acted both cryo- and lyoprotective, while PEGylation induced polyplex aggregation after freeze-drying. In comparison to freshly lyophilized particles, the particle size of naked, HES- and PEG-decorated polymeric complexes was not affected by storage for 10 weeks at 2-8°C, 25°C and 40°C. The gene transfer efficiency of lyophilized, naked polyplexes decreased by a factor of 10 compared to freshly prepared polyplexes, while the coated polyplexes were not negatively affected by the storage for 10 weeks. Benchmarking HES against PEG as shielding agents resulted in distinctly superior lyoprotective performance in the case of polyplexes with HES-coats, with possible consequences for the *in vivo* use, since aggregated particles are not applicable *in vivo*. In summary, our developed HES-coats provided cryo- and lyoprotection to LPEI-based polyplexes after storage without any loss of transfection efficiency compared to freshly prepared HESylated particles.

6 Acknowledgements

The authors would like to thank Dr. Frank Schaubhut (Coriolis Pharma GmbH, Martinsried) for the possibility to use the DynaPro Titan DLS plate reader. We would like to thank Elisabeth Härtl for her kind assistance in preparing and filling hundreds of vials prior to freeze-drying. Raimund Geidobler is kindly acknowledged for his introduction in the lyophilisation technique.

7 References

1. **Greish, K.**, Enhanced permeability and retention of macromolecular drugs in solid tumors: A royal gate for targeted anticancer nanomedicines. *Journal of Drug Targeting*, 2007. 15(7): p. 457 - 464.
2. **Iyer, A.K., G. Khaled, J. Fang, and H. Maeda**, Exploiting the enhanced permeability and retention effect for tumor targeting. *Drug Discovery Today*, 2006. 11(17-18): p. 812-818.
3. **Maeda, H., T. Sawa, and T. Konno**, Mechanism of tumor-targeted delivery of macromolecular drugs, including the EPR effect in solid tumor and clinical overview of the prototype polymeric drug SMANCS. *Journal of Controlled Release*, 2001. 74(1-3): p. 47-61.
4. **Kursa, M., G.F. Walker, V. Roessler, M. Ogris, W. Roedel, R. Kircheis, and E. Wagner**, Novel Shielded Transferrin–Polyethylene Glycol–Polyethylenimine/DNA Complexes for Systemic Tumor-Targeted Gene Transfer. *Bioconjugate Chemistry*, 2003. 14(1): p. 222-231.
5. **Ogris, M., G. Walker, T. Blessing, R. Kircheis, M. Wolschek, and E. Wagner**, Tumor-targeted gene therapy: strategies for the preparation of ligand-polyethylene glycol-polyethylenimine/DNA complexes. *Journal of Controlled Release*, 2003. 91(1-2): p. 173-181.
6. **Petersen, H., P.M. Fechner, D. Fischer, and T. Kissel**, Synthesis, Characterization, and Biocompatibility of Polyethylenimine-graft-poly(ethylene glycol) Block Copolymers. *Macromolecules*, 2002. 35(18): p. 6867-6874.
7. **Hatakeyama, H., H. Akita, and H. Harashima**, A multifunctional envelope type nano device (MEND) for gene delivery to tumours based on the EPR effect: A strategy for overcoming the PEG dilemma. *Advanced Drug Delivery Reviews*, 2011. 63(3): p. 152-160.
8. **Mishra, S., P. Webster, and M.E. Davis**, PEGylation significantly affects cellular uptake and intracellular trafficking of non-viral gene delivery particles. *European Journal of Cell Biology*, 2004. 83(3): p. 97-111.
9. **Fella, C., G.F. Walker, M. Ogris, and E. Wagner**, Amine-reactive pyridylhydrazones-based PEG reagents for pH-reversible PEI polyplex shielding. *European Journal of Pharmaceutical Sciences*, 2008. 34(4-5): p. 309-320.
10. **Miyata, K., Y. Kakizawa, N. Nishiyama, Y. Yamasaki, T. Watanabe, M. Kohara, and K. Kataoka**, Freeze-dried formulations for in vivo gene delivery of PEGylated polyplex micelles with disulfide crosslinked cores to the liver. *Journal of controlled release*, 2005. 109(1): p. 15-23.
11. **Zhu, C., M. Zheng, F. Meng, F.M. Mickler, N. Ruthardt, X. Zhu, and Z. Zhong**, Reversibly shielded DNA polyplexes based on bio-reducible PDMAEMA-SS-PEG-SS-PDMAEMA triblock copolymers mediate markedly enhanced nonviral gene transfection. *Biomacromolecules*, 2012. 13(3): p. 769-778.
12. **Mok, H., K.H. Bae, C.H. Ahn, and T.G. Park**, PEGylated and MMP-2 specifically dePEGylated quantum dots: comparative evaluation of cellular uptake. *Langmuir*, 2008. 25(3): p. 1645-1650.
13. **Noga, M., D. Edinger, W. Rödl, E. Wagner, G. Winter, and A. Besheer**, Controlled shielding and deshielding of gene delivery polyplexes using hydroxyethyl starch (HES) and alpha-amylase. *Journal of Controlled Release*, 2012. 159(1): p. 92-103.
14. **Noga, M., D. Edinger, R. Kläger, S.V. Wegner, J.P. Spatz, E. Wagner, G. Winter, and A. Besheer**, The effect of molar mass and degree of hydroxyethylation on the

- controlled shielding and deshielding of hydroxyethyl starch-coated polyplexes. *Biomaterials*, 2013. 34(10): p. 2530-2538.
15. **Cherng, J.Y., P. van de Wetering, H. Talsma, D.J.A. Crommelin, and W.E. Hennink**, Freeze-drying of poly ((2-dimethylamino) ethyl methacrylate)-based gene delivery systems. *Pharmaceutical research*, 1997. 14(12): p. 1838-1841.
16. **Anchordoquy, T.J. and T.K. Armstrong**, Low molecular weight dextrans stabilize nonviral vectors during lyophilization at low osmolalities: concentrating suspensions by rehydration to reduced volumes. *Journal of pharmaceutical sciences*, 2005. 94(6): p. 1226-1236.
17. **Armstrong, T.K. and T.J. Anchordoquy**, Immobilization of nonviral vectors during the freezing step of lyophilization. *Journal of pharmaceutical sciences*, 2004. 93(11): p. 2698-2709.
18. **Allison, S.D. and T.J. Anchordoquy**, Stabilization of lipid/DNA complexes during the freezing step of the lyophilization process: the particle isolation hypothesis. *Biochimica et Biophysica Acta (BBA)-Biomembranes*, 2000. 1468(1): p. 127-138.
19. **Thomas, M.J., E.S. Parry, S.G. Nash, and S.H. Bell**, A method for the cryopreservation of red blood cells using hydroxyethyl starch as a cryoprotectant. *Transfusion Science*, 1996. 17(3): p. 385-396.
20. **Pasch, J., A. Schiefer, I. Heschel, N. Dimoudis, and G. Rau**, Variation of the HES concentration for the cryopreservation of keratinocytes in suspensions and in monolayers. *Cryobiology*, 2000. 41(2): p. 89.
21. **CLAPISSON, G., C. SALINAS, P. MALACHER, M. MICHALLET, I. PHILIP, and T. PHILIP**, Cryopreservation with hydroxyethylstarch (HES)+ dimethylsulfoxide (DMSO) gives better results than DMSO alone. *Bulletin du cancer*, 2004. 91(4): p. 10097-10102.
22. **Schaffert, D., M. Kiss, W. Rödl, A. Shir, A. Levitzki, M. Ogris, and E. Wagner**, Poly(I:C)-Mediated Tumor Growth Suppression in EGF-Receptor Overexpressing Tumors Using EGF-Polyethylene Glycol-Linear Polyethylenimine as Carrier. *Pharmaceutical Research*, 2011. 28(4): p. 731-741.
23. **Takae, S., K. Miyata, M. Oba, T. Ishii, N. Nishiyama, K. Itaka, Y. Yamasaki, H. Koyama, and K. Kataoka**, PEG-Detachable Polyplex Micelles Based on Disulfide-Linked Block Cationomers as Bioresponsive Nonviral Gene Vectors. *Journal of the American Chemical Society*, 2008. 130(18): p. 6001-6009.
24. **Hatakeyama, H., H. Akita, E. Ito, Y. Hayashi, M. Oishi, Y. Nagasaki, R. Danev, K. Nagayama, N. Kaji, and H. Kikuchi**, Systemic delivery of siRNA to tumors using a lipid nanoparticle containing a tumor-specific cleavable PEG-lipid. *Biomaterials*, 2011. 32(18): p. 4306-4316.
25. **Song, L., Q. Ahkong, Q. Rong, Z. Wang, S. Ansell, M. Hope, and B. Mui**, Characterization of the inhibitory effect of PEG-lipid conjugates on the intracellular delivery of plasmid and antisense DNA mediated by cationic lipid liposomes. *Biochimica et Biophysica Acta (BBA)-Biomembranes*, 2002. 1558(1): p. 1-13.
26. **Masuda, T., H. Akita, K. Niikura, T. Nishio, M. Ukawa, K. Enoto, R. Danev, K. Nagayama, K. Ijiro, and H. Harashima**, Envelope-type lipid nanoparticles incorporating a short PEG-lipid conjugate for improved control of intracellular trafficking and transgene transcription. *Biomaterials*, 2009. 30(27): p. 4806-4814.
27. **Cherng, J.Y., P. Wetering, H. Talsma, D. Crommelin, and W. Hennink**, Stabilization of polymer-based gene delivery systems. *International journal of pharmaceutics*, 1999. 183(1): p. 25-28.
28. **Cherng, J.-Y., H. Talsma, D. Crommelin, and W. Hennink**, Long Term Stability of Poly((2-dimethylamino)ethyl Methacrylate)-Based Gene Delivery Systems. *Pharmaceutical Research*, 1999. 16(9): p. 1417-1423.

29. **Izutsu, K.-i., S. Yoshioka, S. Kojima, T.W. Randolph, and J.F. Carpenter**, Effects of sugars and polymers on crystallization of poly (ethylene glycol) in frozen solutions: phase separation between incompatible polymers. *Pharmaceutical research*, 1996. 13(9): p. 1393-1400.
30. **Gryparis, E., G. Mattheolabakis, D. Bikiaris, and K. Avgoustakis**, Effect of conditions of preparation on the size and encapsulation properties of PLGA-mPEG nanoparticles of cisplatin. *Drug Delivery*, 2007. 14(6): p. 371-380.
31. **Bhatnagar, B.S., S.M. Martin, D.L. Teagarden, E.Y. Shalaev, and R. Suryanarayanan**, Investigation of PEG crystallization in frozen PEG–sucrose–water solutions: II. Characterization of the equilibrium behavior during freeze-thawing. *Journal of pharmaceutical sciences*, 2010. 99(11): p. 4510-4524.
32. **Her, L.-M. and S.L. Nail**, Measurement of glass transition temperatures of freeze-concentrated solutes by differential scanning calorimetry. *Pharmaceutical research*, 1994. 11(1): p. 54-59.
33. **Amin, K., R.M. Dannenfelser, J. Zielinski, and B. Wang**, Lyophilization of polyethylene glycol mixtures. *Journal of pharmaceutical sciences*, 2004. 93(9): p. 2244-2249.
34. **Searles, J.A., J.F. Carpenter, and T.W. Randolph**, Annealing to optimize the primary drying rate, reduce freezing-induced drying rate heterogeneity, and determine Tg' in pharmaceutical lyophilization. *Journal of pharmaceutical sciences*, 2001. 90(7): p. 872-887.
35. **De Jaeghere, F., E. Allémann, J. Feijen, T. Kissel, E. Doelker, and R. Gurny**, Freeze-drying and lyopreservation of diblock and triblock poly (lactic acid)-poly (ethylene oxide)(PLA-PEO) copolymer nanoparticles. *Pharmaceutical development and technology*, 2000. 5(4): p. 473-483.
36. **Hinrichs, W., F. Mancenido, N. Sanders, K. Braeckmans, S. De Smedt, J. Demeester, and H. Frijlink**, The choice of a suitable oligosaccharide to prevent aggregation of PEGylated nanoparticles during freeze thawing and freeze drying. *International journal of pharmaceuticals*, 2006. 311(1-2): p. 237.
37. **Hinrichs, W., N. Sanders, S. De Smedt, J. Demeester, and H. Frijlink**, Inulin is a promising cryo-and lyoprotectant for PEGylated lipoplexes. *Journal of controlled release*, 2005. 103(2): p. 465-479.
38. **Kwoh, D.Y., C.C. Coffin, C.P. Lollo, J. Jovenal, M.G. Banaszczyk, P. Mullen, A. Phillips, A. Amini, J. Fabrycki, and R.M. Bartholomew**, Stabilization of poly-L-lysine/DNA polyplexes for in vivo gene delivery to the liver. *Biochimica et Biophysica Acta (BBA)-Gene Structure and Expression*, 1999. 1444(2): p. 171-190.
39. **Ogris, M., P. Steinlein, S. Carotta, S. Brunner, and E. Wagner**, DNA/polyethylenimine transfection particles: Influence of ligands, polymer size, and PEGylation on internalization and gene expression. *AAPS pharmSci*, 2001. 3(3): p. 43-53.

VI Final summary of the thesis

The current thesis describes the development of novel bioresponsive conjugates based on hydroxyethyl starch (HES) and polyethylenimine (PEI) for controlled shielding and enzymatically-triggered polyplex deshielding under the effect of alpha amylase. HES was tested as biodegradable alternative substitute for non-biodegradable shielding agent polyethylene glycol (PEG) - so far as known - for the first time in the field of polymeric nucleic acid delivery.

In the early stage of the project, a battery of conjugates of several types of HES with different molecular characteristics and linear PEI was synthesized via Schiff's base formation and reductive amination, subsequently purified using preparative ion exchange separation and characterized by ^1H NMR, colorimetry (using the copper assay), and size exclusion chromatography (SEC). Mixtures of the homopolymer LPEI and HES-PEI copolymers were used to produce stable HESylated core-shell nano-dandelions, which was confirmed by AFM- and TEM-measurements, as well as DLS studies. Polymeric complexes with HES coats were found to have similar biophysical properties in terms of particle size and polydispersity compared with naked and PEG-shielded control pDNA polyplexes. Incorporation of hydrophilic polymer HES onto the particle surface resulted in the reduction of the zeta potential by the effect of particle shielding. This effect was most pronounced in the case of high total amounts of high molecular weight HES shields. Shielding the cationic charge of PEI provided by HES coats reduced the DNA binding ability of the homopolymer PEI, however, particle formation at N/P ratio 6.0 was not affected by the HES coatings.

The key issue for overcoming the PEG dilemma in gene delivery is shedding down the disturbing stealth polymer coat after arrival at the target site. HES is a biodegradable polymer, the biocleavage kinetics can be controlled by fine-tuning HES' molecular characteristics. Different analytical tools were used in order to investigate parameters affecting the enzymatic degradation of HES, namely the type and the composition of the buffer, different enzyme concentrations and the effect of the degree of substitution and the molar mass of HES. Initially, the degradation rate and extent of different HES polymers under the effect of AA was studied in the case of the homopolymer using AF4-MALS, using QCM-D in the case of HES-PEI conjugates, and finally using zeta-potential measurements for the HES-coated polyplexes. Degradation studies showed that the rate and extent of biodegradation strongly

correlated with the degree of hydroxyethylation of HES. HES polymers with low degree of substitution were degraded strongly and rapidly, while the biodegradability of the polysaccharide was diminished with increasing degree of hydroxyethylation. The cleavage of α -1,4-glycosidic bonds of HES was monitored as loss of HES molecular weight (AF4-MALS), as mass reduction of adsorbed HES-PEI conjugates (QCM) and as increase in the zeta potential by gradual eating up of the shielding coat over time.

As first proof-of-concept, the effect of polyplex shielding and enzymatic polyplex deshielding was studied *in vitro* in N2A cells. HES coating promoted efficient surface charge shielding and was found to significantly reduce the luciferase gene expression similar to the PEGylated counterparts in comparison to the naked LPEI polyplexes with the highest surface net charge. In presence of alpha amylase the HES coat was gradually degraded and the particle was reactivated resulting in a boost of 2-3 orders of magnitude in gene expression reaching the transfection levels of LPEI polyplexes, while naked as well as PEGylated particles were not affected by the enzyme. Efficient deshielding was only feasible in the case of low substituted HES coats, while high degrees of substitution prevented enzymatic particle reactivation. A satisfying biocompatibility is an important prerequisite for conducting *in vivo* studies. HESylation of cationic polymer LPEI could reduce PEI's cytotoxicity that was confirmed by studies investigating the cellular metabolic activity, the tendency to form aggregates upon incubation with red blood cells and the polymer's hemolytic potency. A second PoC experiment was performed in tumor-bearing A/J mice. The lead polyplex with an amount of 10% shielding agent HES70-PEI was found to significantly reduce the lung accumulation and toxicity provided by LPEI with the effect of up to 3 orders of magnitude and maintained the tumoral gene expression of LPEI polyplexes. Increasing the amount of stealth polymer HES, as well as using non-biodegradable PEG shields resulted in what is known as the PEG-dilemma, namely a safe particle with low transfection activity.

In the last part of the project, the use of HES coats is described for improving the long-term stability of LPEI/DNA complexes. Freeze-thaw and freeze-dry studies confirmed the cryo- and lyoprotective action provided by hydrophilic HES coats. Stabilization by the effect of steric hindrance is considered as reason for HES' beneficial action on the polyplex surface. HES-decorated nano-dandelions showed high particle size resistance against the lyophilization-process and a 10-week storage time with maintained enzymatic activability and high transfection efficiency after freeze-drying and storage. LPEI control particles showed

higher proneness to form aggregates following freeze-thaw- and freeze-dry-stress and significantly reduced gene expression levels after storage. The PEG-shielded particles were found to show high resistance against freeze-thaw stress, however, assumed PEG-crystallization on the polyplex surface induced strong particle clustering following lyophilization, making PEGylated polyplexes unattractive for *in vivo* applications.

PUBLICATIONS ASSOCIATED WITH THIS THESIS

Research articles

Noga M, Edinger D, Rödl W, Wagner E, Winter G, Besheer A. Controlled shielding and deshielding of gene delivery polyplexes using hydroxyethyl starch (HES) and alpha-amylase. *Journal of Controlled Release*, 2012. 159(1): 92-103.

Noga M, Edinger D, Kläger R, S.V. Wegner, J.P. Spatz, Wagner E, Winter G, Besheer A. The effect of molar mass and degree of hydroxyethylation on the controlled shielding and deshielding of hydroxyethyl starch-coated polyplexes. *Biomaterials*, 2013. 34(10): 2530-2538.

Noga M, Edinger D, Wagner E, Winter G, Besheer A. Characterization and biocompatibility of hydroxyethyl starch-polyethylenimine copolymers for DNA delivery. *submitted*

Noga M, Edinger D, Wagner E, Winter G, Besheer A. Lyophilized HESylated pDNA polyplexes for increased nanoparticle stability and maintained gene transfer efficiency – A benchmark study against PEG. *In preparation*

Review article

Noga M, Winter G, Besheer A. Enzyme-responsive stealth coats for long-circulating nanomedicines. *In preparation*

Patent

Besheer A, Noga M, Winter G, Wagner E, Edinger D. Method for the controlled intracellular delivery of nucleic acids. 2013, WO/2013/021056.

PRESENTATIONS ASSOCIATED WITH THIS THESIS

Oral presentation

Noga M, Edinger D, Wagner E, Winter G, Besheer A. Can HES-decorated polyplexes overcome the PEG-dilemma. DPhG Doktorandentagung, Weimar, Germany, November 2012.

Poster presentations

Noga M, Edinger D, Wagner E, Winter G, Besheer A. Controlled shielding & deshielding of HES-decorated polyplexes using alpha amylase. 39th Annual Meeting & Exposition of the Controlled Release Society, Québec City, Canada, July 2012.

Noga M, Edinger D, Wagner E, Winter G, Besheer A. Can nano-dandelions overcome the „PEG-dilemma“ in gene delivery? – Designing HES-decorated core-shell polyplexes with controlled shielding & deshielding. 8th World Meeting on Pharmaceutics, Biopharmaceutics and Pharmaceutical Technology, Istanbul, Turkey, March 2012.

Noga M, Winter G, Besheer A. HES-PEI copolymers for gene delivery: synthesis, characterization and generation of HES-decorated polyplexes. 8th World Meeting on Pharmaceutics, Biopharmaceutics and Pharmaceutical Technology, Istanbul, Turkey, March 2012.